AN INVESTIGATION OF THE IMPACTS OF *ACACIA MEARNSII* PLANTATIONS ON SECONDARY AQUIFER SYSTEMS WITHIN THE TWO - STREAMS CATCHMENT, KWAZULU-NATAL, SOUTH AFRICA.

By

Caiphus Zimise Ngubo

211560631

Supervisors: Prof. Simon Lorentz and Dr. Molla Demlie

Submitted in fulfilment of the academic requirements for the degree of Master of Science: Hydrology

College of Agriculture, Engineering and Science
School of Agriculture, Earth and Environmental Science
Discipline of Environmental Hydrology
University of KwaZulu-Natal
Pietermaritzburg
South Africa

March 2019

PREFACE

The research contained in this dissertation was completed by the candidate while based in the Discipline of Environmental Hydrology, School of Agricultural, Earth and Environmental Sciences of the College of Agriculture, Engineering and Science, University of KwaZulu-Natal, Pietermaritzburg Campus, South Africa. The contents of this work have not been submitted in any form to another university and, except where the work of others is acknowledged in the text, the results reported are due to investigations by the candidate.

_____ _____

Signed (Supervisor) Date

DECLARATION

I, Caiphus Zimise Ngubo, declare that:

1. The research in this dissertation, except where otherwise indicated, is my original research.

2. This dissertation has not been submitted for any degree or examination at any other university.

3. This dissertation does not contain other person's data, pictures, graphs or other information, unless specifically acknowledged as being sourced from other persons.

4. This dissertation does not contain other person's writing, unless specifically acknowledged as being sourced from other researchers. Where other written sources have been quoted, then:
    A. Their words have been re-written but the general information attributed to them has been referenced.
    B. Where their exact words, then their writing has been placed in italics, inside quotation marks and referenced.

5. This dissertation does not contain text, graphics or tables copied and pasted from the internet, unless specifically acknowledged, their source detailed within the dissertation and in the reference section.

Signed: Caiphus Zimise Ngubo

Date :

ABSTRACT

The Two-Streams catchment, located in the Seven Oaks District in the KwaZulu-Natal midlands of South Africa has been used as an experimental catchment over the past decade to investigate the impacts of *Acacia mearnsii* stands on hydrological processes. As part of the ongoing hydrological study, the hydrogeology of the Two - Streams catchment covering an area of about 0.74 km^2 is investigated and characterized to understand the impacts of *Acacia Mearnsii* plantations on groundwater. A combined hydrological, hydrogeological, hydrochemical and environmental isotope methods were employed in characterizing the hydrogeology of the study catchment. Geologically, the study area is underlain by three units, namely; top weathering profile, mainly of clay, which is underlain by weathered shale. The shale is in turn underlain by granite basement rock. Two hydrostratigraphic units are identified: a water table or unconfined aquifer occurring along the weathered shale and the underlying regional weathered and fractured semi confined basement granitic aquifer. The regional weathered and fractured granitic aquifer is characterised by a transmissivity that ranges from 0.15 to 0.48 m^2/day and a hydraulic conductivity of 0.04 m/day. The Two-Streams catchment receives a mean annual rainfall of 778 mm, average annual evapotranspiration of 802 mm, average annual stream discharge of 20387 m^3 and average annual recharge of 31.9 mm or 4.1 % of MAP. Hydrochemical data indicates both groundwater and stream samples are characterised by mean specific electrical conductivity (EC) of 28.5 mS/m and Ca-HCO_3 and Ca-Cl dominant hydrochemical facies. All samples have δD and $\delta^{18}O$ isotopic values that plot on or above the local and global meteoric water lines, indicating recharge from rainfall with insignificant evaporation during or prior to recharge. Seasonal stream isotope data analysis indicates that groundwater is the main contributor of streamflow during dry season. Furthermore, the impacts of *Acacia mearnsii* trees on groundwater through direct groundwater uptake by roots and impacts of trees on recharge, groundwater levels and baseflow were investigated. The results show that direct groundwater uptake by tree roots from the saturated zone at Two-Streams would not be possible due to limiting root depth. Thus, in instances where the regional groundwater table is not available for direct abstraction by tree roots, *Acacia mearnsii* trees can have a large impact on groundwater through extracting water from within the unsaturated zone, reducing the proportion of rainfall that eventually contributes recharge to the aquifers and baseflow, without necessarily having direct access to the groundwater proper.

Key words/Phrases: *Acacia mearnsii;* Baseflow separation; Environmental isotope; Groundwater Recharge; Hydrochemistry; Two-Streams Catchment; South Africa.

ACKNOWLEDGEMENTS

This report was made possible through determined hard-work, patience, and guidance from my supervisors; Dr. Molla Demlie, Prof. Simon Lorentz and Prof. Colin Everson who presented me with an opportunity to engage myself with hydrological studies in the highly researched Two-Streams catchment and who remained relentlessly prepared to share their views and expertise to see the completion of this report, I thank you. In particular, I would like to thank Dr. Molla Demlie who served as my internal supervisor for his support, inspiration and always having an open door and willing to listen and provide advice, without him, this dissertation would not have been possible.

Furthermore, I would like to stretch my acknowledgment and my sincere appreciations to the following people and institutions:

- Water Research Commission and Department of Environmental Affairs: Working for Water, for providing funding for research work in the Two Streams catchment.
- Centre for Water Resources Research (CWRR) and South African Observation Network (SAON) for providing hydrological monitoring data.
- Department of Water and Sanitation, in particular Mr. Vukani Tshabalala, Mr. Siboniso Dube, Mr. Sakhile Mndaweni Mr. Mofokeng Setjhaba for their assistance during geophysical surveying and pumping test.
- Mr. Siphiwe Mfeka, Sphelele Ngubo and Philani Ndlela for their assistance during water sampling programs.
- Postgraduates students: Sphelele Ndlovu and Hlumela Mduduma for their assistance with Aquachem, Coraldraw and Surfer analysis software programs.
- My family, EDTEA Bramhill office colleagues and friends for their support and encouragement.
- Finally, I would like to thank my wife, Nobuhle and my daughters Amahle, Snothile and Zemvelo for their immense support, patience and understanding throughout my studies.
- Additionally, I would like to thank every individual or an organisation that may be intentionally or unintentionally included or excluded from the above acknowledgements, which have directly or indirectly contributed to the completion of this report. I Thank You.

Table of Contents

LIST OF FIGURES

LIST OF TABLES

CHAPTER ONE: INTRODUCTION AND BACKGROUND

1.1. Introduction

Acacia Mearnsii plantations are originally from Australia and were brought to South Africa in 1864 for timber and paper-making (De Beer, 1986; Stirton, 1987). They survive in South African conditions by developing adaptation strategies, such as developing deep root systems that can access alternative sources of water (De Wit *et al*., 2001). A review study conducted by Le Maitre *et al.* (1999) concluded that woody plantations can develop deep root systems, which are capable of extracting large volumes of groundwater from depths of up to 10 m. In a semi-arid country like South Africa, the sustainable management of water resources requires sound understanding of the availability of water and how it is influenced by climate, soil and vegetation. Vegetation plays a key role in the interactions between surface and groundwater systems, because of its direct and indirect influence on recharge, evapotranspiration and the dependence of vegetation species on groundwater (Le Maitre *et al*., 1999). Tree plantations can reduce streamflow and groundwater recharge relative to shallow-rooted grass and agricultural crops (Benyon *et al.*, 2006). Many hydrological studies from across the world (Hibbert, 1967; Bosch and Hewlett, 1982; Holmes and Sinclair, 1986; Zhang *et al*., 1999) have demonstrated that woody plantations commonly use more water than grasses and non-irrigated agricultural crops. In South Africa, the impacts of forest plantations are thought to be predominantly due to increased transpiration, rather than increased interception losses (Scott and Lesch, 1997). The studies conducted in South Australia (Holmes and Colville, 1970b; Allison and Hughes, 1972; Colville and Holmes; 1972) indicated that once the canopy of tree plantations has fully closed, there is little, if any, groundwater recharge under these plantations because of interception losses. However, none of these early studies indicated whether deep-rooted tree plantations obtain water from the groundwater system. In South Africa, most of the work undertaken on the impacts of trees on groundwater resources has been conducted in the Zululand coastal plain. These studies highlighted the impact of vegetation on recharge through water extraction from the unsaturated zone and abstractions from shallow groundwater. Thus, these plants reduce the proportion of rainfall that eventually recharges groundwater, by interfering with the passage of precipitation from the atmosphere to the water table (Kelbe *et al.*, 1995).

1.2. Background to Two-Streams Catchment Research Studies

The Two Streams catchment has been used as an experimental catchment over a decade to investigate the effect of *Acacia mearnsii* tree stands on hydrological processes. These studies have focused mainly on evaporation and soil hydrological processes, and concluded that evaporation rates exceeded rainfall by 46% (Burger, 1999; Jarmain and Everson, 2002; Clulow *et al*., 2011, Everson *et al*., 2014). However, little attention was given into the characterization of the hydrogeology of the catchment and investigation of the impacts of deep-rooted *Acacia mearnsii* plantations on the groundwater system. At an international level, Baldocchi and Xu (2007) reported that *Quercus douglasii* plantations were able to survive extended periods without water, as the total evaporation was also found to exceed rainfall. This suggested that tree roots were accessing subsurface water and depleting soil water reserves from the deep soil profile, which raised concerns about the effects of deep rooted plantations on groundwater.

The net aquifer discharge through the direct uptake of groundwater by tree roots in secondary aquifer systems has not been established. The impacts of deep rooted tree plantations on groundwater resources need to be understood and quantified, which will enable improved understanding of the beneficial or adverse effects on groundwater supplies and groundwater dependent ecosystems. The groundwater recharge originating from rainfall under *Acacia mearnsii* plantations in the Two-Streams catchment has not been estimated. The site-specific factors, such as aquifer characteristics and linkages, and preferential flow paths which can be interpreted to understand the hydrogeological behaviour of the catchment, also remain poorly understood. Therefore, the Two-Streams catchment provides an opportunity to fully investigate effects of deep rooted tree plantations on secondary aquifer systems in the South African context. Hence, this research envisages to investigate the site specific factors of the catchment such as aquifer characteristics, preferential flow paths and groundwater recharge, which are interpreted to understand the impacts of *Acacia mearnsii* plantations on the groundwater system using the Two-Streams catchment as a case study.

1.3. Research Aims and Objectives

The aims of this M.Sc. research are to characterize the hydrogeology of the Two-Streams catchment, understand the mechanisms by which water is extracted by deep-rooted *Acacia mearnsii* plantations and its impact on groundwater.

The specific objectives are:

- To study the aquifer characteristics, recharge rates and mechanisms as well as groundwater flow behavior using different hydrological techniques, including estimating the thickness of different hydrogeological units, characterize the aquifers and local groundwater flow patterns;
- To characterize hydrochemical parameters and isotope signatures of groundwater from boreholes, seepage areas and streams;
- To develop a conceptual hydrogeological model of the study area; and
- To characterize mechanisms that make groundwater available for use by *Acacia mearnsii* plantations and its impact on groundwater.

1.4. Significance of the Study

Vegetation plays a key role in controlling surface and groundwater systems, because of its direct and indirect influence on recharge, discharge and the dependence of vegetation communities on groundwater. There is little information available on the effect of *Acacia mearnsii* plantation on the groundwater system. Therefore, the significance of this study are to:

- Improve the understanding of the groundwater regimes of the catchment, in terms of the potential local and regional impacts, groundwater recharge, storage and potential preferential flow paths in the catchment.
- Improve understanding of the mechanisms that make groundwater water available for extraction by deep-rooted plantations in the secondary aquifer systems, and thus to provide information necessary for water use allocation and licensing for the forestry sector.

1.5. Thesis Structure

Chapter 1

This chapter presents an introduction into the dissertation. It provides a brief overview of the worldwide problem of vegetation interfering with surface and groundwater systems, the history of hydrological research studies that have been conducted in the Two-Streams research catchment as well as the paucity of research on the interaction between deep-rooted tree plantations and groundwater systems. The aims, objectives and the significance of the study are also contained in this chapter.

Chapter 2

This chapter presents the description of the study area, its physiographic settings and a brief description of soils, geology and hydrogeological settings. The site instrumentation set-up is also presented in this chapter.

Chapter 3

This chapter contains the literature reviewed related to hydrogeological characterization and groundwater mechanisms that make water available for extraction by deep-rooted tree plantations. The following topics are covered in this chapter: groundwater distribution and dynamics in hillslope catchments, groundwater storage and distribution, residence time of water, water use by tree plantations, vegetation water uptake in hillslope catchments, root depth of trees, water uptake in the unsaturated and saturated zones, environmental tracers in groundwater provenance as well as aquifer hydraulic characterization.

Chapter 4

This chapter presents a detailed account of the materials and methods that were employed during the study for data acquisition and interpretation. The following methods were employed: electrical resistivity tomography for geophysical surveying, streamflow, rainfall and groundwater measurements, stream hydrograph and borehole hydrograph analysis, aquifer testing, recharge estimation as well as, hydrochemical and isotope sampling and analysis.

Chapter 5

This chapter presents the results from the investigation and provides detailed discussions of the results. The chapter is concluded by developing a hydrogeological conceptual model of the study site, comprising a simplified but quantified description encompassing all aspect of the local hydrology and hydrogeology of the area.

Chapter 6

This chapter presents the conclusions of the research and ends with recommendations for future research, which is then followed by a comprehensive list of references.

CHAPTER TWO: DESCRIPTION OF STUDY AREA

2.1. Location

The Two-Streams catchment is located in the small town of Seven Oaks, approximately 70 km from Pietermaritzburg, within the uMvoti local municipality in the KwaZulu-Natal midlands, South Africa (Figure 2.1) and covers an area of about 0.74 km^2. The catchment characteristics as described in Everson *et al*. (2014) is part of the midlands mist-belt grassland Bioregion. The catchment is generally hilly with rolling landscapes and a high percentage of arable land. It is dominated by forb-rich, tall, sour *Themeda triandra* grasslands of which only a few patches remain due to invasion of native *Aristida junciformis.*

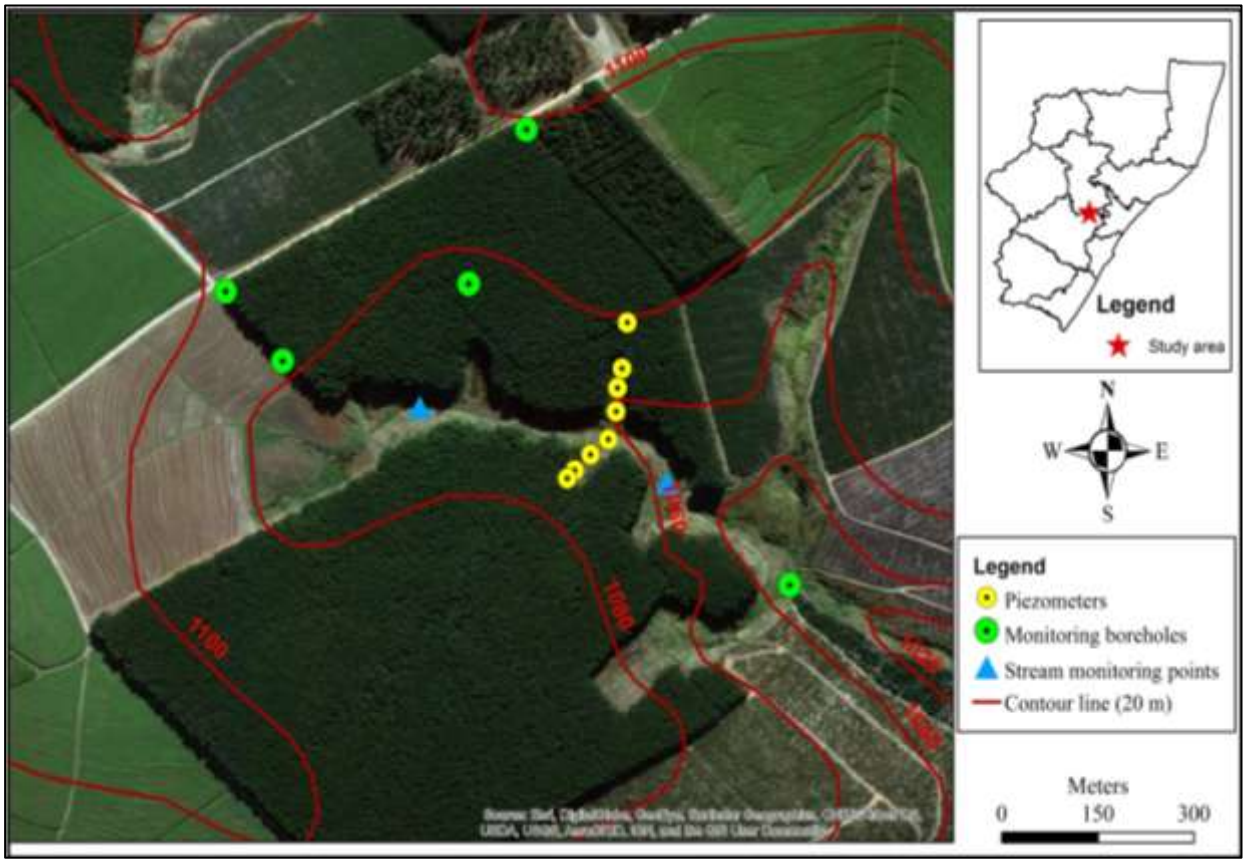

Figure 2.1. Location of Two-Streams catchment study area in KwaZulu-Natal province.

2.2. Climate

The Two-Streams catchment study site lies in the warm sub-tropical climate of South Africa, where summer is hot, humid and it is the main rainy season, while winter is cold and dry. The rainfall is commonly derived from summer thunderstorms or cold fronts. The long-term mean

annual precipitation (MAP) for the area is 853 mm (Clulow *et al*., 2011). However, the MAP for the monitoring period 2006 to 2017 using the two long-term gauges in the study area is 778 mm (Figure 2.2). The average minimum temperature occurring in July is 4.5 ^{0}C and the average maximum temperature occurring in March is 31.7 ^{0}C (Appendix A). Mist can be heavy and frequent and add significantly to precipitation. Moderate frosts, droughts, hail and berg winds are also common to the area (Clulow *et al*., 2011).

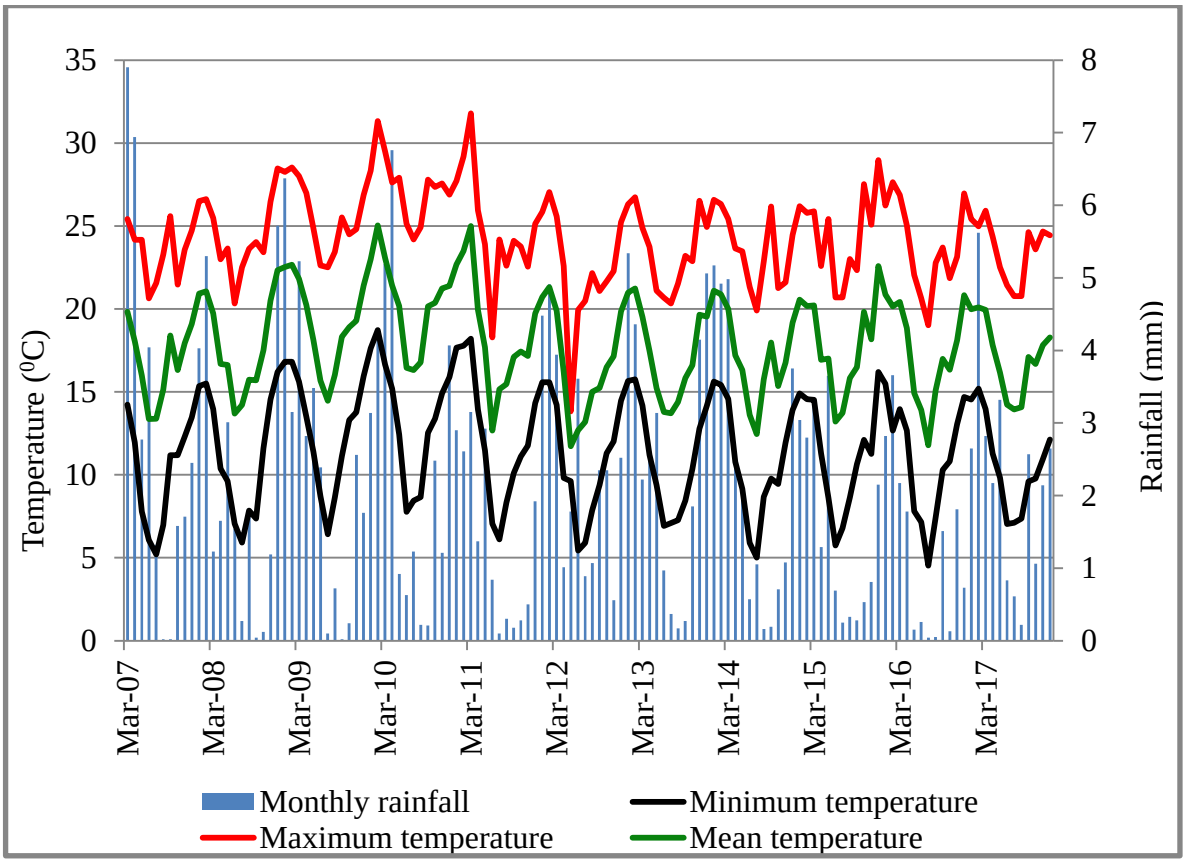

Figure 2.2. Minimum, maximum and mean temperature with corresponding monthly rainfall in the study area.

2.3. Topography and Drainage

The topography of the study area is generally hilly with a rolling landscape and dips towards the south east, giving rise to a surface drainage from north west to south east. The catchment area is positioned along slope between 1060 m amsl (low) and 1110 m amsl (high). The catchment is drained by two streams (Figure 2.3), which are the basis on which the catchment is called and drains into Mateku River on the south east. The Mateku River then joins the Mbalane River which is the main tributary of the uMvoti River in the east. The uMvoti River eventually drains into the Indian Ocean near Stanger in the South.

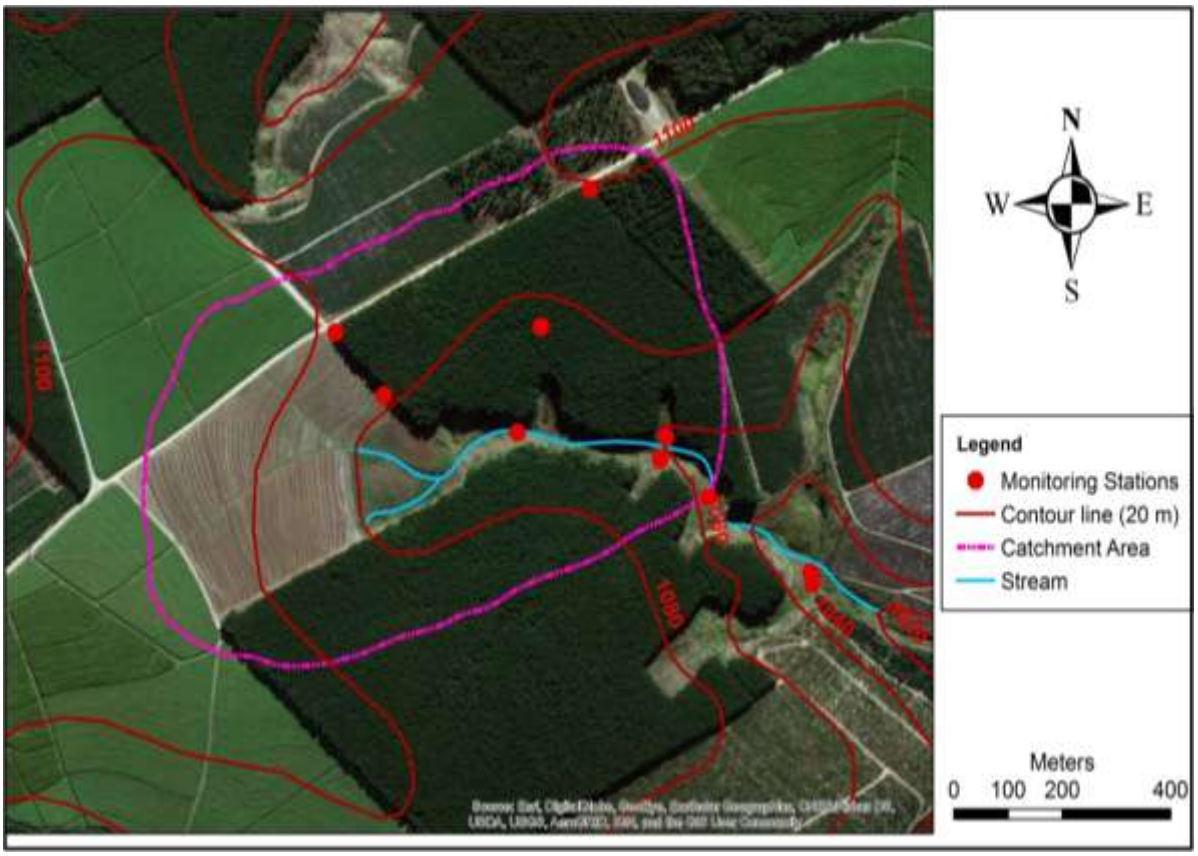

Figure 2.3. Map showing the Two-Streams catchment area.

2.4. Geology and Soils

According to the 1:250 000 geological map series 2930 Durban (Council for Geoscience, 1992), the study site is underlain by ancient basement granite of the Natal Metamorphic Province. These basement rocks are overlain unconformably by the Natal Group Sandstone comprising mostly of coarse-grained arkosic to subarkosic sandstone; micaceous sandstone with subordinate siltstone and mudstone lenses. The Natal Group is in turn overlain unconformably by the Ecca Group of the Karoo Supergroup sediments of the Pietermaritzburg formation, comprising mainly of dark grey shale; carbonaceous shale; siltstone and subordinate sandstone. Dolerite intrusions in the form of dykes and sills are common in the area. Numerous faults and fractures are present in the area associated mainly with Gondwana breakup (Figure 2.4). Faults and fracture zones are preferential groundwater storage and circulations zones in secondary aquifers and as such are typical targets for groundwater exploration. Soil types bear a close association with the underlying geology in that the sedimentary lithologies generally support sandy, more freely drained apedal soils. The soil formed in the study site as described in Clulow *et al*. (2011), are red sandy and yellow apedal freely drained soils derived mainly from the Ecca Group rocks and dolerite intrusions in the form of dykes or sills.

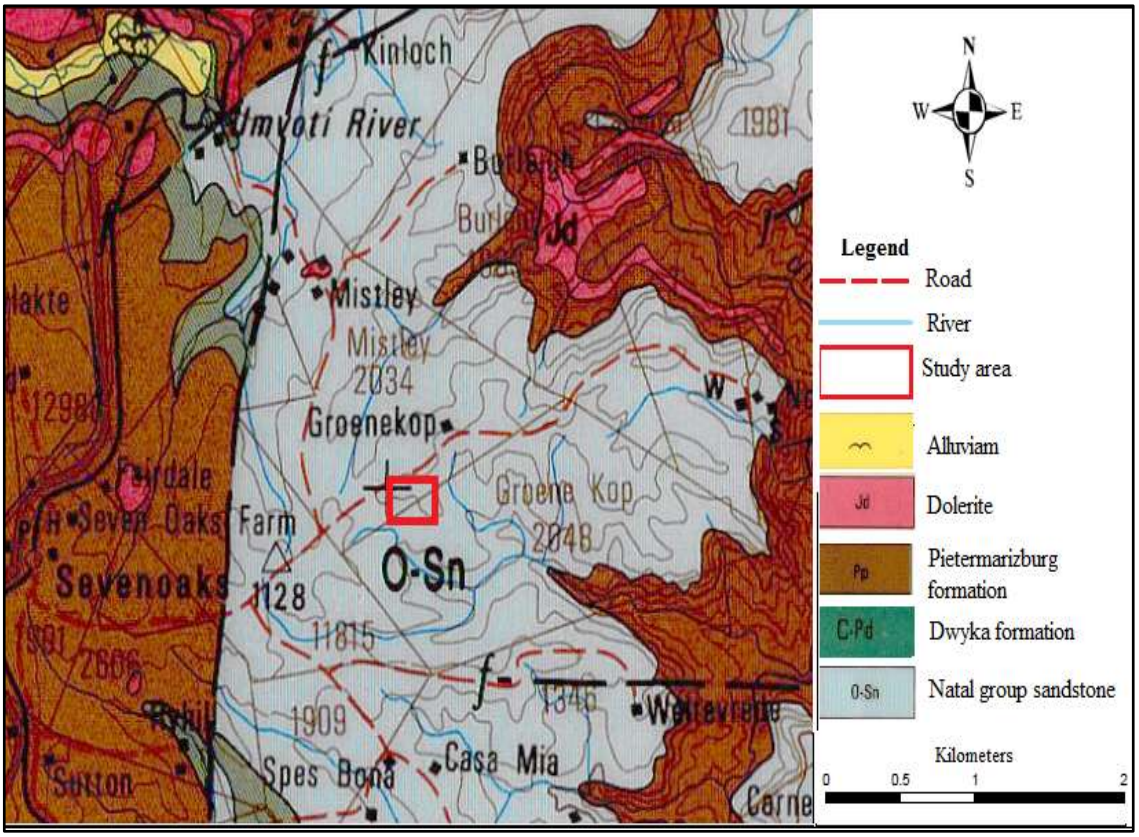

Figure 2.4. Geological map of the Two-Streams catchment modified from the 1:250 000 geological map series 2930 Durban (Council for Geoscience, 1992).

2.5. Hydrogeology

Groundwater occurs in porous geological material, hence the geology of the aquifer material has an impact on groundwater occurrence. It is of great importance to consider site geology if one is going to study its hydrogeology. Generally, the more porous the material is, the more water it can contain in its pores. The geological material may have a high porosity, but that does not guarantee it as good source of water. It is the interconnection of pores that make water to readily flow into springs and wells during pumping. Hence, the formation with high transmissivity is the main focus for groundwater exploration and development. Hiscock (2005) defined transmissivity as the measure of the ease with which groundwater flows in the subsurface. The more transmitting the material is, the more likely it is to have good yields, provided there is high storage and good recharge. The baked zone near dolerite dyke is highly fractured and has high transmissivity (DWAF, 1995). The fractured geological material becomes a target in groundwater exploration, thus confirming the importance of studying the geology of the area when conducting groundwater related investigations. The study site is underlain by the basement complex and cemented and compacted sedimentary strata of the

Natal Group Sandstone and Karoo Supergroup rocks. These strata have negligible primary porosity and permeability. The occurrence of groundwater is thus controlled by the development of secondary permeability in the ostensibly impermeable lithologies through features such as weathering, fracturing and jointing. These secondary aquifers are considered to have low groundwater potential and hence limited storativity and transmissivity. According to the hydrogeological map series 2928 Durban (DWAF, 1998), the study site falls within the fractured aquifers (b3) mode of groundwater occurrence associated with fractures, fissures and joints as shown in Figure 2.5. Borehole yields fall into the poor to moderate category varying between 0.5 and 2 litres per second, with expected hydraulic conductivities ranging between 0.4 and 7.7 m/day as well as the storativity of between 0.0005 and 0.005. However, faults, fractures, joints and dykes can play a primary role in the storage and transmission of groundwater. Therefore, moderate to good yields can be realized along these major structures. Groundwater recharge occurs as surface water infiltrates the soil especially through exposed fractures and weathered zones. Du Preeze (2007) reported an estimated overall recharge between 3 and 5% of MAP in similar geological formations in the region. The groundwater chemistry in the region is generally good with field electrical conductivity values seldom exceeding 70 mS/m (DWAF, 1995).

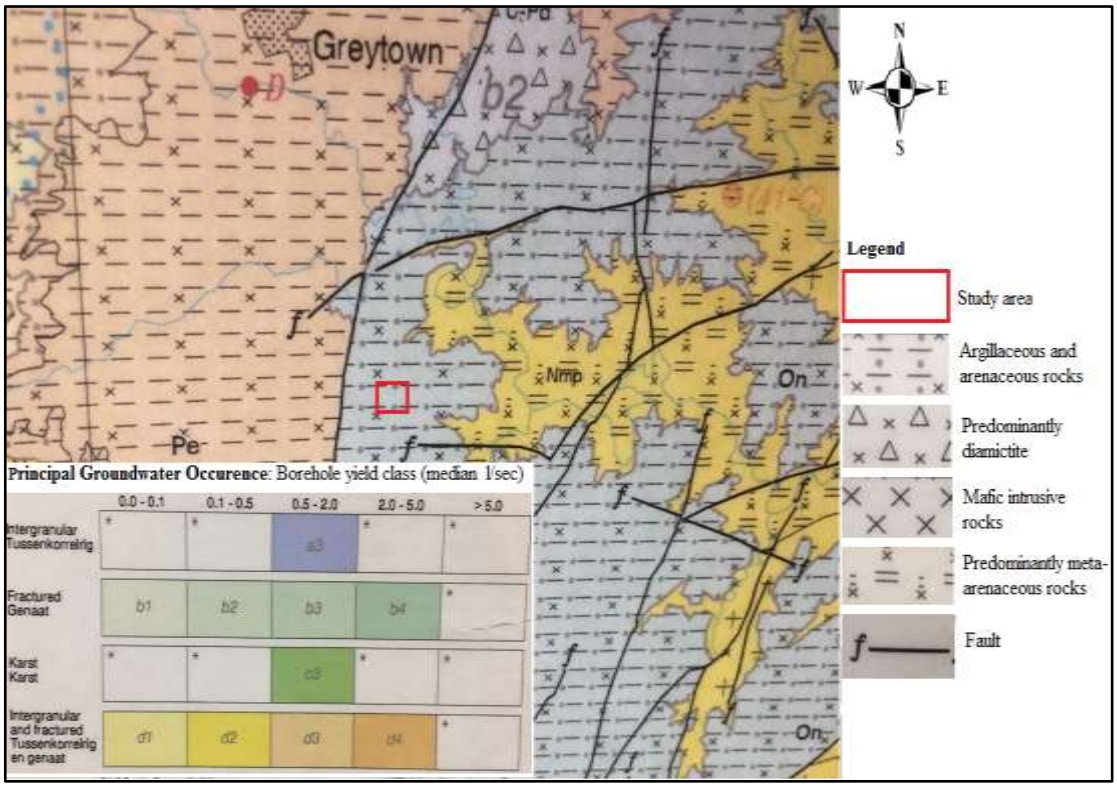

Figure 2.5. Hydrogeological map of the study area modified from the 1:500 000 hydrogeological map series (DWAF, 1998).

2.6. Site Set-up

The study site consists of five (5) deep groundwater monitoring boreholes and eight (8) shallow piezometers drilled to intercept the soil/bedrock interface. The four deep groundwater monitoring boreholes are 60 m deep each and the fifth borehole located at the center of the plantation is 40 m deep. One deep borehole located at catchment outlet is artesian. Three stream hydrochemistry monitoring points were selected at an up-stream point, midpoint (weir) and down-stream near the artesian borehole as shown in Figure 2.6. The site also consists of 457.2 mm 90^0 V-notch weir to monitor catchment runoff and a tipping bucket rain gauge to monitor the rainfall.

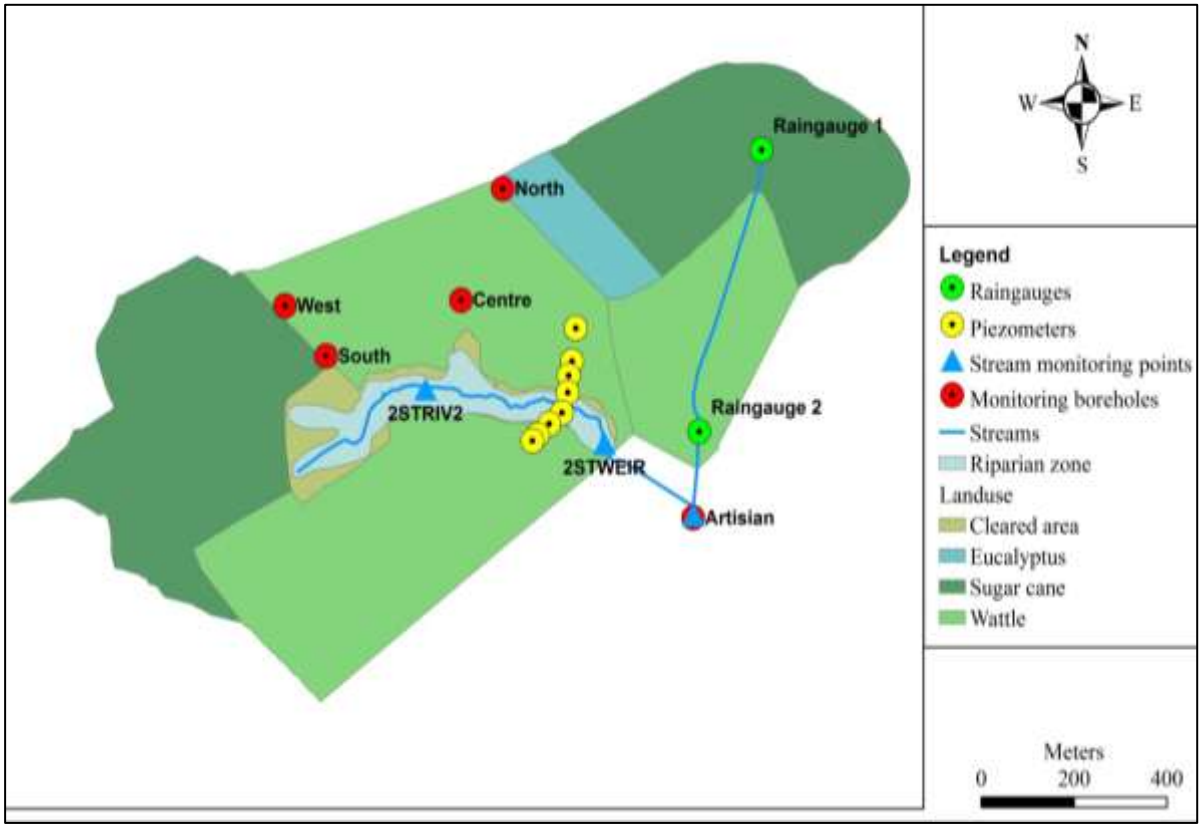

Figure 2.6. Map showing spatial distribution of monitoring stations within the study area.

CHAPTER THREE: LITERATURE REVIEW

3.1. Introduction

Acacia mearnsii plantations occur naturally in Southern Australia, where it forms part of the undergrowth in Eucalyptus forests or grows in dense stands along roads (De Beer, 1986). It grows well in high rainfall areas on deep, well-drained soils, but also establishes on shallow soils if there is sufficient water (Stirton, 1987). Literature indicates that the first *Acacia mearnsii* seed was brought to South Africa in 1864 by John van der Plank, an English seafarer who settled on the farm in Camperdown area in Natal (De Beer, 1986; Stirton, 1987). The seed was distributed to travellers by van der Plank, which led to *Acacia mearnsii* spreading far from the original introduction locality (De Beer, 1986). It is not certain whether trees in the Cape descended from the original van der Plank progeny, as there are records of seed being received from Australia in Cape Town around the late 1800s and that it was already in the Cape Town Botanical Gardens by 1858 (Stirton, 1987).

Acacia mearnsii is cultivated in vast plantation for firewood, paper manufacturing, charcoal and parquet flooring industries. Its bark is used in the process of tanning leather (De Beer, 1986; Stirton, 1987). Apart from its commercial value, it could produce poles for fencing and house building, windbreaks and shade for stock. Furthermore, as a legume, it enriches the soil through fixing the atmospheric nitrogen (Scott and Le Maitre, 1998). Smith *et al.* (1992) identified *Acacia mearnsii* as potential useful species in mine site rehabilitation, because water use by trees on mining sites is viewed as a strategy for the reduction of acid rock drainage. *Acacia mearnsii* is among plant species declared as invaders and categorised as category two species, henceforth may only be grown in areas demarcated for that purpose, because they have the most impact on the water resources of South Africa (Gorgens and Van Wilgen, (2004). The effect of *Acacia mearnsii* plantations on water resources has been reported by researchers to certain extent. The following topics cover a detailed review of the body of literature from local and international sources to understand processes that govern vegetation and groundwater interactions: groundwater distribution and dynamics in hillslope, vegetation water uptake in hillslope, environmental tracers in groundwater provenance and groundwater recharge estimation methods.

3.2. Groundwater Distribution and Dynamics in Hillslope Catchments

3.2.1. Flow paths

Three major water flow pathways exist in a typical hillslope, namely; overland flow, subsurface lateral flow and bedrock flow (Ticehurst *et al.*, 2007). These flow paths are not mutually exclusive, as water tends to move between them. Some flow paths are only connected when hillslope is wet. Hillslope water flow paths are controlled by topography, soil characteristics, macro-pore network and parent material at the base of the soil (Mosley, 1982). Hydrological conditions are influenced by soil depth, pore size, organic matter distribution, tortuosity, surface and subsurface topography (Sidle *et al*., 2001).

3.2.1.1. Overland flow

Overland flow occurs either as infiltration excess or as saturation excess. The steep slope of the upper-slope generates a large volume of overland flow with significant erosive energy. In some areas, A1 and A2 horizons are eroded completely, leaving the B2 horizon exposed (Figure 3.1). Thinner A horizons usually indicate that the overland flow is dominant, in thicker soils, more infiltration can be expected due to the greater volume of water needed to saturate the soil. The assumption can be made that thicker soils support more vegetation and this causes a decrease in the overland flow proportion (Ticehurst *el al*., 2007). At the break of slope (between upper and waning slope), the change in gradient causes slower movement of water and therefore a decrease in the runoff (Figure 3.1). Generally, soils at the break of the slope are thicker, due to the deposition of alluvial material and organic matter, which enhance infiltration. On the lower-slope, runoff rate tend to be slow, because of smaller gradient. These soils are however, the wettest in the hillslope and saturated conditions reduce infiltration rate. Ticehurst *et al.* (2007) indicated that saturation excess is conducive to overland flow. Some of water moves as overland flow down the slope, but encounters an area where soil moisture deficit has not yet been satisfied, then infiltrates. This is called the run-on pathway and is often ignored in rainfall and runoff studies. The water available for infiltration then includes precipitation and water supplied from upper-slope (Nahar *et al*., 2004). The amount of overland flow is also greatly affected by the texture of the soil, specifically the percentage of clay and sand. Generally, sand is more permeable and has a greater hydraulic conductivity than clay and therefore infiltration excess induced overland flow seldom occur in sandy soils. In a study reported in Karnoven *et al*. (1999), the conductivity of sandy loam soils are 15 times higher than clayey soils. Return flow as overland flow at the foot and the toe-slope is related to a great amount of precipitation.

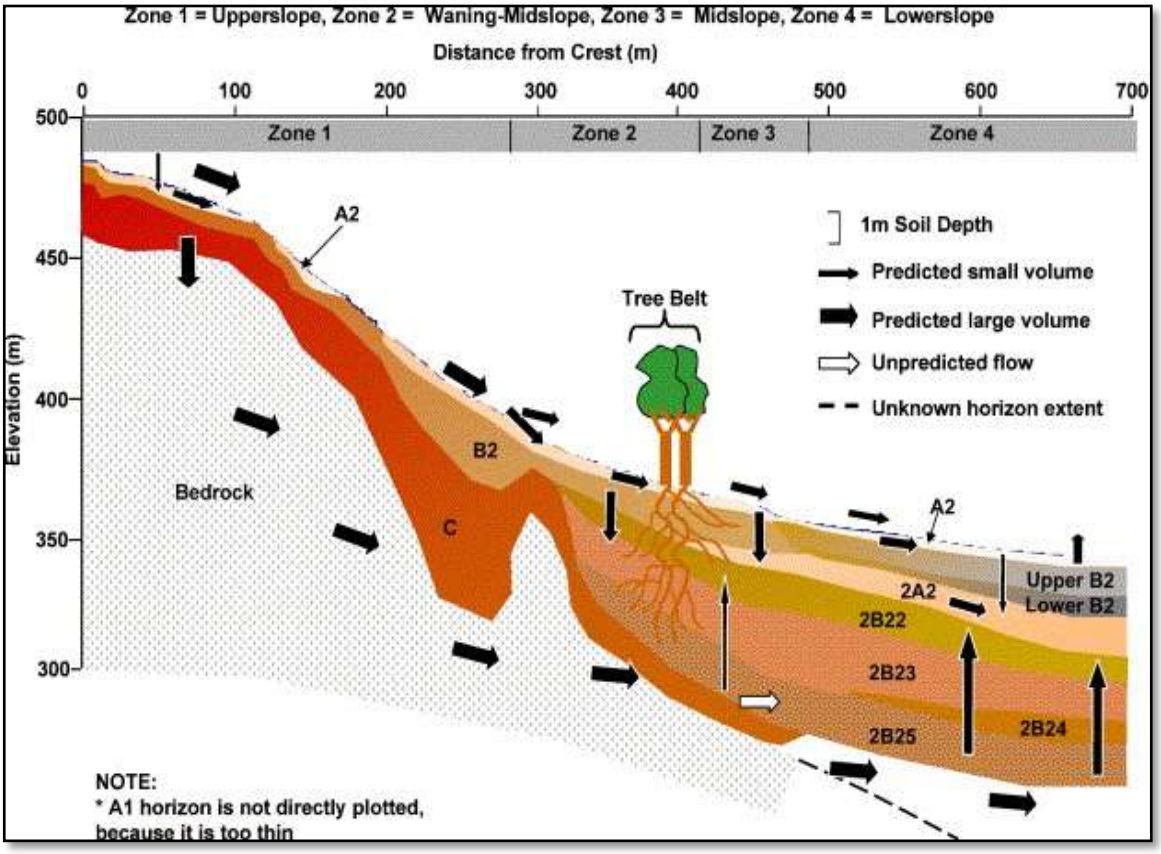

Figure 3.1. Flow paths on a hillslope in south eastern Australia (Ticehurst *et al*., 2007)

3.2.1.2. Subsurface lateral flow

Four major subsurface flow paths exist in a typical hillslope; (1) subsurface macro-pore flow, (2) subsurface lateral flow at A and B horizons interface, (3) return flow at foot-slope, toe-slope, and (4) flow at soil-bedrock interface, as described in a conceptual model of a hillslope (Figure 3.2), that elaborates the patterns of soil moisture distribution along the hillslope within a soil profile (Lin *et al*., 2006).

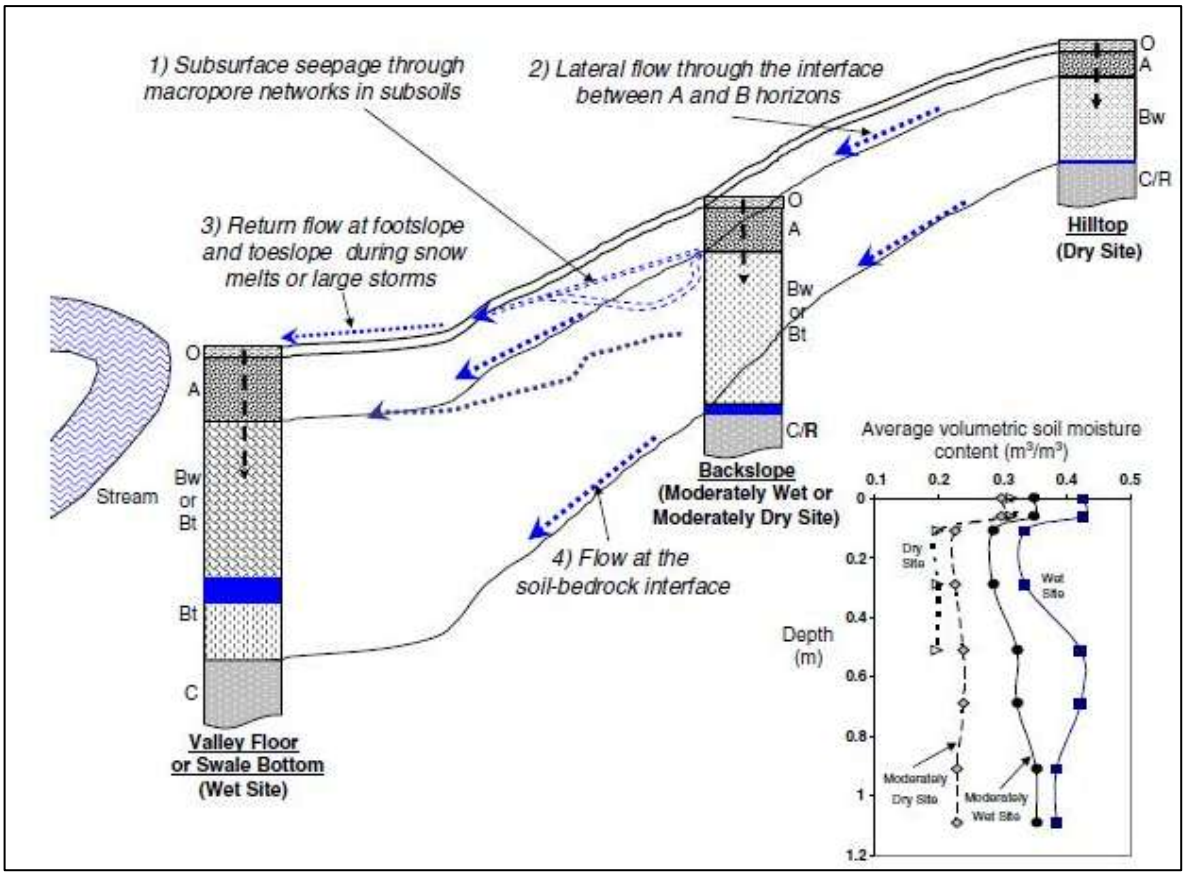

Figure 3.2. Flow pathways of a conceptual hillslope (Lin *et al*., 2006).

According to Lin *et al*. (2006), the movement of water through macro-pores conducts a considerable volume of water during large storms in forested catchments. Flow paths can exist in homogeneous soils due to unpredicted pathways caused by cracks, plant roots and biological activity (Figure 3.2). Cracks are usually present in soils with high 2:1 clay content (Lin *et al*., 2006). There are three factors that determine the contribution of subsurface macro-pore flow of water: (1) size of macro-pores, (2) accessibility, and (3) continuity of pores (van Tol *et al*.,, 2008). The continuity of pores increases with increasing soil moisture content (Nieber *et al*., 2006). Soil pipes are usually flow pathways parallel with the slope and are formed by soil fauna (moles and mice) and dead root channels. They contribute a significant amount of subsurface water to stream flow and are usually quick to respond to rainfall. The second pathway is the lateral flow at the interface between A and B horizons. This flow occurs due to differences in structures, densities and hydraulic conductivities of the horizons. The smallest hydraulic conductivity measured by Ticehurst *et al*. (2007) was 43 mm/h for the A2 horizon and 1 mm/h for the B horizon. The vertical flow would then be delayed and water would tend to move laterally in the more permeable A2 horizon. The flow path is important in conditions of saturation of the B horizon and thus becomes more significant in the waning mid-slopes.

The third pathway in hillslope catchment is the return flow at the foot-slope or toe-slope, where the stream channel is located. This flow pathway is seasonal, but once activated it may contribute considerable volume of water to the stream (van Tol *et al.*, 2008). The low gradient of the lower slope would limit this lateral flow and cause water logging and overland flow due to excess saturation. The fourth pathway is the flow at the interface between the bottom of the soil profile and underlying weathered and fractured parent material, largely in areas with shallow depth to bedrock. The continuous flow after a storm event with little moisture in the top of the profile suggests that the water moves vertically in the upper slopes and then laterally at or near the soil-bedrock interface (Lin *et al.*, 2006). Permeability, depth and differentiation between horizons would affect the amount of water moving through this flow path.

3.2.1.3. Bedrock flow

The study conducted by Ticehurst *et al*. (2007) reported that soils in the upper slope are important intake for water that supplies bedrock flow path. The general movement of water in this region is vertical except near the shoulder. Most water moves through the B2 horizon into C horizon on the upper slope, and is likely to move laterally on top of and through the saprolite and over solid bedrock. The water that does not move on top of bedrock moves through cracks in the bedrock or on solid bedrock within the saprolite (Figure 3.2). On the mid-slope the depth of this flow path is about six metres. The bedrock flow accumulates in the waning slope, thus causing a periodic water table. In the lower slope, the accumulating water table causes the saturation of the B horizon (Wilding *et al*., 1983; Fanning and Fanning, 1989 and Ticehurst *et al*., 2007). Bedrock flow is extremely important for the recharge of the lower slope and groundwater.

3.3. Groundwater Storage and Distribution

Water below surface occurs in two zones; an upper unsaturated zone and deeper saturated zone. In the unsaturated zone, most of open spaces are filled with air, but water occurs as soil moisture and in a capillary fringe that extends upward from the water table (Parsons, 2004). Soils and rocks serve either as confining units or aquifers. A confining unit is characterized by low permeability that does not readily permit water to pass through it. An aquifer has sufficient permeability to permit water to flow through it with relative ease. Water occurs in aquifers under two conditions, unconfined and confined conditions (Figure 3.3). An unconfined aquifer has a free water surface that rises and falls in response to differences in recharge and discharge.

A confined aquifer is overlain and underlain by aquicludes and water is under sufficient pressure to rise above the base of the confining bed or top of the aquifer. In some cases, water is under sufficient pressure to rise above land surface, such as in the case of artesian wells (Hiscock, 2005). An unconfined aquifer is usually recharged directly from the surface, while a confined aquifer is recharged via zones of aquifer outcrop (Freeze and Cherry, 1979; Hiscock, 2005; Pinder and Celia, 2006) and leakage through aquitards.

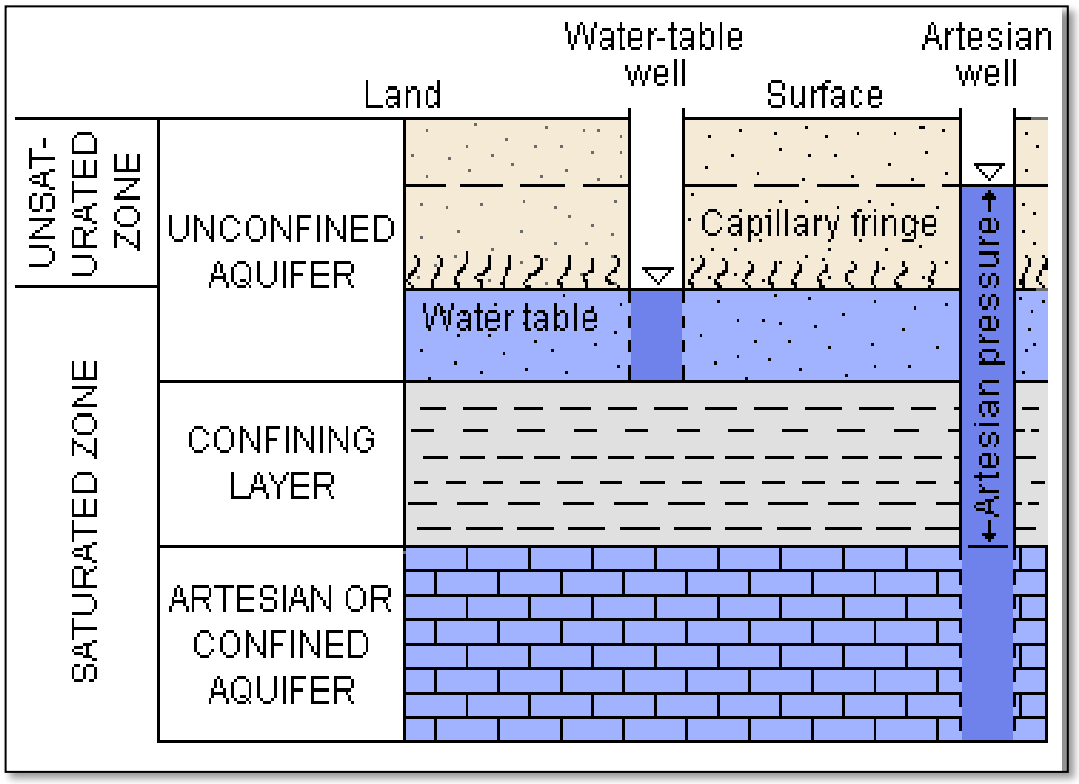

Figure 3.3. Unconfined and confined aquifers systems (Groundwater primer, 1997)

In the saturated zone, the movement of water is lateral under the influence of gravity rather than vertical as in the unsaturated zone. As long as groundwater is being recharged, it also discharges to the surface, either as springs, seepage or through evapotranspiration aided by capillarity (Vegter, 1995). Although earlier literature suggests that regional water table is the only contributor to baseflow, Lorentz *et al*. (2007) reported that the regional water table in a research catchment is very deep and therefore may not be a contributor to baseflow. Two water table systems exist; regional and perched water tables. The regional water table lies at greater depth under hills than it does under valley (van Tol *et al.*, 2008). A perched water table occurs above the regional water table in the unsaturated zone. Two basic types of perched water tables can be recognized: perched under solum (on rock) or perennial groundwater and perched within solum (on clay) or transient groundwater (Le Roux *et al*., 1999). Perennial groundwater is defined as the saturated area on top of bedrock and is usually associated with G horizons.

This water table shows a close correlation with topography. The presence of this water table can be attributed to the accumulation of enormous amount of water moving through the bedrock flow path. Transient groundwater occurs due to a clay layer within the solum with restricted permeability and usually associated with E horizons (Le Roux *et al*., 1999; Ticehurst *et al*., 2007).

3.4. Residence Time of Water

Residence time implies the rate at which a parcel of water remains in a component of the hydrological system. In hillslope hydrology, it is the time taken by the parcel of water to reach the stream (van Tol *et al.*, 2008). A distinction is made between residence time and transit time, where residence time implies time spent within the reservoir and transit time is the time it takes to exit a flow system (McGuire and McDonnell, 2006). Residence time reveals information on dominant flow paths, storage and sources of water. Since most chemical and biochemical reactions are time related, residence time of water will significantly influence the quality of water. Although the impact of soil properties may be averaged out in larger catchments, Schulze (1995) reported that the most important parameter controlling hillslope hydrological behaviour is the soil. Soil depth has a greater influence on residence time than the length of the upslope contribution area. Soil porosity, infiltration capacity, infiltration rate, clay content and soil moisture content all have an influence on the residence time.

3.5. Water Use by Tree Plantations

The effect of vegetation changes on water yield has been investigated in all parts of the world at a catchment scale (Bosch and Hewlett, 1982). In South Africa, research has focused on regions where forestry research stations were established and several long term experiments were laid out and monitored since 1940 (Le Maitre *et al*., 1996). The results from these stations have been used to model water use of vegetation and have established relationships between cover, biomass and their resultant effect on streamflow reduction (Le Maitre *et al*., 1996; Scott and Smith, 1997; Scott *et al*., 1998). There have been a number of models published and/or previous models reviewed of which most notable is a preliminary assessment of alien invading plants and water resources in South Africa (Versveld *et al*., 1998). Versveld *et al*. (1998) reported that the total water use of alien invaders in South Africa over a condensed area of 1.7 million hectares is estimated to be 3300 million m^3 per year. *Acacia mearnsii* is reported as one

of the worst invaders in South Africa and covers a condensed area of 131 341 hectares. This amounts to an estimated 576.58 million m^3 water used for alien plant invaders in South Africa (Versveld *et al*., 1998). Smith *et al.* (1992) estimated the average water use for an *Acacia mearnsii* tree (diameter 9.2 cm) at approximately 30 l/day, whereas Poulter *et al*. (1994) used two *Acacia mearnsii* (diameter 14.7 cm and 17.2 cm) in their comparisons and found an average water use of 20 l/day. It is standard practice for plantation managers to avoid planting trees in the riparian zone to avoid the risk of soil erosion close to the channel, and to minimise water use of plants in these areas (Scott and Lesch, 1995, 1996; Van Der Zel, 1987). Trees growing in the riparian zone have direct access to water that feeds streams and are able to transpire freely and meet evapotranspirative demands. Whereas, trees further away from streams are limited by soil water availability (Le Maitre *et al*., 1996). Various researchers (Le Maitre *et al*., 1996; Scott and Lesch, 1995, 1996) reported that trees growing in the riparian zone use proportionately more water.

3.6. Vegetation Water Uptake in Hillslope Catchments

Water used by land plants is absorbed from the soil by roots. The primary factor affecting the pattern of water extraction by plants from the soil is rooting depth (Nuberg *et al*., 2009). Forests are thought to play an important role in groundwater dynamics, through their capacity to extract water from permanent and deep groundwater table to the atmosphere even during the dry season. Water absorbed and transported through plants is moved by negative pressure generated by the evaporation of water from the leaves, through a process commonly known as Cohesion-Tension (C-T) mechanism. Figure 3.4 illustrates the representation of water transport pathways along the soil-plant-atmosphere continuum (SPAC), where tension is generated by the evaporation of water molecules during leaf transpiration and transmitted down the continuous cohesive water columns through the xylem and out of the roots to the soil.

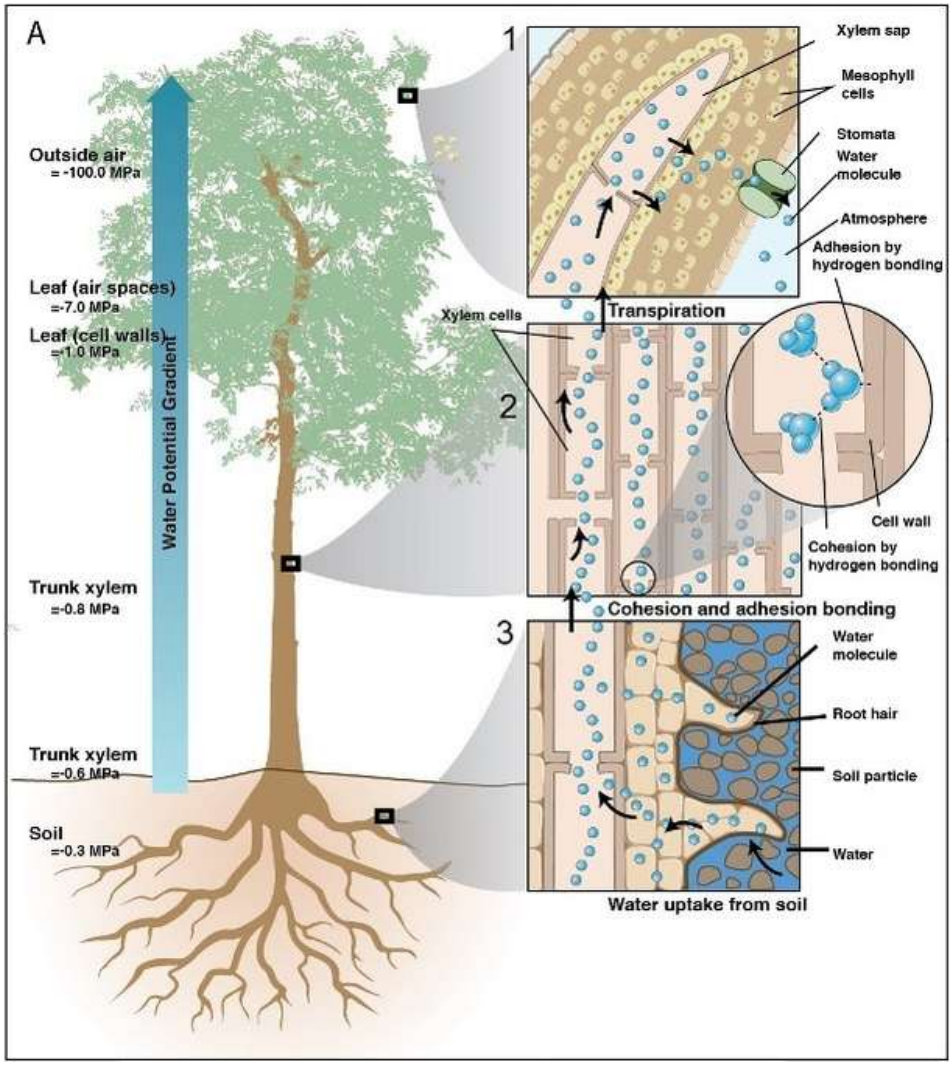

Figure 3.4. Representation of water transport pathways along the Soil-Plant-Atmosphere Continuum (modified from McElrone *et. al*., 2013).

The hillslope organises itself into three distinct regions; an uphill recharge and downhill discharge zones separated by midline zone on which there is on average, no recharge or discharge (Famiglietti *et al*., 1998). The variability in soil water dynamics can be attributed to several factors including meteorological factors, total water content, water table depth, soil properties, vegetation composition and topography. All these factors and their interaction with one another influence water movement and uptake through the hillslope on temporal and spatial scale (Famiglietti *et al*., 1998). Figure 3.5 illustrates the overview of water movement and uptake in a typical hillslope catchment.

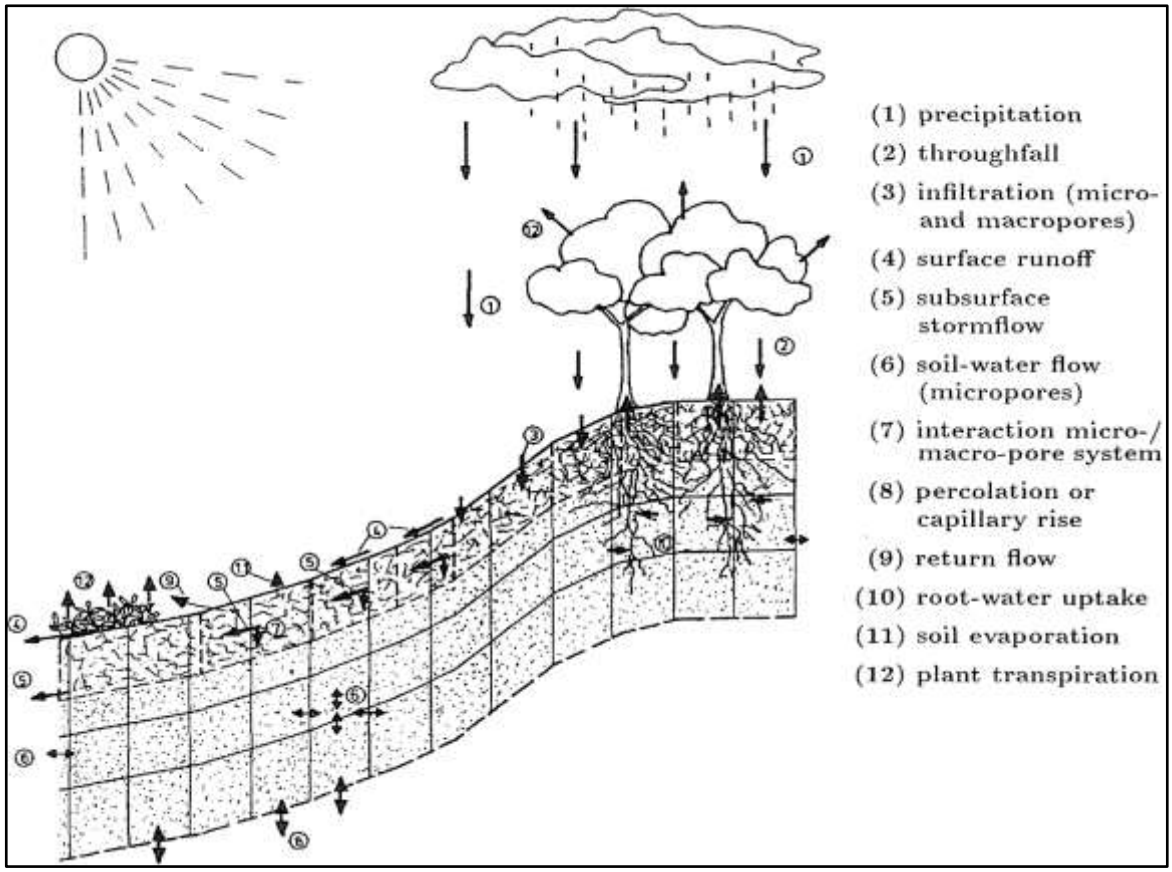

Figure 3.5. Overview of the hydrological system, water movement and uptake in hillslope (Modified from Bronstert and Plate, 1998).

3.6.1. Root depth of *Acacia mearnsii* trees

The depths of tree root systems are highly variable, in many cases roots extend much deeper than shallow, agriculturally defined soil profile. The studies of root systems in plants show that roots will penetrate as deep into the soil as required to reach the available water. However, penetration will be restricted by soil or regolith characteristics that prevent rooting or by permanent water table (Cannon, 1949; Stone and Kalisz, 1991; Nepstad *et al*., 1994; Stone and Comerford, 1994). *Acacia mearnsii* rooting development is rapidly being able to reach 0.2 m before the tree has developed any leaves. The main tap root of the tree often does not reach more than a metre in depth with the lateral roots continuing to grow down vertically until they encounter physical constraints such as water tables or bedrock, and only slowdown in the rate of growth when there is competition for space or the physical properties of the soils prohibit the growth. The *Acacia mearnsii* roots can reach depths of 3-35 m and even greater than 53 m was observed in one recorded case (Scott and Le Maitre, 1998). Depending on soil characteristics, the lateral rooting systems of the tree can often exceed the equivalent height of the tree in order to maximise water uptake (Sherry, 1971).

3.6.2. Water uptake in the unsaturated zone

Vegetation plays a key role in the interactions between surface and groundwater systems, because of its direct and indirect influence on recharge. Root systems may affect groundwater by decreasing recharge through extracting water from the unsaturated zone and creating an additional storage capacity in the unsaturated zone to later transpire without there being a direct abstraction from groundwater (Le Maitre *et al*., 1999). In South Africa, the impacts of forests are thought to be predominantly due to increased transpiration rather than increased interception losses (Scott and Lesch, 1997). The study conducted by Clulow *et al.* (2011) indicated that *Acacia mearnsii* plantations were using more water than is available from rainfall. Another study of *Acacia mearnsii* trees by Kok (1976) found that groundwater recharge was reduced from the expected 10% of annual rainfall under grassland to nil at 5 to 8 years after planting, presumably because of increased transpiration rates. In another study by Dye and Poulter (1995) in Mpumalanga, eucalyptus trees were denied rainfall by means of plastic sheeting over the ground. Trees showed little stress relative to the control trees outside the covered area. Although the trees were clear felled at an age of 16 years, streamflow did not return to normal until further five years later (Scott and Lesch, 1997). These results imply that, where there is deep soil, deeply fractured or decomposed rock, vigorous woody plantations can have a large impact on groundwater without necessarily having access to the groundwater.

3.6.3. Water uptake in the saturated zone

The capillary zone is defined as the saturated band above the water table where water is held by capillary forces against gravity. The thickness of the capillary zone is determined by soil texture and other characteristics. Very small pores in clay soils may support the capillary fringe of up to 1.5 m. In coarse material, the capillarity is reduced such that the saturated zone in medium textured sands would be around 0.4 m (Brunel *et al*., 1995). Above the capillary zone, the unsaturated upward movement of water is driven by matrix suction up to the point where it is equal to the gravitational forces (approximate maximum of 3 m above the water table in clay soils). Above this, water movement would need to be in the form of vapour diffusion. This flux would be small because of large resistances to vapour movement. Hence, where water tables are below 3 m deep, upward water fluxes driven by evaporation would be minimal. Except where water tables are shallow, the primary loss of groundwater would have to be through root extractions or groundwater discharge (Scott and Le Maitre, 1998). The water extraction by plants is driven by very low water potentials in the atmosphere around the plant canopy.

However, the extraction of water by roots is not practically constrained by atmospheric demand, but rather by the nature of the plant, physical obstructions in the soil, e.g. impenetrable layers, and the costs to the plant of rooting to great depths given that deep penetration is possible (Scott and Le Maitre, 1998).

3.7. Environmental Tracers in Groundwater Provenance

3.7.1. Environmental isotopes tracers

Environmental isotope tracers have been amongst the most powerful tools employed to understand sources of mixing water in surface and groundwater systems (Clark and Fritz, 1997). The stable isotopic composition of water is modified by meteoric processes, and so the recharge water in a particular environment will have a characteristic isotope signature. This signature then serves as a natural tracer for the provenance of groundwater. Stable isotopes commonly used in the field of hydrogeology include ^{1}H, ^{2}H, ^{18}O, and ^{16}O. Hydrogen occurs in nature as a mixture of isotope ^{1}H (Proteum) and ^{2}H (Deuterium), while oxygen is found as isotopes of atomic masses ^{18}O, ^{17}O, and ^{16}O. The ratios of the least abundant isotope to the most abundant differ with locations and water bodies. For example, ocean water contains two ^{18}O atoms for every thousand ^{16}O atoms, whereas the situation is different in freshwater (Singh and Kumar, 2005).

Due to different masses, stable isotopes behave slightly differently during physical, chemical and biological processes. During evaporation and condensation, the stable isotopes of $^{1}H/^{2}H$ and $^{18}O/^{16}O$ become fractionated (Singh and Kumar, 2005). The resulting small variations in isotopic concentrations may yield information on the climate at the point of infiltration or the origin of the water. The concentration of stable isotopes is normally given as the ratio of the least abundant isotope over the most abundant isotope and expressed relative to a known standard in the delta notation (Equation 3.1). In the case of water, the international standard used is the Vienna Standard Mean Ocean Water (VSMOW). The isotopic abundances and changes in these abundances are generally small, and denoted using δ notation, which expresses the deviation of the isotopic ratio in a sample with respect to the ratio in the standard.

$$\delta_{sample} = \frac{(R_{sample} - R_{standard})}{R_{sample}} \text{ X } 1000 \qquad (3.1)$$

Where,

δ - Value expresses the abundance of isotope in a sample,

R- Denotes the isotope ratio of the heavier to the lighter isotope (i.e., $^{18}O/^{16}O$) in the sample (R_{SAMPLE}) or the standard ($R_{STANDARD}$), respectively. The result is multiplied by the factor 1000 and expressed in per mil (‰), due to the small amount detected (Singh and Kumar, 2005).

3.7.1.1. Application of stable environmental isotopes

Stable environmental isotopes tend to behave differently when exposed to different chemical, biological and physical environments due to their differing mass numbers. In this regard, changes in ^{18}O and ^{2}H concentrations along groundwater flow path is an effective tool to determine the altitude of groundwater recharge, estimations of mixing proportions of different component flows and the relationships between surface and groundwater (Gat, 1996). When water is in an open water body such as a dam or lake, lighter isotopes (^{16}O) would be evaporated easily into vapour phase, while heavier isotopes would likely remain in the liquid phase. The opposite occurs during condensation, heavier isotopes (^{18}O) would condense with ease into liquid phase. The basic principle is that the enrichment of lighter isotopes ^{16}O occurs in vapour during evaporation, as opposed to the loss of the heavy isotopes ^{18}O from the vapour first during condensation. This is a natural distillation or fractionation process which continues with the rainfall. Therefore, precipitation in a certain area would have a distinctive stable isotope concentration (Leketa, 2011). As a result of evaporation and condensation processes, a plot of isotopes $\delta^{18}O$ versus $\delta^{2}H$ provides a straight line for the meteoric water known as the Global Meteoric Water Line (GMWL).

Most rain water will plot close or parallel to this line. After the alteration of the isotopic concentrations in the atmosphere during evaporation and condensation, the isotopic pair $\delta^{2}H$ and $\delta^{18}O$ will plot to the right of the meteoric water line and make an evaporation line of a lesser slope (s) and lowered than the GMWL. Vapour masses moving inland are subject to equilibrium isotopic exchange processes with the continued depletion in heavy isotopes in vapour travelling inland as a result of rainout. Condensation readily washes out heavy isotopes than lighter isotopes, so as clouds move inland, the heavy isotopes remain closer to the coast while the lighter ones are carried more inland. As a result of this, the stable isotopic content of meteoric water lies on a GMW regression line represented by Equation 3.2.

$$\delta^{2}H = s*\delta^{18}O + d \qquad (3.2)$$

The GMWL is characteristic of a line with s = 8 and d = +10. The slope is controlled by the rainfall and seasonal variations in precipitation, while the ^{2}H-excess (d) is controlled by the deuterium in the vapour source region. Generally, the isotopic concentration in groundwater becomes fixed from the surface because of the end to atmospheric effects such as evaporation and condensation. Evaporation losses from groundwater generally occur under isotopic equilibrium. This causes the isotopic concentrations of groundwater to be closely equivalent to the isotopic concentration state of the water just before infiltration. As a result of this, it becomes possible to identify groundwater that has recharged from precipitation and groundwater that has recharged from a surface water body on condition that sufficient evaporation took place in that water body. Water that has recharged from precipitation would have a high concentration of the lighter isotopes, hence the low concentration of the heavier isotopes that plot on the GMWL. On the other hand, water that has recharged from the water body would have a high concentration of the heavier isotopes and shall therefore plot on the evaporation water line (Leketa, 2011).

3.7.2. Isotopic variations in waters recharging aquifers

3.7.2.1. Isotopic composition of precipitation

Precipitation is formed by condensation of atmospheric vapour derived from the evaporation of water and land surfaces. The water vapour of the atmosphere is depleted in heavy stable isotopes because of their lower vapour pressure (Fette, 2005). Isotopic fractionation takes place during evaporation and condensation of water. The extent of condensation is determined by the decrease of temperature, which thus becomes the main factor controlling stable isotope composition of precipitation (Kendall and McDonnell, 1998). The isotopic composition of raindrops is primarily determined by equilibrium fractionation processes, which occurs when there is a depletion or enrichment of heavier isotopes as the liquid content in the clouds increases or dissipates (Gat, 2010). The temperature and isotopic composition of the condensing parent vapour are the major factors that control stable isotope composition of precipitation at any given location. The temperature of condensation and physical state of the condensate determines the isotopic partitioning during condensation (Kendall and McDonnell, 1998). The isotopic composition of precipitation exhibits the following variations in the concentration of heavy isotope: temperature effect, evaporation effect, amount effect, altitude effect and continental effect.

3.7.2.2. Isotopic composition of surface waters

The isotopic composition of river water reflects that of precipitation over catchment basin. The head water of most rivers and streams would reflect the isotope composition of local precipitation, however, all sources would control the isotope contents downstream. If the basin largely consists of mountains, where rains are often more abundant, river water would be depleted in heavy isotopes, as a consequence of the altitude effect. In this case, groundwater would be depleted as well with respect to local precipitation. Other isotopic variations in rivers are caused by heavy rains after a relatively dry period. In this case, different isotopic and chemical compositions of rain and groundwater allow direct contribution of rainwater to river discharge to be distinguished from that of groundwater (Kendall and McDonnell, 1998). According to Singh and Kumar (2005), surface water bodies like lakes lose water by evaporation and therefore are characterized by enrichment of heavy isotope species of Deuterium and ^{18}O. The isotope enrichment follows a characteristic evaporation line from the meteoric line.

3.7.2.3. Isotopic composition in the unsaturated zone

The infiltration of precipitation through the unsaturated zone is an isotopically non-fractionating process. However, there are processes that have an indirect effect on the isotopic composition of the infiltrating water (Gat and Tzur, 1967). Only rain falling above a certain threshold rate contributes to recharge. The threshold value depends on the climatic conditions and vegetation type. For instance, rains over bare karst terrains will seep easily and rapidly through joints and fissures. The same applies for rains over surfaces covered by gravel and coarse sand. In these cases minor change in isotopic composition of precipitation can be expected. On the other hand, a significant proportion of rain falling on vegetative catchments is intercepted by plants and re-evaporated. The throughfall that reaches land surface will infiltrate slowly in small proportions, with most of it removed by evapotranspiration. Thus, certain enrichment in heavy isotope of infiltrating water may occur due to evaporation (Kendall and McDonnell, 1998). The maximum enrichment at the drying front creates a concentration gradient along the soil column. The accumulation of $H_2{}^{18}O$ and ^{2}HHO begin to move downward by aqueous diffusion, giving a characteristic exponential profile as shown in Figure 3.6. The shape of the profile is controlled by the relative rates of isotope diffusion downward and the capillary flow of water upward. The trend to low $\delta^{18}O$ near the top of the profile is due to exchange between the evaporated-depleted vapour and residual pore water above the zone of

liquid flow (Clark and Fritz, 1997). Figure 3.6 shows the profile of ^{2}H in soil column undergoing evaporation, the depth of maximum enrichment marks the boundary between a lower zone of liquid flow and an upper zone of vapour movement by diffusion to the surface.

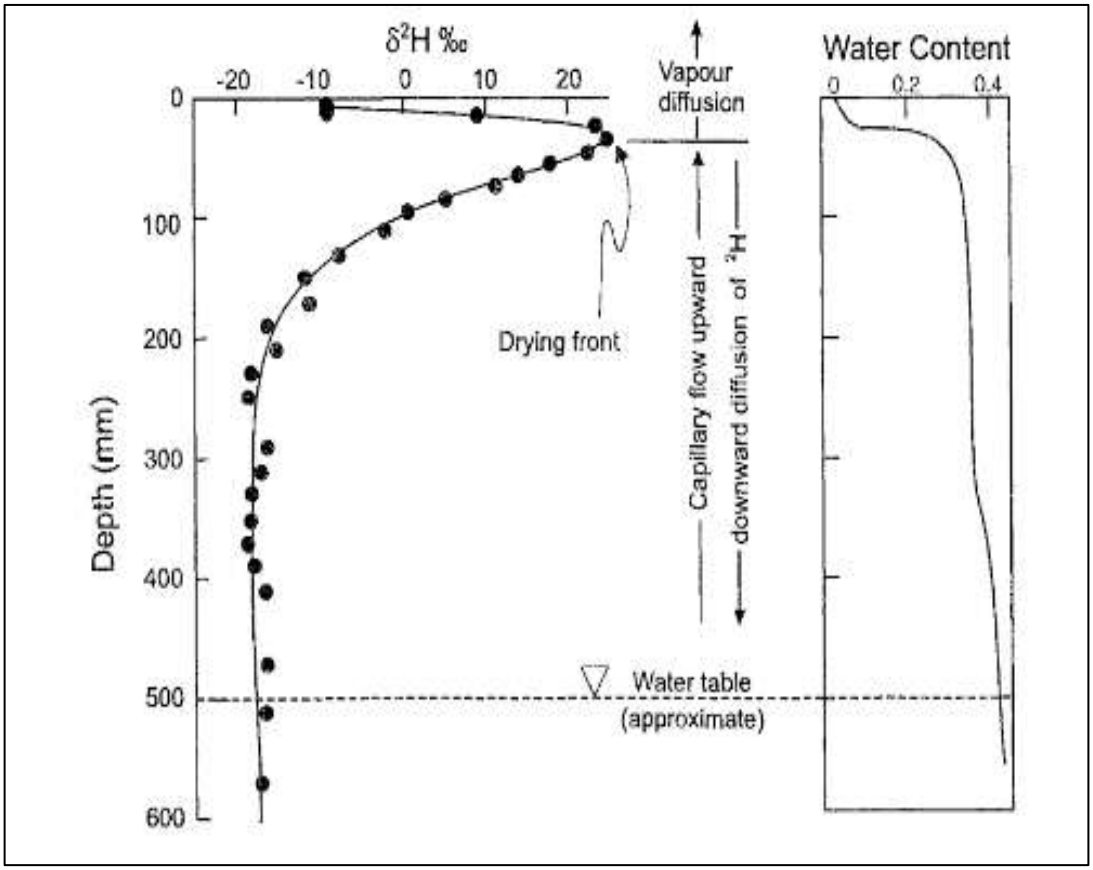

Figure 3.6. Profile of ^{2}H in soil column undergoing evaporation (modified from Allison *et. al*., 1984).

3.7.2.4. Isotopic composition of groundwater

The origin of groundwater can be characterized using stable isotopes with a reasonable degree of confidence, provided that it is not exposed to temperatures of above 60 ^{0}C to 80^{0}C. This is due to the conservative nature of the stable isotope composition of water in an aquifer. According to Singh and Kumar (2005), groundwater can be grouped into a number of categories based on their origin, namely: meteoric water, palaeowaters, geothermal and saline groundwater. In many cases, the isotopic composition of meteoric groundwater matches the mean composition of precipitation over the recharge area. Because of this property, shallow and locally derived groundwater is used to characterize the isotope content of meteoric water provided it is not subjected to high temperature (Singh and Kumar, 2005). The compositional fluctuations of individual rainfalls are smoothened out by transition of water through the

unsaturated zone. In arid conditions, an enrichment of heavy isotope species in groundwater is observed. This is due to evaporation process as there is delay of water near the surface before infiltration. Further infiltration of water and evaporation of soil water from uppermost soil layers also contribute to enrichment. The isotopic compositions of aquifers vary from place to place and also as a function of depth in unconfined conditions. Many of the sources of salinity, such as seawater or surface brines are associated with water of a characteristic isotopic composition. Fossil brines, formation waters and magmatic or geothermal fluids display a variety of isotopic compositions. Most of these waters also show distinctive chemical and trace-element composition, so that their admixture to fresh groundwater can be identified readily through combined chemical and isotopic analysis (Singh and Kumar, 2005). Formation water is encountered during drilling operation and found in association with various geological formations below aquifer systems. Most formation waters have been in contact with their formation for extended periods of time, mostly at elevated temperatures. As a result, both salinity and isotopic compositions are modified and in most cases approaching equilibrium with mineral phases that they contacted with (Singh and Kumar, 2005).

The loss of seasonal variations during infiltration through the unsaturated zone is a function of the physical characteristics of the unsaturated zone, length of flow-path and residence time. A critical depth can be defined where the isotope variations is less than the 2σ error of the ^{18}O analysis (Figure 3.7). In a fine-grained soil without fast flow-paths, the critical depth may be reached at 3 to 5 m (Clark and Fritz, 1997). The critical depth is often situated below the water table. In such aquifers, minor seasonal variations are preserved in shallow groundwater. These too are eventually lost due to advective dispersion during flow under confined conditions. In advection dominated systems with a single type of porosity, pistol-flow models may be used to determine the critical depth (Clark and Fritz, 1997). The isotope variability below the critical depth and/or along a single flow path in a confined aquifer, generally does not exceed the 2σ analytical precision. When it does, this signifies preferential pathways or mixing of different recharge waters. Generally, variations in confined aquifers are due to groundwater mixing (Clark and Fritz, 1997). Figure 3.7 shows the schematic of attenuation of seasonal isotope variations (^{18}O and ^{2}H) in recharge waters during infiltration through the unsaturated zone and movement within the saturated zone, and the critical depth below which variability is less than the analytical precision.

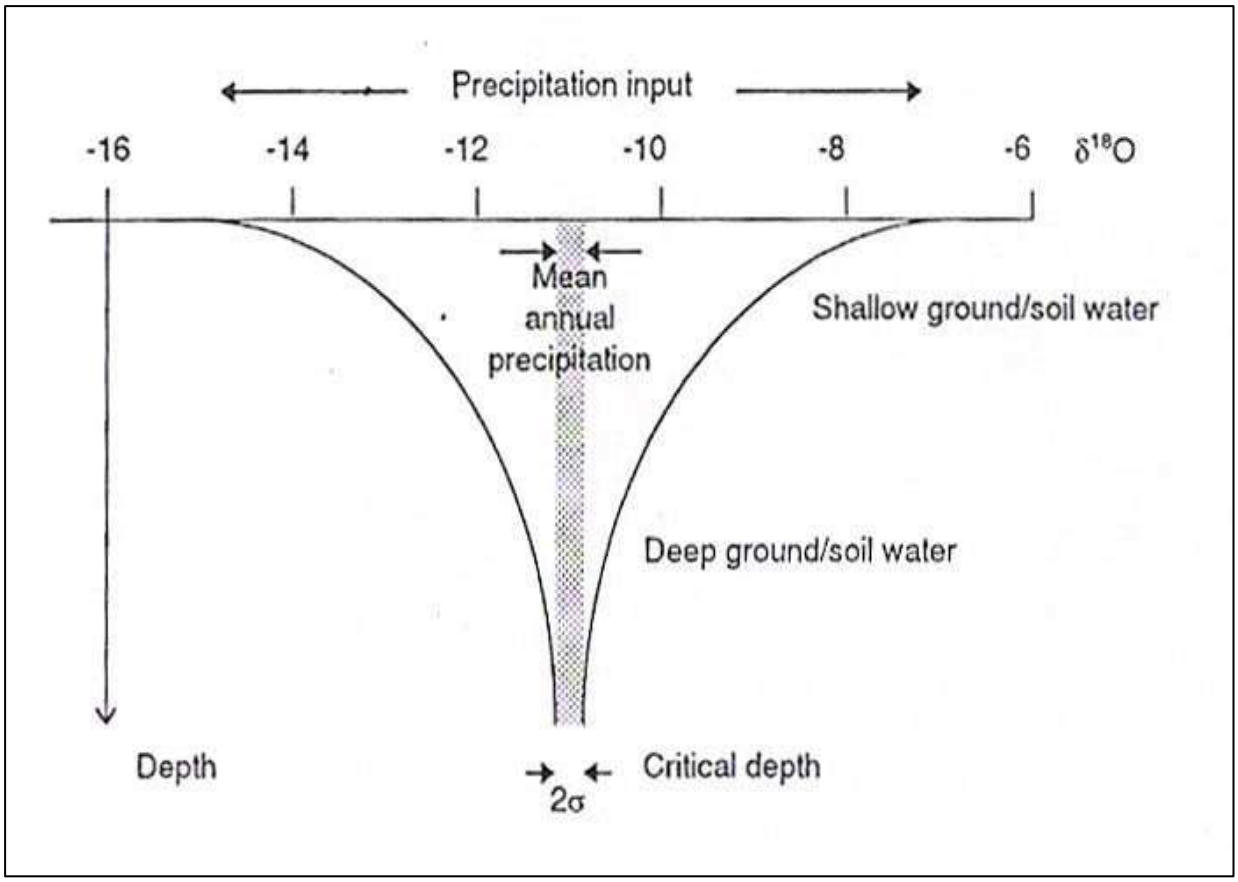

Figure 3.7. Schematic attenuation of seasonal isotope variations in recharge waters during infiltration through the unsaturated zone and movement within the saturated and the critical depth (Clark and Fritz, 1997).

3.7.3. Hydrochemical data analysis

Water quality analysis is one of the most important aspects in groundwater studies. The hydrochemical study reveals quality of water whether it is suitable for drinking, agriculture and industrial purposes. Furthermore, it is possible to understand the change in quality due to rock water interaction or any type of anthropogenic influence. Groundwater often consists of major ions such as Ca^{+2}, Mg^{+2}, Na^{+}, K^{+}, Cl^{-}, HCO_3^{-}, and SO_4^{-2}. These hydrochemical parameters of groundwater play a significant role in classifying and assessing water quality. Groundwater generally originates from precipitation that infiltrates through the soil and later occupies pore spaces and fractures of underlying geological materials. As rainwater infiltrates through soil and geological materials, its chemical composition is altered by the effects of a variety of soil and geochemical processes. Organic matter in the soil zone is decomposed by microbes, producing high concentrations of dissolved carbon dioxide (CO_2). Excess CO_2 in water produces carbonic acid (H_2CO_3), which causes the reduction of pH in soil water. The corrosive nature of carbonic acid causes a number of mineral-weathering reactions, which results in

bicarbonate ion (HCO_3^-) being the most abundant anion in water. The contact times between water and minerals in shallow groundwater paths are usually short and therefore dissolved solids concentrations become generally low. The chemical composition of deeper groundwater is usually different from surface and shallow groundwater, due to longer contact times and geochemical processes. The initial reactions that occur in the soil zone, giving rise to bicarbonate ions are replaced over time by chemical reactions between water and minerals. As weathering progresses, the relative abundance of major inorganic chemical species changes, the rate of change is dependent on the weathering process (Kelly *et al.*, 1998*)*. Therefore, by investigating the chemistry of groundwater in a catchment, a conceptual model of the geology in which water is stored in a catchment can be constructed.

3.7.3.1. Groundwater chemistry data presentation methods

Presentation of chemical analysis in graphical form makes understanding of complex groundwater system simpler and quicker. The most common approaches to describe the abundance or relative abundance of ions in individual water samples are Piper diagram, Stiff patterns diagram, Durov diagram and bar graphs.

Piper diagrams: Piper Diagrams are one of the most useful ways of representing and comparing water quality. The piper trilinear diagram presents the concentrations of K^+, Na^+, Ca^{2+} and Mg^{2+} expressed as % milliequivalent per liter (meq/l) plotted on the cation triangle. The relative abundance of Cl^-, SO_4^{2-} and HCO_3^{2-} are then plotted on the anion triangle. The two data points on the cation and anion triangle are then combined into the main diamond shaped field of Piper diagram that shows the overall chemical property as to how the water sample is defined. The water is then classified depending on the position of that point (Figure 3.8), which shows the projection of the cation and anion triangles onto a diamond shape of the Piper diagram. These tri-linear diagrams are useful in bringing out chemical relationships among groundwater samples in more definite terms rather than with other possible plotting methods. The Piper Diagram also conveniently reveals similarities and differences among groundwater samples. Those samples with similar qualities will tend to plot together as groups (Todd and Mays, 2005). Figure 3.8 shows the projection of the cation and anion triangles onto a diamond shape of a Piper diagram and the hydrochemical facies.

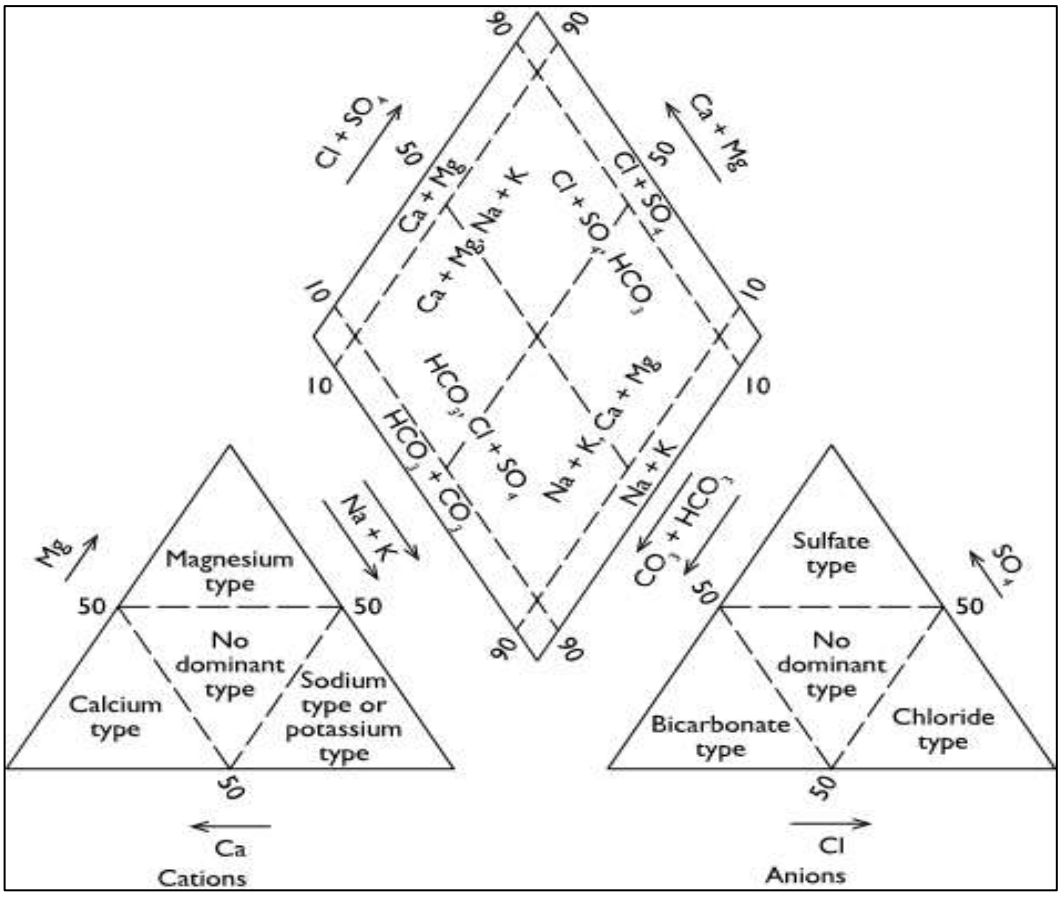

Figure 3.8. Piper diagram for describing hydro-chemical facies variation (Freeze and Cherry, 1979).

3.8. Hydraulic Characterisation of Aquifers

The methods of determining hydraulic characteristics of aquifers involve pumping tests and tracer tests. The determination of aquifer parameters through pumping tests has become a standard step in the evaluation of groundwater resource potential of an area (Freeze and Cherry, 1979).

3.8.1. Pumping tests

Pumping tests involve pumping out water from a borehole at a known rate and observing the resulting decline in water level (drawdown) in the aquifer in the vicinity of the well. Pumping tests can provide information on the type of flow that occurs within an aquifer system and they are the simplest means of characterizing aquifers in terms of their parameters, such as transmissivity (T), hydraulic conductivity (K), storativity (S) and specific yield (Sy) amongst others. Aquifer tests can be classified into slug tests, step-tests, constant discharge rate tests and recovery tests.

3.8.1.1. Slug tests

A slug test is an important tool in obtaining a cost effective quick estimate of the hydraulic properties of an aquifer. It involves disturbing the static water level in the borehole and monitoring the time it takes to recover back to initial water level. If the water table is shallow, the water level can be disturbed using a bailer or a bucket. A small volume of water is removed from the borehole after which the rise of the water level in the borehole is measured. Alternatively, a closed cylinder can be submerged to raise the water level and monitor the time it takes for the water level to lower back to the static water level. In some instances a small slug of water is poured into the borehole and the subsequent fall of the water level is measured (Kruseman and De Ridder, 1994). Aquifer transmissivity and hydraulic conductivity can be determined from the slug test measurements. If aquifer transmissivity is higher than 250 m^2/d, the recovery will be so quick that manual measurements cannot be used but rather automatic recording devices would be needed (Kruseman and De Rider, 1994). In South Africa, slug tests are conducted for the following reasons:

- To estimate the hydraulic conductivity (K) and Transmissivity (T) of the aquifer in the vicinity of the borehole (Van Tonder and Vermeulen, 2005).
- To obtain a first estimate of the yield of a borehole (Vivier *et al.*, 1995).

3.8.1.2. Constant discharge rate test pumping

In the constant discharge rate test, the borehole is pumped at a constant rate that is enough to cause drawdown in the borehole and not too much to cause drawdown to reach the pump inlet or main water strike (Kotze, 2001). The drawdown is monitored in the pumping boreholes as well as observation boreholes where applicable. The choice of how long the test should be conducted depends on the required precision in sustainable yield, capability as well as the intended use of the borehole. Most pumping tests in South Africa are conducted within 48 hours (Kotze, 2001). Despite the advantages of a slug test, the constant discharge test is a better method of analysing the physical properties of aquifers, because the influence goes beyond the immediate vicinity of the pumping borehole, hence a wider cone of depression may be caused. Van Tonder and Vermeulen (2005) reported that when estimating aquifer parameters that are to be used in numerical management models, constant discharge rate test is the most important aquifer test and it is set as the minimum requirement for aquifer parameter estimation.

3.8.1.3. Recovery tests

The evaluation of recovery data may be used to confirm the aquifer parameters determined from the main test. The recovery of the water level should be measured from the time the pump is switched off, at the same interval as during constant discharge test for a period equal to the duration of the main test or until the water level has fully recovered (Leketa, 2011).

3.8.2. Aquifer parameters

The characterization of aquifer parameters involves the determination of the aquifer behaviour defined by its transmissivity, hydraulic conductivity, storativity, Darcy velocity, groundwater flow direction, porosity and other physio-chemical characteristics.

Transmissivity: Transmissivity (T) is defined as the rate at which water is transmitted through a unit width of an aquifer under a unit hydraulic gradient (Hiscock, 2005). It therefore indicates the ease with which water moves through the subsurface and is given by the product of the hydraulic conductivity (K) and the thickness of the saturated aquifer (equation 3.3).

$$\mathbf{T = Kb} \qquad (3.3)$$

Where,

T- transmissivity in m^2/day,

H- hydraulic or aquifer conductivity in m/day;

b- thickness of the aquifer in meters.

Transmissivity can be obtained from the pumping test data, preferably from the constant discharge rate test. The first estimate of the T-value of the formation can be obtained by using the Logan equation (FC Program, Van Tonder *et al*., 2001), given by:

$$\mathbf{T = \frac{1.22Q}{s}} \qquad (3.4)$$

Where,

Q - abstraction rate in m^3/d,

s - drawdown at the end of the test (m).

A qualified guess method can also be used to find the value of T if the maximum yield of the borehole is known, using equation 3.5:

$$\mathbf{T = 10Q} \qquad (3.5)$$

Where,

Q - maximum yield in l/s,

Hydraulic conductivity: The groundwater dictionary defines hydraulic conductivity as the volume of water that would move through a porous medium in a unit time under a unit hydraulic gradient through a unit area. It depends on the size and arrangement of particles (in an unconsolidated formation), size and the character of crevices, fractures and solution openings in a consolidated formation as well as the viscosity of the fluid. The hydraulic conductivity may change with any of these parameters (Hiscock, 2005). Short time-budget slug tests are a cheaper way of determining the hydraulic conductivity of the aquifer in the vicinity of the borehole (van Tonder and Vermeulen, 2005). In mathematical models, aquifers are usually assumed to be homogeneous. In real situation, there is a lot of heterogeneity, hence the value of K obtained from a slug test is site specific and only valid for that borehole. The hydraulic conductivity of unconsolidated material can be obtained using infiltration tests. Table 3.1 shows the hydraulic conductivities of different geological materials.

Table 3.1. Hydraulic conductivities of various rock types and unconsolidated matter (Brassington, 2006).

Rock Type	**Grain size (mm)**	**Hydraulic Conductivity K (m/d)**
Loose unconsolidated matter		
Clay	$5x10^{-4}$- $2x10^{-3}$	10^{-8} - 10^{-2}
Silt	$2x10^{-3}$- $6x10^{-2}$	10^{-2} - 1
Fine Sand	$6x^{-2}$ - $25x^{-2}$	1-5
Medium Sand	0.25 - 0.50	5-20
Coarse Sand	0.50 - 2	20 - 100
Gravel	2 - 64	$1x10^{-2}$ - $1x10^{3}$
Sedimentary rocks		
Shale	small	$5x10^{-8}$ - $5x10^{-6}$
Sandstone	medium	10^{-3} - 1
Limestone	variable	10^{-5} - 1
Igneous rocks		
Basalt	small	$3x10^{-4}$ - 3
Granite	large	$3x10^{-4}$ - 0.03
Slate	small	10^{-8} - 10^{-5}
Schist	medium	10^{-7} - 10^{-4}

3.9. Groundwater Recharge

Groundwater recharge represent that portion of the rainfall which reaches the saturated zone, either by direct contact in the riparian zone or by downward percolation through the unsaturated zone (Bredenkamp *et al*., 1995). A measure of the rainfall that is available for recharge is provided by the mean annual effective rainfall. Adams *et al.* (2004) identified several factors that affect natural groundwater recharge. At the land surface, recharge is affected by the topography and land cover in addition to the magnitude, intensity duration and spatial distribution of precipitation. Steep terrain supports fast fluxes and therefore favours surface runoff in preference to infiltration. A similar effect is achieved by a rainfall event of high intensity and low duration in the absence of preferential flow pathways to the saturated zone. Lerner *et al*. (1990) defined three mechanisms for natural groundwater recharge; (1) direct recharge, (2) indirect recharge, and (3) localised recharge (Figure 3.11). Direct recharge refers to the replenishment of water to the aquifer from precipitation after subtracting interception, runoff and transpiration. Localised recharge results from ponding of surface water in the absence of well-defined channels of flow, whilst indirect recharge refers to percolation to the water table from surface watercourses. Each type of mechanism is more prevalent in some climatic condition than others (Lloyd, 1986).

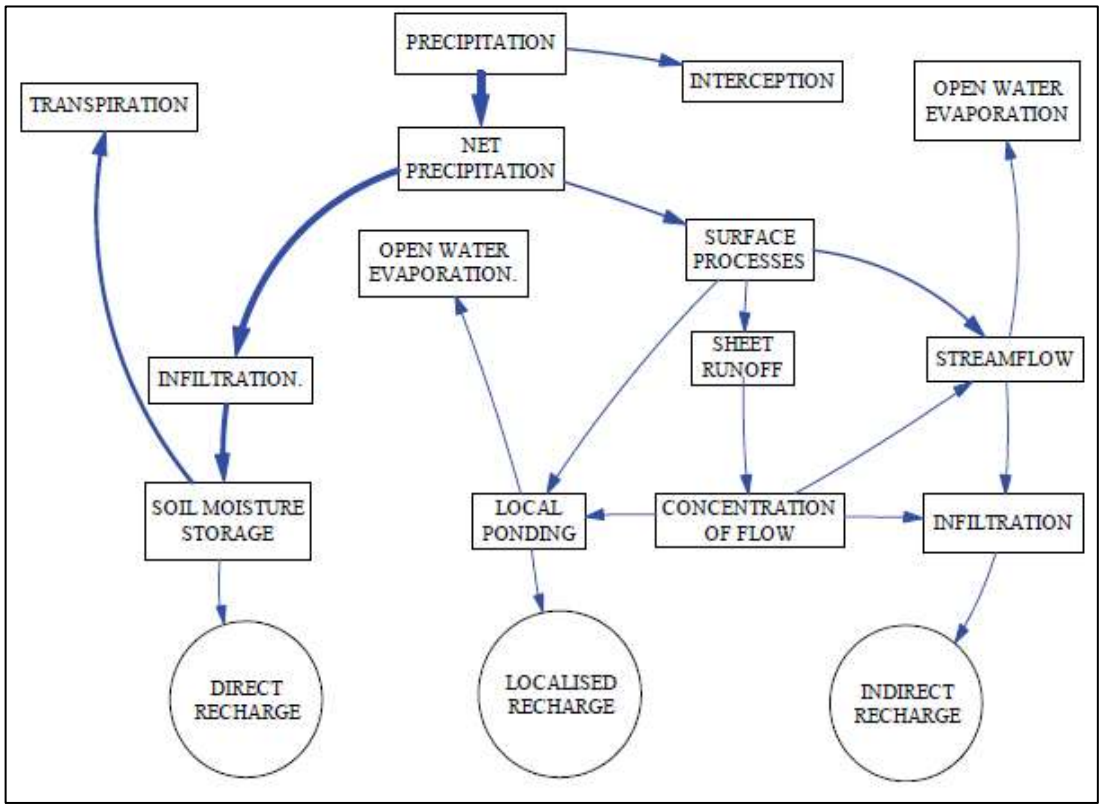

Figure 3.9. Various elements of recharge in a semi-arid area (Lloyd, 1986).

3.9.1. Groundwater recharge processes

Natural groundwater recharge can be defined as the downward movement of surface water, originating from precipitation to the groundwater storage irrespective of recharge mechanisms (Lerner *et al.* 1990). Natural groundwater recharge is considered as the primary method for aquifer replenishment (Bredenkamp *et al*. 1995). The spatial and temporal variability of recharge is dependent on several factors Lerner *et al*. (1990), which have been identified as climate, geology, topography and land cover. The spatial-temporal variability of precipitation is one of the major contributors to the spatial and temporal variability of groundwater recharge. The occurrence of precipitation alone is not enough to guarantee recharge, but rather recharge is dependent on the intensity, amount and duration of the precipitation. Topography is responsible for driving both surface water and groundwater, which is the case in unconfined aquifers where the water table is likely to follow the surface topography. Areas with steep topography are prone to facilitating mountain front recharge, but they can also promote runoff depending on geology, soil characteristics, slope angle, rainfall intensity and duration (Lloyd, 2010). In the case of runoff occurrence, it eventually reaches streams where indirect recharge can occur. Besides controlling the spatial distribution of recharge, topography can also dictate where and how much precipitation occurs known as the orographic effect.

Land cover is also an important factor that controls the spatial variability of groundwater recharge. In general, groundwater recharge tends to be lower in highly vegetated areas because precipitation is being intercepted by plants. Furthermore, evapotranspiration (ET) would be greater because of high transpiration whereby plant roots take up the available soil moisture thus decreasing precipitation that could have been potential recharge. The soil texture, thickness and the moisture content are important for groundwater recharge. Favourable conditions for recharge to occur are thin soils with a low clay content, high permeability and high soil moisture content. The type of geology would have an influence on the amount of recharge that occurs. The structural features, type of aquifer, aquifer materials and hydrogeological parameters of an aquifer would determine the extent to which recharge occurs. Fractured aquifers where flow is facilitated only by fractures and the weathered zone(s) would experience less recharge than karst aquifers where flow occurs through karst structures (Healy, 2010).

3.9.2. Groundwater recharges estimation methods

The quantification of the rate of groundwater recharge is vital for efficient groundwater resource management or sustainable management of groundwater sources (Bredenkamp *et al*., 1995). The prediction of sustainable yields of aquifers is dependent on the amount of water recharging the aquifers. Several methods have been developed over the last few decades to determine the groundwater recharge originating from direct, indirect and localised mechanisms. However, no two methods if applied to the same area will provide similar recharge rates (Xu and Beekman, (2003). Groundwater recharge estimation techniques are divided into physical techniques, tracer techniques and numerical models. The applicability of any recharge estimate depends on the availability and potential to obtain data, characteristics of the area and the cost of obtaining data. A summary of available groundwater estimation methods is provided in Appendix B.

3.9.3. Commonly used recharge estimation methods in Southern Africa

Groundwater recharge estimation studies in South Africa have been conducted using direct and indirect techniques and methodologies in the unsaturated and saturated zones. In the unsaturated zone recharge has been assessed using lysimeter studies, tritium profiling, soil moisture balance and chloride profiling techniques. Bredenkamp *et al*. (1995) noted that lysimeter results indicate an apparent annual threshold value of rainfall below which no recharge takes place. Tritium profiling yielded estimates that were generally less than those derived from water balance methods. The soil moisture balance method was found to be too dependent on the assumed equivalent soil moisture available to the vegetation (Bredenkamp *et al*., 1995). In general, recharge rates estimated through chloride profiling were found to correspond well with values obtained using other techniques (Bredenkamp *et al*., 1995). The saturated volume fluctuation (SVF) and cumulative rainfall departure (CRD) methods were used to estimate groundwater recharge in the saturated zone in South Africa. Hydrograph and spring flow analysis were used in areas where spring flow analysis and discharge data were available. Adams *et al.* (2004) applied the (SVF) method to estimate the groundwater recharge in dolomite aquifers, using recorded water level, rainfall, spring flow data and computer simulated groundwater level data. Recharge rates of between 10 – 14% of the average annual rainfall were estimated. Such values agreed closely with those obtained from the chloride profile approach. Bredenkamp *et al*. (1995) and Xu and Beekman (2003) identified chloride mass balance (CMB), cumulative rainfall departures (CRD), saturated volume fluctuations

(SVF), watertable fluctuations (WTF), groundwater models (GM) and EARTH model as the most promising recharge estimation methods for application in semi-arid Southern Africa conditions. The applicability of any recharge estimation method depends on the availability of data, potential to obtain data, characteristics of the area and the cost of obtaining data. Given that there is no single method that would produce good estimates of recharge in all cases, the chloride mass balance (CMB), cumulative rainfall departure (CRD) and saturated volume flux (SVF) methods were identified to be relevant for application in the present study. The description of each method is provided in the next section.

3.9.3.1. Chloride mass balance (CMB) method

The chloride mass balance (CMB) method is often used as a first approximation of recharge due to its simplicity and relatively low cost (Kotze, 2001). The method was first applied in the saturated zone by Eriksson and Khunakasem (1969) and has become one of the most widely used recharge estimation methods. The method makes use of the relationship between chloride concentrations in rainfall and in groundwater. It assumes that the increase of chloride concentrations has resulted from evapotranspiration losses and that no additional chloride has been added by contamination, leaching of rocks or from the overburden (Woodford and Chevallier, 2002). Chloride has the advantage over other tracers involving the water molecule (^{18}O, ^{2}H, ^{3}H) in that atmospheric inputs are conserved during the recharge process, allowing a mass balance approach to be used (Edmunds and Gaye, 1994). The CMB method is applicable in areas of high evapotranspiration where the infiltrating water becomes concentrated (Johansson, 1987). The CMB method entails determining recharge coefficient from the ratio of average chloride in rainfall to that of chloride concentration in groundwater. This relationship can be represented by equation 3.6 as defined by Adams *et al*. (2004).

$$\boldsymbol{Re = Rf x \frac{Clrf}{Clgw}} \qquad (3.6)$$

Where,
Re - average annual recharge (mm),

Rf - average annual rainfall (mm)

Cl_{rf} - chloride concentration in rainfall (mg/l)

Cl_{gw} - chloride concentration in groundwater (mg/l)

3.9.3.2. Cumulative rainfall departure (CRD) method

The CRD method is based on the premise that water level fluctuations are caused by rainfall events (Xu and Beekman, 2003). Wentzel (1936) demonstrated that the cumulative rainfall departure (CRD) series correspond to fluctuations of the groundwater level. According to Bredenkamp *et al*. (1995), the CRD method conforms to the concept that equilibrium conditions develop in an aquifer over time until the average rate of losses equal the average recharge of the system. The rationale behind the departure method is that in any area, despite large annual variations in precipitation, equilibrium is established between the average annual precipitation and the hydrological response (Bredenkamp *et al*., 1995). The CRD method was revised by Van Tonder and Xu (2000) to accommodate for trends in rainfall time series. The recharge is calculated using equation 3.7 below (Van Tonder and Xu, 2000):

$$\boldsymbol{Re = rCRDi = Sy}\left[\boldsymbol{\Delta hi} + \frac{\boldsymbol{(Qpi+Qouti)}}{\boldsymbol{ASy}}\right] \quad (3.7)$$

Where,

Re - average annual recharge

rCRD - fraction of a CRD which contributes to recharge

Sy - specific yield

Δhi - water level change during a month i

Qp - groundwater abstraction

Qout - Natural outflow

A - recharge area

3.9.3.3. Saturated volume flux (SVF) method

The SVF method comprises an inventory of inputs in relation to outputs over a specific time period of the water balance. It also comprises the change in the system caused by an imbalance between components. The method provides a combined picture of the water level response of an aquifer. It determines effective recharge and aquifer storativity and allows these to be quantified reliably as lumped parameters. The method presents one of the most valuable contributions to water balance interpretations, in that it determines average annual rainfall and annual variability of recharge (Adams *et. al*., 2004). It is suitable for most hydrological analysis and aquifer management applications (Bredenkamp et al., 1995). The method is based on the saturated water balance given by equation:

$$\boldsymbol{I - Q + Re - O = S}\frac{\boldsymbol{\Delta V}}{\boldsymbol{\Delta t}} \quad (3.8)$$

Where,

I - lateral inflow
Q - net discharge
Re - recharge
O - lateral outflow
S - storativity/specific yield
V - saturated volume of aquifer

t - time

CHAPTER FOUR: MATERIALS AND METHODS

4.1. Site Geology

It is of great importance to consider the geology of the site if one is going to study its hydrogeology, since the geology of the aquifer has an important bearing on groundwater occurrence. Geological methods commonly used include field surveys, geological maps, aerial photography and satellite imagery. All these methods only provide the properties of the earth surface rather than the understanding of subsurface geology. Therefore, electrical resistivity tomography (ERT) surveys together with geological logs from air percussion drilling were used to understand the geology of the study site. The ERT was selected as one of the geophysical techniques proven to be efficient in characterizing lithology and hydrogeological settings of the site. The geo-electrical techniques have been widely used in groundwater exploration to correlate between the electrical properties of geologic formations and their fluid content. The electrical resistivity of a formation depends mainly on the salinity of fluid content, saturation, aquifer lithology and porosity.

4.1.1. Description of resistivity method used in this study

Electrical resistivity measures the earth's resistivity properties by injecting a direct current (DC) into the ground through current electrodes and measuring resulting potential created in the subsurface. An apparent resistivity of the subsurface is calculated from the ratio of the electrical current and the measured potential difference. By using different spacing for current and potential electrodes, apparent resistivity is calculated for different depths of investigation. Apparent resistivity is then inverted by means of inversion algorithms to obtain the information of subsurface resistivity distribution. The inverted resistivity data is then related to various geological and hydrogeological parameters of interest such as, minerals and fluid content, porosity, degree of water saturation in the rock and dissolved ions in groundwater. Resistivity investigations can thus be used to identify zones of different electrical properties, which can thus be referred to different geologic strata. Considering accuracy, in the present study a two-dimensional (2-D) model, which measures resistivity changes in both vertical and horizontal direction along a survey line, was selected. In this case it was assumed that resistivity does not change in the direction that is perpendicular to the survey line.

4.1.2. Resistivity data collection and processing

Electrical resistivity surveys were conducted with a two-dimensional ABEM Terrameter (ABEM SASI100), using Wenner-Schlumberger short and long protocols. The Wenner array has a good sensitivity to vertical changes in subsurface resistivity, while the Schumberger array has a good sensitivity to horizontal changes in the subsurface resistivity. The Wenner-Schumberger array is a new hybrid between the Wenner and Schumberger arrays, where the sounding and profiling techniques are integrated to provide information on both lateral and vertical extent of the subsurface (Loke, 2000). A modified form of this array so that it can be used on a system with the electrodes arranged with a constant spacing is shown in Figure 4.1. The "n" factor is the ratio of the distance between the C1-P1 (or P2-C2) electrodes to the spacing between the P1-P2 potential pair. The sensitivity pattern for the Schlumberger array is slightly different from the Wenner array with a slight vertical curvature below the centre of the array, and slightly lower sensitivity values in the regions between the C1 and P1 (C2 and P2) electrodes. There is a slightly greater concentration of high sensitivity values below the P1-P2 electrodes, meaning that this array is sensitive to both horizontal and vertical structures.

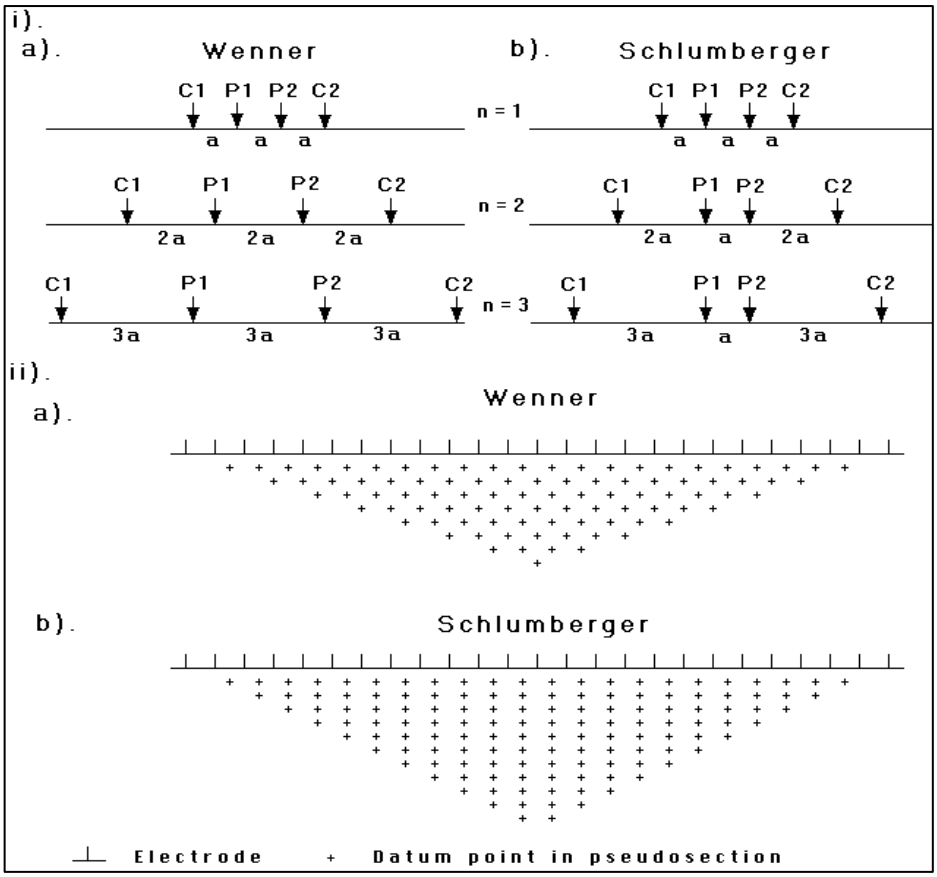

Figure 4.1. A comparison of the (i) electrode arrangement and (ii) pseudosection data pattern for the Wenner and Wenner-Schlumberger arrays (Loke, 2000).

There were four electrical resistivity tomography (ERT) surveys that were conducted during geophysical surveying in the Two Streams catchment. Traverses 2ST001, 2ST002 and 2ST003 were positioned on a standard 5 m electrode spacing along a 600 m survey line corresponding to 128 electrodes. Traverse 2ST004 was run on 2.5 m electrode spacing over a 160 m survey line also corresponding to 128 electrodes. Traverses 2ST001, 2ST002 and 2ST004 were run along the slope in a south to north direction, whereas traverse 2ST003 was run across the slope from west to east direction. Historical ERT datasets for the catchment were used to compare current results with historical ERT datasets (T1, T2, T3 and tstert2, tstert 3) as shown in Figure 4.1. The Trimble™ Pro-XPS Differential Global Positioning System (DGPS) was used to survey each electrode spacing point on a traverse line. The topographic data from the 1:50 000 topographic sheet for the area were added to correct for lateral effects resulting from the changes in elevation.

Figure 4.1. Google earth image showing the location of electrical resistivity traverses conducted at the study site.

The apparent resistivity data measured from four traverses and from previous studies were examined in order to identify and remove erratic data that could affect the inversion routine. The data was then inverted using the two-dimensional inversion software (RES2INV), which makes use of the smoothness-constrained least-squares method and automatically determines a 2-D resistivity model of the subsurface. A smoother resolution with a cell width of half the electrode spacing was used for more accuracy as large resistivity variations were depicted near the ground surface. The 5 m and 2 m electrode spacing transects were inverted using 2.5 m and 1 m electrode spacing respectively. ERT results were interpreted using borehole geological logs, previous hydrological reports and the table of the resistivity of rocks, soils and minerals (Loke, 2000) as shown in Appendix D and E. The data inversion of the ERT survey indicated a high number of missing data points, resulting from bad electrode contact with the ground during data acquisition. Missing data points affect the accuracy of the model of the resistivity section obtained after invasion. Therefore, it was decided to compare current ERT survey with previous survey results, in order to provide more accurate evaluation and interpretation of the geophysical characteristics of the catchment. Two sets of previous electrical Resistivity Tomography (ERT) survey results were selected, namely:

- Electrical Resistivity Tomography (ERT) survey conducted in February 2007 along three transects (T1, T2, T3), reported in Clulow *et.al.* (2011).
- ERT survey dataset conducted in November 2009 along two transects (tstert 2, tstert 3), sourced from the database of the CWRR, UKZN- Pietermaritzburg.

4.2. Streamflow Analysis

Streamflow in the Two-Streams catchment has been monitored continuously since 1999 from a 457.2 mm, 90^0 V-notch weir using a stream flow recorder. Streamflow hydrograph is commonly conceptualised to include baseflow and a runoff component. The former represents the relative steady contribution to stream discharge from groundwater, while the latter represents the streamflow contributed by shallow subsurface flow and direct surface runoff. The separation of baseflow from direct runoff in a hydrograph assists in determining the influence of different hydrological processes on discharge from the catchment. Several methods have been developed to separate the contribution of baseflow from total streamflow. In the present study, the Web-based hydrograph analysis tool (Lim *et al.* 2005), which incorporates digital filter methods into local minimum methods for baseflow separation and stable isotope techniques were used to separate baseflow from direct runoff in the catchment.

4.2.1. Web-based hydrograph analysis tool (WHAT)

Digital filtering methods have become common in hydrograph separation and have proven useful for hydrograph analysis. The WHAT system developed by Lim *et al.* (2005) incorporates digital filter methods into local minimum methods for baseflow separation. Thus, three baseflow separation modules are available in the WHAT system namely; local minimum method, one parameter digital filter method and the recursive digital filter method. The local minimum method searches and uses the minimum flow for each time interval, and minimum flows for each time interval are connected by a straight line to describe the baseflow portion from the hydrograph. This method does not consider the duration of flow and often over-estimate baseflow when multiple high peaks occur within a short period. To utilise either one parameter digital filter or recursive digital filter method for baseflow separation, the user must provide a filter parameter for one parameter filter and BFI_{max} value for the recursive digital filter method. Eckhardt (2005) found that the filter parameter is not very sensitive to the filtered results, while the BFI_{max} value greatly influences the results.

The general approach of the baseflow filtering method as proposed by Eckhardt (2005) included in the WHAT system is given by the following equation:

$$b_k = \frac{(1- BFI_{max})\, a.\, b_{k-1} + (1- a)\, .\, (BFI_{max} y_k)}{1 - a\, .\, BFI_{max}} \qquad (4.1)$$

Where,

b_k - is baseflow at time k, subject to bk </= yk

BFI_{max} - is maximum value of long term ratio of baseflow to total streamflow

a - is a baseflow filter parameter (default: a = 0.98)

y_k - is the total flow at time k

4.2.2. Base flow separation using stable isotope technique

Isotope tracers have been most useful in terms of providing new insights into the hydrological processes, because they integrate small scale variability to provide effective indication of catchment scale processes. Stable oxygen and hydrogen isotope composition can be used to determine the contribution of old and new water to a stream, because the rain that triggers the runoff is often isotopically different from the water already in the catchment (old water). The use of stable isotope tracers allow to separate the runoff hydrograph into the water stored in the

catchment prior to the rainfall event and the water brought by the rainfall event. The respective contributions can be used to calculate the proportion of streamflow that consists of new and old water at any point during a storm event for which isotope samples have been collected by using the following mass balance equation (Ladouche *et al*., 2001):

$$Q_t = Q_g + Q_r \quad (4.2)$$

$$Q_t \,.\, \delta_t = Q_g \,.\, \delta_g + Q_r + \delta_r \quad (4.3)$$

Thus,

$$Q_g = Q_t * (\delta_t - \delta_r)/(\delta_g - \delta_r) \quad (4.4)$$

Where,

Q_g - Baseflow (m^3/d)

Q_t - Streamflow (m^3/d)

δ_t - Isotope composition of streamflow (‰)

δ_r - isotope composition of rainfall (‰)

δ_g - Isotope composition of groundwater (‰)

The following are assumed when using stable isotope techniques for baseflow separation:

- The isotope content of the event and the pre-event water are significantly different.
- The event water maintains a constant isotope signature in space and time, or any variations can be accounted for.
- The isotopic signature of the pre-event water is constant in space and time or any variations can be accounted for.
- Contributions from the vadose zone must be similar to that of groundwater.
- Contributions from surface water storage are negligible.

4.3. Groundwater level Measurements

4.3.1. Determination of groundwater flow direction

Groundwater flows from areas of high hydraulic head to areas of low hydraulic head and eventually drains into streams, lakes or any other water body. Although there is a premise that groundwater flow usually follows surface topography, however this is not always the case. It is therefore inappropriate to always assume the direction of groundwater flow considering topography alone. There are methods available to determine the direction of groundwater flow in the areas (Brassington, 2006).

In the present study, a three point system and hydraulic heads were used to determine the direction of groundwater flow in the Two Streams catchment. This technique only applies to boreholes intercepting the same aquifer system (Leketa, 2011) with an idea to determine the direction of groundwater flow in the aquifer system. If a deep borehole intercepts both a shallow unconfined aquifer and a deep confined aquifer, the confined aquifer has a high piezometric head, such that water level in that borehole may rise above other boreholes that did not intercept the deeper confined aquifer. This may yield wrong calculation of groundwater flow direction if tri-well technique was used. Water levels and elevations in boreholes were measured and related to a common datum. The data obtained (Table 4.1) was used to plot groundwater flow directions in the catchment using Surfer 15 software.

Table 4.1. Groundwater data used for determining groundwater flow direction in the Two Streams catchment

Site Name	**Latitude**	**Longitude**	**Altitude** (m amsl)	**Borehole Depth** (m bgl)	**Collar Height** (m)	**depth to GW level** (m bgl)	**Date**	**GW elevation** (mamsl)
2STBH1	29.20542	30.65072	1107	40	0.30	28.166	28-09-18	1079
2STBH2	29.20925	30.65522	1024	60	0.50	0.000	28-09-18	1024
2STBH3	29.20336	30.65153	1110	60	0.38	45.745	28-09-18	1064
2STBH4	29.20550	30.64731	1105	60	0.47	33.060	28-09-18	1072
2STBH5	29.20644	30.64811	1091	60	0.16	34.790	28-09-18	1056
Satin Farm	29.20859	30.59805	1122	102	0.70	15.765	28-09-18	1106
Botha Farm	29.21877	30.64662	1044	100	0.00	24.170	28-09-18	1020
Mondi Village	29.19338	30.66397	1077	120	0.00	82.840	28-09-18	994
Mowbray spring	29.19100	30.71526	1051	Spring	0.00	0.000	28-09-18	1051

4.3.2. Groundwater level monitoring

Groundwater level fluctuates in response to precipitation, evapotranspiration, barometric pressure and groundwater abstraction, among others. A good set of reliable groundwater level measurements is the best foundation to an understanding of groundwater system. Within the Two-Streams, groundwater level has been monitored from groundwater monitoring boreholes (Figure 2.3), using Solinist dip meter (model 101) and Solinst water level loggers (model 3001), so as to analyse the hydrogeological response of the catchment.

4.4. Aquifer Testing

Hydraulic characterization of the aquifer in the study area has never been determined in the past, hence a constant discharge rate (CDR) test was performed to provide the preliminary estimation of aquifer parameters. A CDR test is a field experiment in which a well is pumped at a controlled rate and water-level response (drawdown) is measured in the pumped well as well as monitoring boreholes. The response data from the pumping test was used to estimate the hydraulic properties of aquifers, such as transmissivity (T) and hydraulic conductivity (K). A submersible pump was used to pump 2STBH1 borehole at a rate of 0.03 litres per second (l/s) and resulting effects in water level was measured manually in the pumping and nearby observation boreholes (2STBH3, 2STBH4 and 2STBH5) using deeper meters. Pumping lasted for 40 minutes after which pump inlet was reached, pump was stopped and residual water level was monitored against time immediately using a dipper meter. A recovery test was carried out up to 86% of the original water level over a period of 40 minutes. This allowed for a better understanding of the aquifer hydraulic characteristics of the geological formations.

4.5. Groundwater Recharge Estimation

The quantification of groundwater recharge is an essential task for water resource management. There are several methods available to estimate groundwater recharge rates and all have their own limitations. Simmers (1998) and Bredenkamp *et al.* (1995) state that the use of multiple recharge estimation techniques provides more reliable results than using only a single method. Recharge estimation techniques used in this study are chloride mass balance (CMB) and water balance methods, with results verified against RECHARGE spreadsheet program developed by Van Tonder and Xu (2000) which incorporates CMB, Saturated Volume Flux (SVF), Cumulative Rainfall Departure (CRD) and qualified guess methods.

4.5.1. Chloride mass balance (CMB) method

When the overall water input is supplied into the soil, some of the water will be lost through evapotranspiration, some used by plants, and only a portion percolates to successively reach the surface of the water table. The CMB method is often used as a first approximation of recharge due to its simplicity and relatively low cost (Kotze, 2001). The method makes use of a relationship between chloride concentrations in rainfall and chloride concentrations in groundwater. The method utilizes the chloride concentrations in precipitation to that in groundwater. Recharge is estimated by dividing the input flux divided by the chloride concentration in groundwater (equation 3.6). Several assumptions are considered inherit for successful application of the CMD method. These assumptions included that there should be no production or removal of salts, dry salt deposition should be added to the total salt load, groundwater chloride only represents vertically recharged water and not laterally transported salts (Xu and Beekman, 2003; van Wyk *et al.*, 2011).

4.5.2. RECHARGE spreadsheet program

The excel-based RECHARGE program developed by van Tonder and Xu (2000) was used to provide an estimate of recharge in the study area. The RECHARGE program includes groundwater estimation methods such as Qualified Guesses (Vegter's recharge map, Acru map, Harvest potential map, and the Groundwater component of river baseflow map), saturated volume flux (SVF), cumulative rainfall departure (CRD) and chloride mass balance (CMB) methods. Van Tonder and Xu (2000) caution that the estimated recharge value obtained from the RECHARGE program indicates the effective groundwater recharge and that trees taping water from the unsaturated zone could reduce the effective recharge value.

4.6. Catchment Water Balance

The concept of water balance provides a framework for studying the hydrological behaviour of the catchment. It assumes that all water entering an aquifer system is equal to the water leaving it, plus or minus any change in groundwater storage (Brassington, 2006). The water balance method involves identifying all inflow and outflow components that occur within an area and quantifying each one individually using field records and long-term records. The water balance of an area can be mathematically represented as:

$$\text{Inflow} - \text{Outflow} = \pm \text{ change in storage} \quad (4.5)$$

The water balance of the Two Streams catchment for any given time period can be expressed by the following equation (modified after Hiscock, 2005):

$$P - ET - S_R - G_R = \pm \Delta S \quad (4.6)$$

Where,

P_{recip} is the precipitation in the catchment

ET is evapotranspiration measured in the catchment

S_R is surface runoff

G_R is groundwater discharge

$\pm \Delta S$ is the change in surface and groundwater storage

To calculate the water balance of the catchment, the inflow and outflow components of equation 4.6 need to be defined. The rainfall, surface runoff and evapotranspiration data for *Acacia mearnsii* and Eucalyptus grandis stands, were obtained from the Two Streams catchment database run by the Centre for Water Resources Research (CWRR), University of KwaZulu-Natal, Pietermaritzburg. Groundwater discharge as baseflow was computed using baseflow separation techniques applied in the present study.

4.7. Hydrochemical and Environmental Isotope Sampling and Data Collection

4.7.1. Sampling procedure

Water samples for hydrochemical and environmental isotope analyses were collected from deep boreholes, shallow piezometers, stream and an automated rainfall sampler on monthly basis over a one year period, following standard methods of water sampling reported in Weaver *et al*. (2007). Down-the-hole hydrochemical profiling was carried out using a multi-parameter probe which measures temperature, specific electrical conductivity (EC), dissolved oxygen, pH and the oxidation reduction potential at each borehole. Cations, anions and environmental isotope samples were taken in separate sampling bottles. During each sampling campaigns, depth to groundwater at each borehole was measured prior to borehole purging for sampling and on-site measurements of physiochemical parameters including on-site titration. Hand-held pH and EC meters (Hanna combo HI 98121 and 98312 models) were used to measure on-site

pH, temperature (T), EC, total dissolved solids (TDS) and oxidation reduction potential (ORP). On-site acid titration was conducted to determine the concentration of total alkalinity and bicarbonate (HCO_3^-) content of water samples using a 0.02M hydrochloric acid solution and Bromocresol green as indicator. Prior to taking groundwater samples, each borehole was purged so as to ensure that the groundwater sample subsequently taken was representative of groundwater drawn from the aquifer rather than stagnant water from the borehole. Hydrochemical samples were filtered on-site through a 0.45 µm polyethersulfone syringe filter. Cation samples were acidified on-site with nitric acid (HNO_3) to a pH of below 2 immediately after sampling. Prior to taking every water sample, each bottle was washed three times with deionized water and again with a filtered sample. All samples were clearly marked, kept cool in a cooler box immediately after sampling. Prior to analysis, samples were stored in the fridge at a temperature of less than 4 ^{0}C to minimise sample deterioration.

4.7.2. Hydrochemical and stable isotope analysis

4.7.2.1. Major cations

Major cations (Ca^{2+}, Mg^{2+}, Na^+ and K^+) in water samples were analysed using Inductively Coupled Plasma Optical Emission Spectrometry (ICP-OES) technique run by the School of Chemistry at the University of KwaZulu-Natal, following standard procedures for analysis of water samples by ICP-OES methods described in (Thermo Fisher Scientific, 2011). Seven standard solutions ranging from 0.2-30 mg/l for Ca^{2+}, Mg^{2+}, Na^+ and 0.5-10 mg/l for K^+ (Table 4.2) were prepared for use in ICP-OES instrument.

Table 4.2. Calibration standards used for major cation analysis by ICP method

Parameter	**STD1** (mg/l)	**STD2** (mg/l)	**STD3** (mg/l)	**STD4** (mg/l)	**STD5** (mg/l)	**STD6** (mg/l)	**STD7** (mg/l)
Ca^{2+}	0.2	5	10	15	20	25	30
Mg^{2+}	0.2	5	10	15	20	25	30
Na^+	0.2	5	10	15	20	25	30
K^+	0.5	1	1.5	3	4	5	10

4.7.2.2. Major anions

Major anions (SO_4^{2-}, Cl^-, NO_3^- and F^-) in water samples were analysed using a Thermo Scientific Gallery Discrete Analyser which uses ready to use reagents at the Soil Science laboratory, University of KwaZulu-Natal. Analyses were completed following standard operating procedure as prescribed in the Gallery Reference Manual (Thermo Fisher Scientific, 2011). The gallery analyser utilises a discrete cell technology which enables simultaneous analyses of several different parameters from the same sample. It runs steps including sample and reagent dispensing, colorimetric reading and data processing.

4.7.2.3 Stable isotope analysis

Deuterium and oxygen-18 analysis were conducted using the isotope laser spectrometer (Los Gatos Research DLT-100 Liquid Water Isotope analyser), run by the Centre for Water Resources Research (CWRR) at the University of KwaZulu-Natal. The analyser uses infrared absorption spectroscopy to quantify the measurements of $^2H/^1H$ and $^{18}O/^{16}O$ ratios of water samples in an optical cell. The spectrum of the analyser was verified and the sub-sampling of the auto-sampler was programmed. Each sample and standard was sub-sampled and analysed six times. Since the analyser does not report values on a V-SMOW scale, post-processing requires the determination of ratios for standards, developing a relationship between known V-SMOW δ values and the measured ratios of the standards, and then applying the relationship to the sub-sample measured ratios. Three standards were prepared by calibration against known standards as shown in Table 4.3 and placed into an auto-sampler tray before every five samples to be analysed and after the last five samples to allow for calibration. Post-processing checks included temperature variation, sub-sample density and deviation of $^2H/H$ and $^{18}O/^{16}O$ ratios (Pretorius, 2014).

Table 4.3. Standards used for stable isotope analysis (adapted from Pretorius, 2014)

Standard	Name	$\delta\ ^2H$	$\delta\ ^{18}O$
1	LGR2	177.00	-15.55
2	VSMOW2	0.00	0.00
3	IA-RO53	-61.97	-10.18

CHAPTER FIVE: RESULTS AND DISCUSSIONS

This chapter presents the results obtained through the methodology applied in the course of the research to characterise the hydrogeology of the Two Streams catchment study area and as such to understand the impact of *Acacia Mearnsii* plantation on weathered and fractured aquifer systems, using the Two-Streams catchment as a case study. Aquifer characterisation techniques included geophysical surveying, interpretation of streamflow data, groundwater level monitoring, the determination of groundwater flow directions in the catchment, aquifer testing, groundwater recharge estimation as well as hydrochemical and isotope characterisation.

5.1. Geological Conceptual Model

The results of the electrical resistivity tomography (ERT) survey together with the geological logs of boreholes in the study area were used to develop the conceptual geological model of the study site. The ERT results are based on a principle that the resistivity of a formation largely depends on the moisture content and on the physical and chemical properties of saturated water. Lower resistivity would indicate that the formation is partially or totally saturated or the formation is conductive material such as clay. In order to evaluate the accuracy of the results obtained from the current ERT survey at Two-Streams catchment, two sets of previous ERT results were selected. The first set was referenced from Clulow *et al*. (2011) report and the second obtained from the Centre of Water Resources Research database, University of KwaZulu-Natal. The results of the current resistivity investigations undertaken at the study site were assessed by comparing them with previous ERT investigations in the catchment and the geological logs (Figure 5.2). The results are displayed in Figure 5.1 in the form of a two-dimensional resistivity sections corresponding to ERT survey lines conducted in the study site. The two-dimensional (2D) resistivity sections of all transect conducted in the study site (both current and previous) are presented in Appendix C.

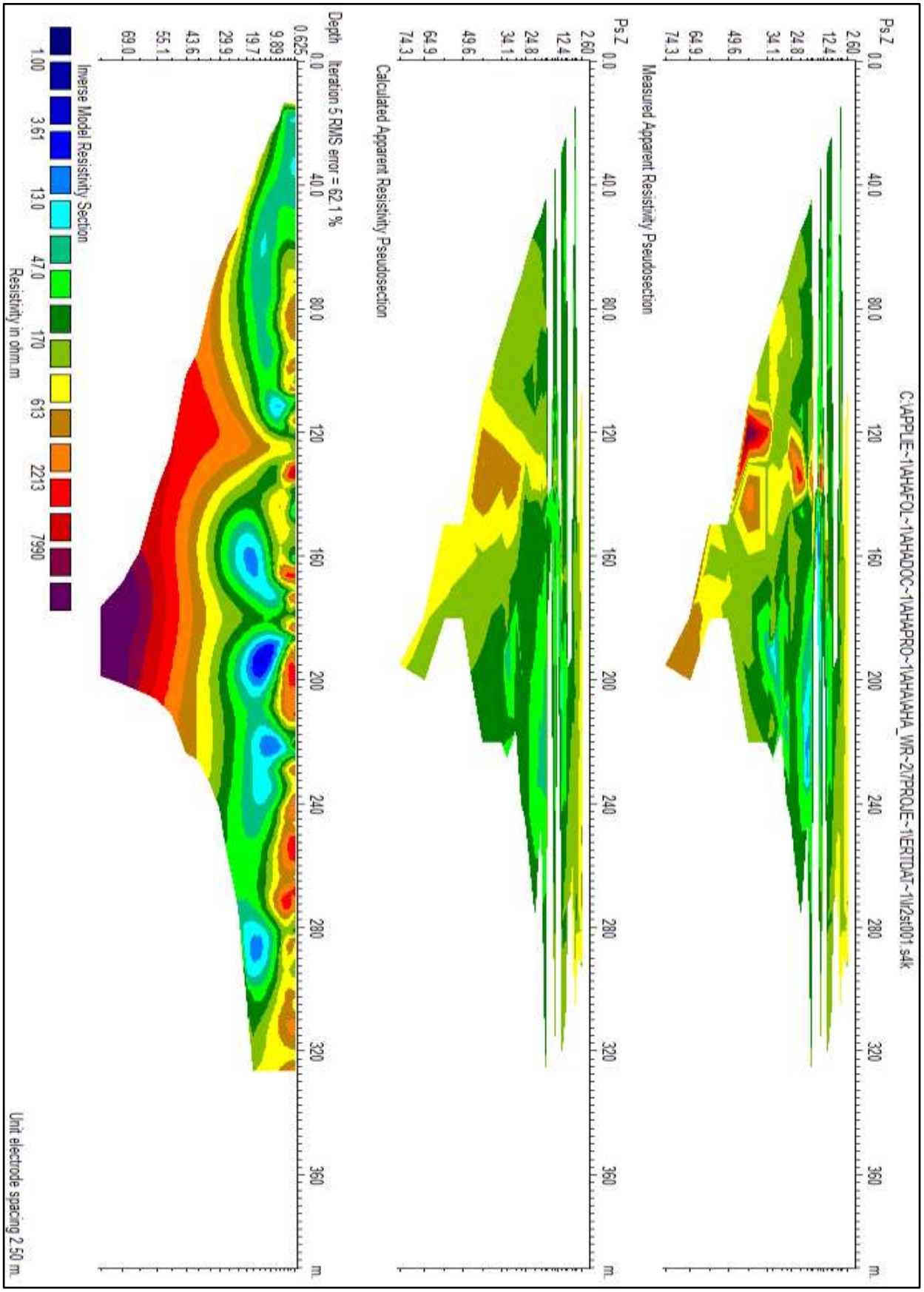

Figure 5.1. Two-dimensional geo-electric resistivity model of the subsurface along transect 2ST001 in the Two Streams catchment site.

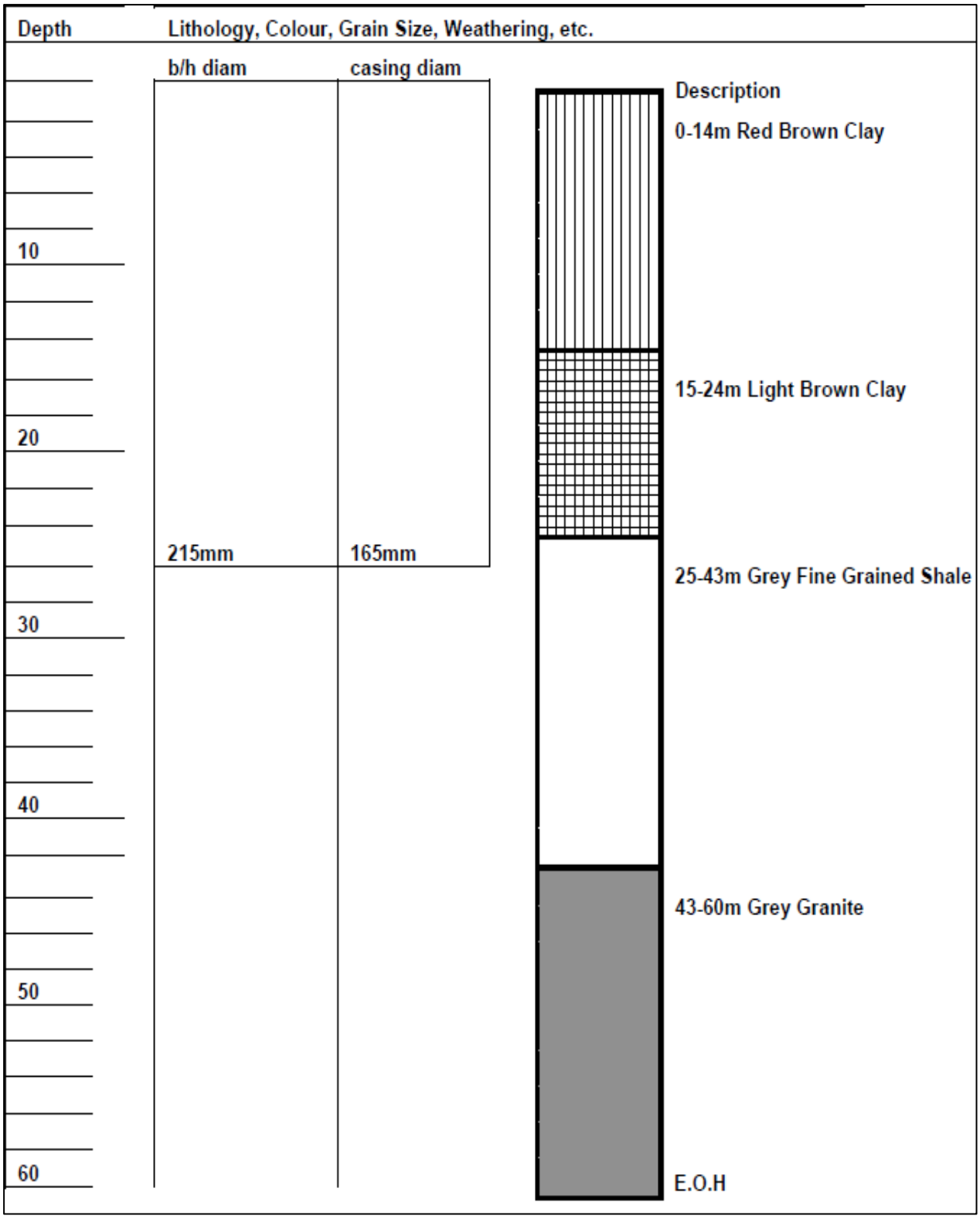

Figure 5.2. Geological logs recorded during the drilling of 2STBH3 borehole.

From the two dimensional (2D) resistivity sections presented in Figure 5.1 and Appendix C as well as borehole logs (Figure 5.2 and Appendix D), the following observations are made:

- The geo-electrical section or models of the subsurface displays a shallow contrast of resistivity distribution ranging between 100 Ωm and 1000 Ωm, indicating lateral variations of water content distribution from moist to dry material. The thickness of this layer along ranges between 24 m at the crest, 15 m mid-slope and decreases to nearly zero towards the toe of the slope. When referring to borehole logs of 2STBH3 (North borehole) as shown in Figure 5.2, this layer can be related to a brown clayey material which has a thickness of up to 24 m deep at the crest.
- The clayey layer is underlain by a weathered material with a lateral change in layer thickness, decreasing towards the toe of the hillslope. The layer base is located at approximately 44 m bgl up-gradient and at approximately 25 m bgl down-gradient. Borehole logs (Figure 5.2) indicate that this layer is grey fine-grained shale. The layer consists of two conducive materials, some pockets of clay material with resistivity values ranging between 1 Ωm and 20 Ωm and a weathered material with resistivity ranging between 20 Ωm and 100 Ωm. Although the presence and depth of a perched water table cannot be identified from the resistivity section, however, the observed low resistivity values suggest that the clayey layer is at least partially saturated. The material can be interpreted as a water bearing formation, since water seepages were observed at 31 m bgl and 41 m bgl during the drilling of 2STBH3. Borehole logs further indicate that the water strike with a 0.5 l/s yield observed at 41 m bgl relates to the contact zone between shale and basement granite rock.
- The conductive layer (weathered grey fine-grained shale) is in turn underlain by a deep contrasting layer that is identified from 45 m bgl to 77 m bgl, with high resistivity values of above 1000 Ωm and it is shallow at the stream bed. According to borehole drilling logs (Figure 5.2 and Appendix D), this layer may be related to basement granite.

Based on the results of the geophysical survey and borehole drilling logs, it can be concluded that the study site is underlain by three geological formations. Namely: clayey material consisting of lateral variations of water content distribution from moist to dry material with a thickness of 24 m, saturated weathered shale material with a thickness of approximately 22 m and deep basement granite rock. The main aquifer occurs at the contact between the shale and granite formations. The geological conceptual model of the study site is given in Figure 5.3.

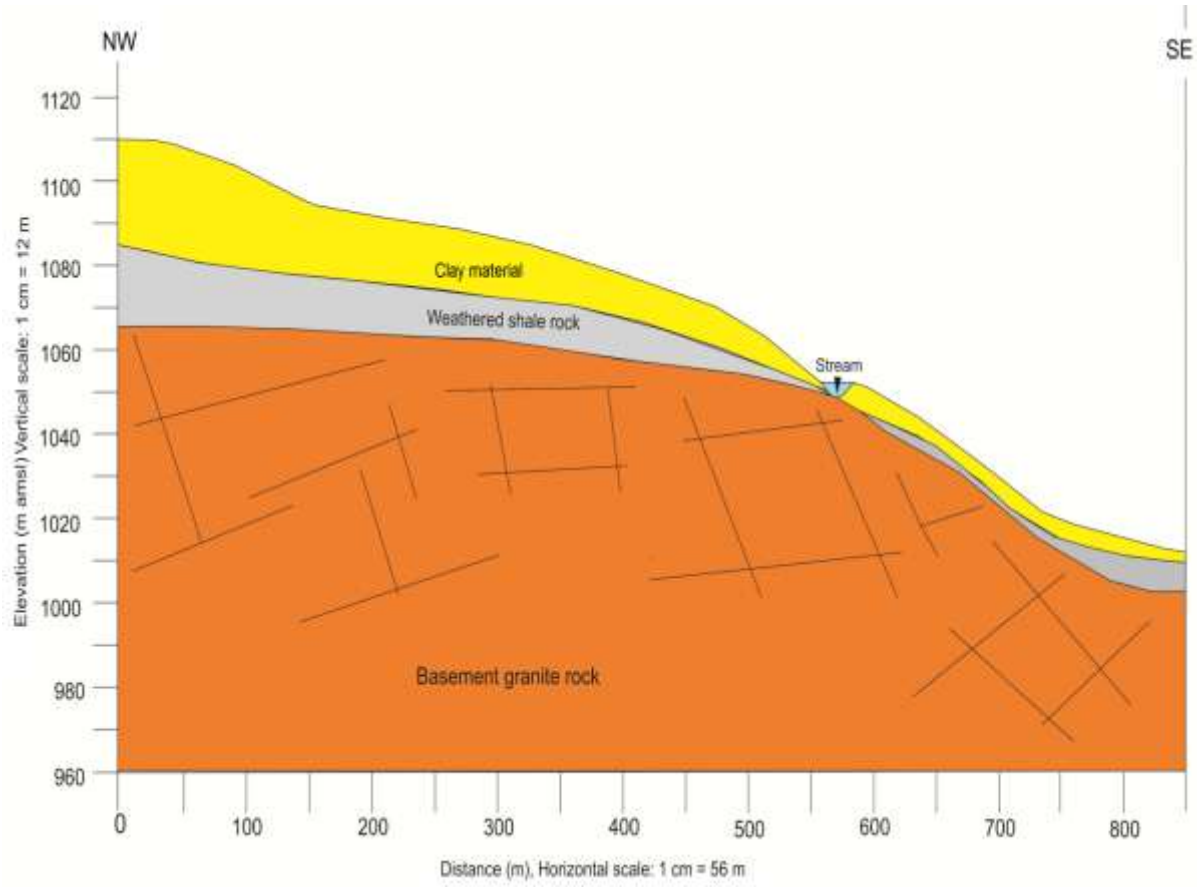

Figure 5.3. Geological conceptual model of the Two Streams catchment.

5.2. Streamflow Characteristics at Two-Streams catchment

5.2.1. Streamflow

Daily streamflow with corresponding rainfall from January 2006 to December 2017 is shown in Figure 5.4. The rainfall and streamflow data show a well-identified seasonal rainfall and streamflow fluctuations. As expected, rainfall is high in summer rainy season than in dry winter season and the streamflow also behaves in a similar way as the rainfall. The high streamflow observed in January 2013 corresponds well with high rainfall recorded for the same period, thus confirming a strong relationship between streamflow and rainfall in the study area. The results of streamflow indicate that as trees continue to grow, water flow in the stream is gradually reduced irrespective of rainfall inputs. It is observed from Figure 5.4 that the stream has failed to return to original water flow levels that were observed when the trees were just planted in 2006. This is an indication that the *Acacia mearnsii* trees have a direct impact on streamflow by reducing baseflow that sustains streamflow in the catchment. Furthermore, despite low rainfall in winter, the stream has continued to flow for the past 11 years from 2006 to 2017, suggesting that during dry periods, streamflow is mainly sustained by groundwater.

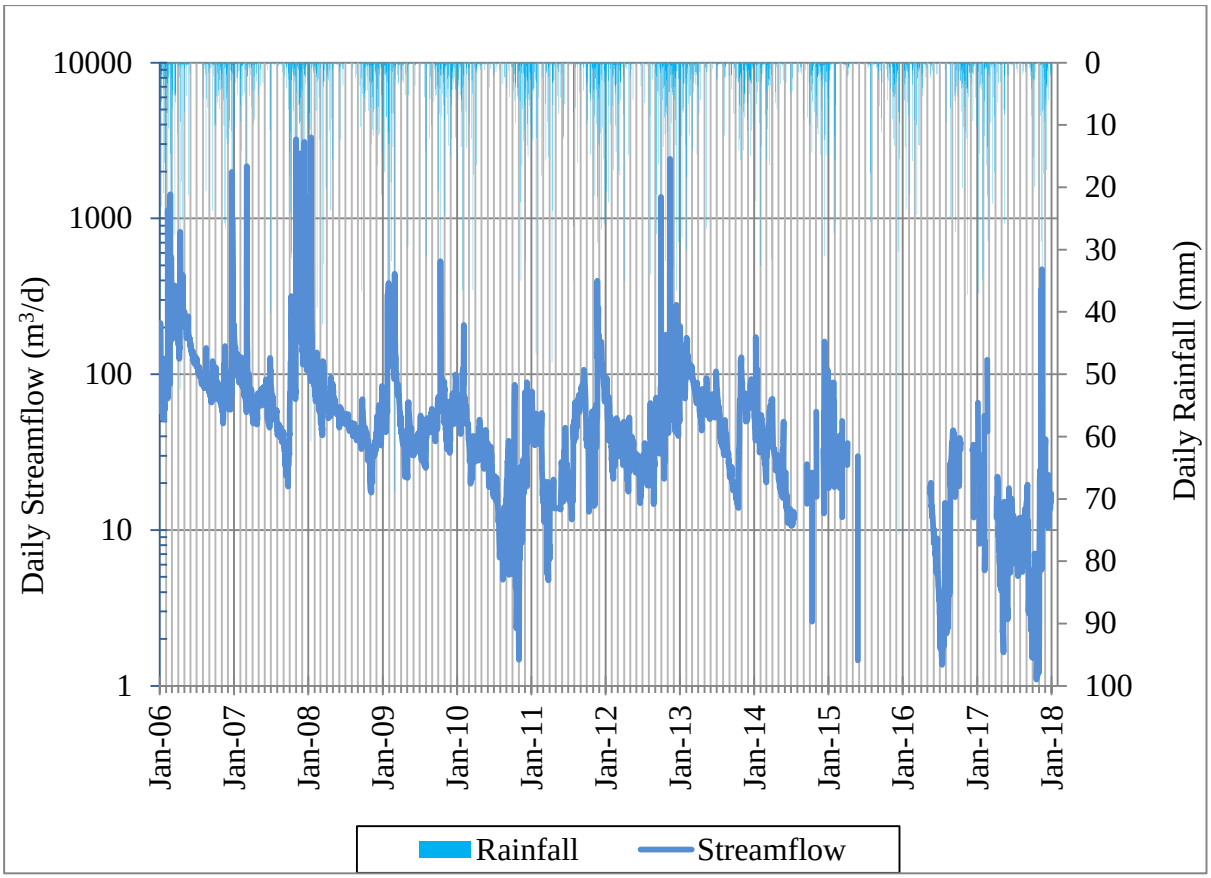

Figure 5.4. Daily streamflow with corresponding daily rainfall in the Two Streams catchment.

5.2.2. Baseflow separation

The sustainability of a river system is equated to the rate at which that river system is being replenished by baseflow. The Web-based hydrograph analysis tool (WHAT) system and stable isotope techniques were used to determine the contribution of baseflow to streamflow in the study area, using daily streamflow values between 29 February 2012 and 31 December 2014. These were the days that had both streamflow values and isotope data for rainfall, stream and groundwater to enable the comparison of isotope techniques and graphical methods in baseflow separation. The baseflow filter parameter of 0.98 (a = 0.98) and BFI_{max} = 0.25 as proposed by Eckhardt (2005) were used for graphical baseflow separation. In order to explore whether the digital filter methods incorporated in the WHAT system performed better than the local minimum method, baseflow was computed using two digital filter methods included in the WHAT system and compared to the local minimum method for streamflow data from 2STWEIR monitoring site.

The baseflow results obtained from digital methods did not appear to have over-estimated baseflow compared to values obtained from the local minimum method, which had typically shown over-estimates of baseflow values. However, baseflow values of the recursive digital method did not appear to be realistic, as these values were very low and not rising even during high rainfall periods. This is expected from the recursive method as it is commonly used to remove high frequency quickflow signals to derive a low frequency signal (Indarto *et al.*, 2015). According to the baseflow analysis from the one parameter digital filter method included in the WHAT system (Figure 5.5), the total streamflow is estimated to be 1216.74 m^3/yr with a direct runoff volume of 527.97 m^3/yr which is equivalent to 43% of the total streamflow. The remaining 688.78 m^3/yr which is equivalent to 57 % of the total volume of streamflow is attributed to baseflow contribution. Channel precipitation is negligible in the catchment. This result suggests that the rainfall contributes significantly to the shallow aquifer in the upper slope of the catchment, which in turn discharges into the stream as baseflow. Therefore, tree plantations are most likely to affect the streamflow by reducing the amount of water available for baseflow that sustains streamflow in the catchment and also likely to reduce water available for recharging the regional aquifer.

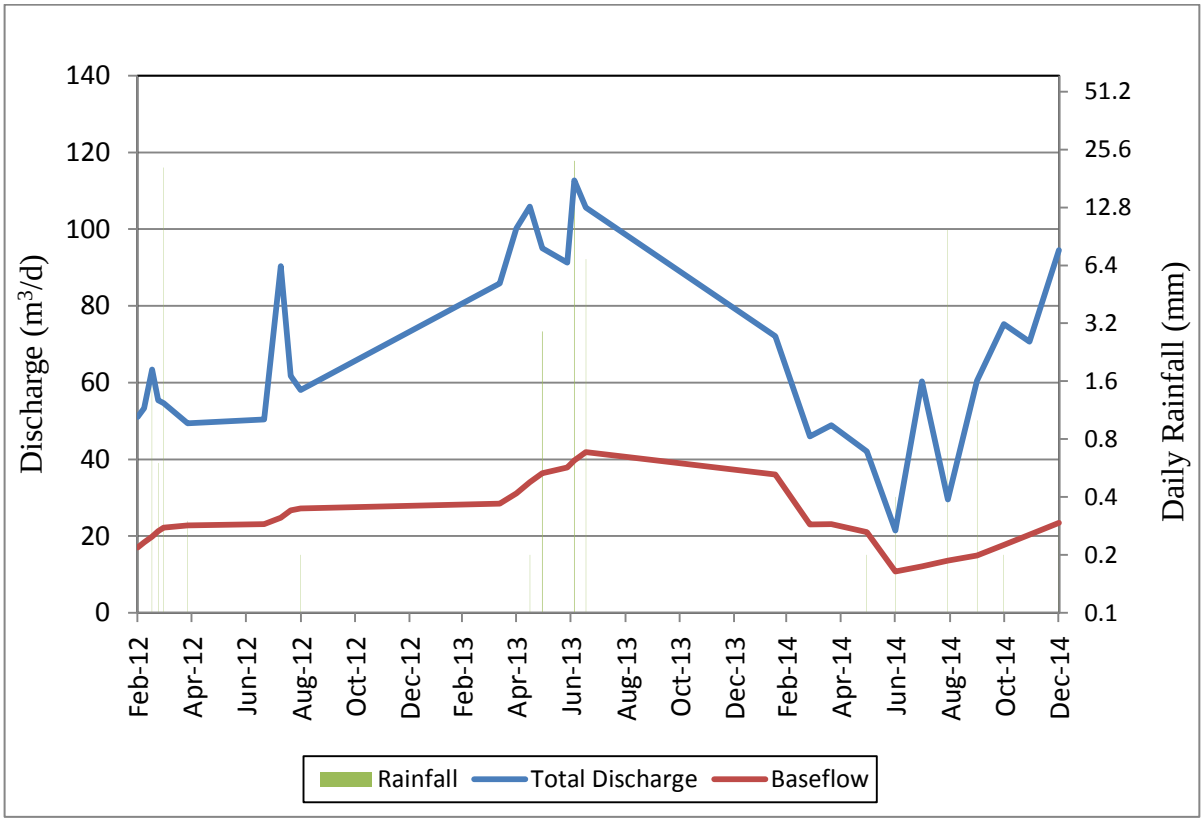

Figure 5.5. Baseflow separation using one parameter digital filter method in the Two-Streams catchment (February 2012 to December 2014).

In addition to baseflow separation using digital filter methods, isotope based separation method was used to separate baseflow from the total streamflow in the catchment for the same period (29 February 2012 to 31 December 2014). Isotope techniques were employed because the isotopes of water molecule are an ideal, conservative tracer since they are part of the water molecule, added naturally during precipitation events and once free from evaporation expose, are only subject to changes due to mixing. The isotope based hydrograph separation (Figure 5.6) shows that the stream hydrograph of the catchment is dominated by pre-event water with a baseflow contribution of 1097.2 m^3 (90 %) of total stream discharge and only 119.6 m^3 (10 %) contribution resulted from direct runoff. This baseflow value is much greater than the baseflow contribution value of 688.78 m^3 (57%) obtained from using the one parameter digital filter method contained in the WHAT system. This suggests that the isotope hydrograph separation technique has over-estimated the contribution of baseflow to streamflow in the catchment. Berman *et al.* (2009) found that some forested catchments with runoff ratio above 50% may display no detectable rainfall in channel storm flow, even at the peak of storm flow, indicating the over estimation of baseflow contribution.

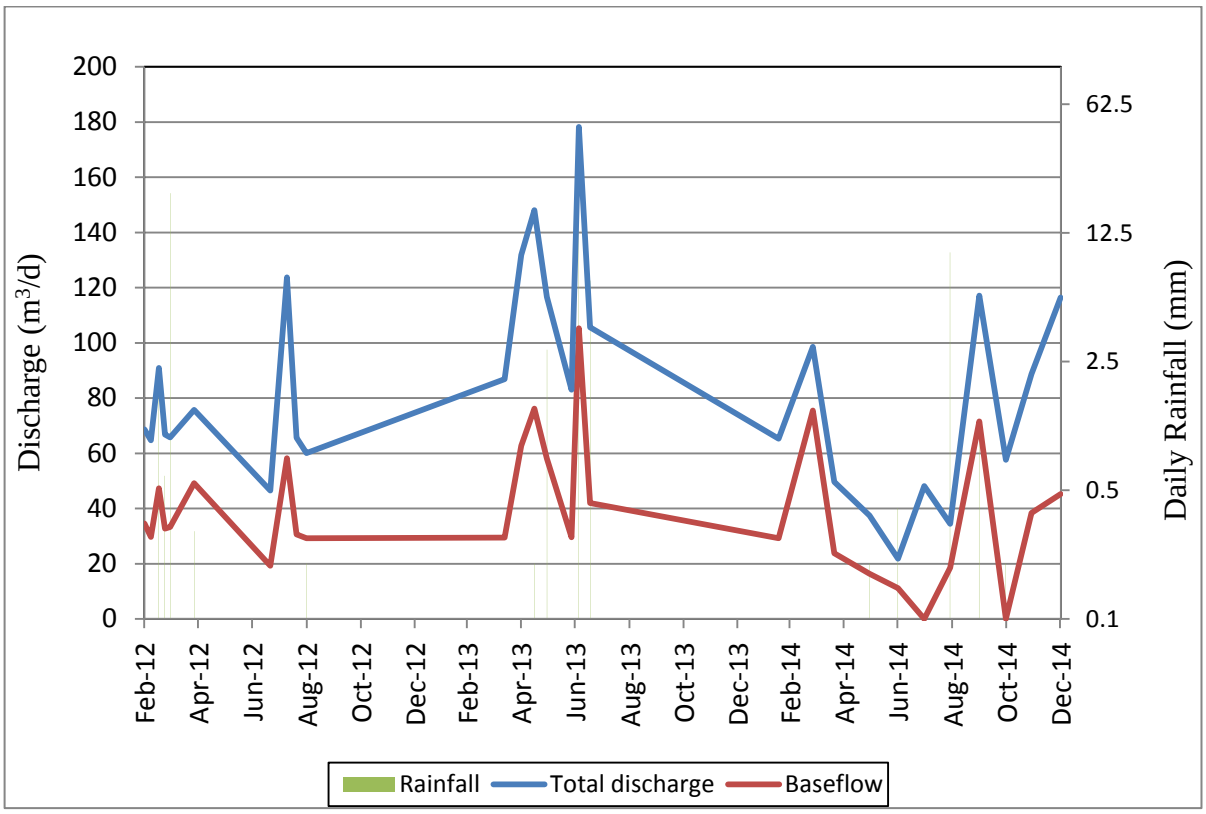

Figure 5.6. Baseflow separation using isotope techniques in the Two-Streams catchment from February 2012 to December 2014.

Figure 5.7 shows daily total streamflow and daily rainfall measured in the study area in relation to baseflow contribution determined from the one parameter digital filter baseflow separation method, whilst Table 5.1 shows mean annual streamflow separated into direct runoff and baseflow over a 12 year period (2006 to 2017). According to Table 5.1, the mean annual runoff in the catchment is 20387.42 m^3 of which approximately 14768.28 m^3 (72.4 %) is baseflow contribution into the total streamflow. The years with the highest mean annual runoff were 2006, 2007 and 2008; as expected baseflow contributions to total streamflow were also at the highest during these years. The year 2017 had the lowest catchment runoff (4191 m^3) of which 2331.8 m^3 (55.6%) was baseflow contribution. These results are an indication that *Acacia mearnsii* plantations over 10 years old have the capacity to reduce baseflow contribution to streamflow significantly, which in turn reduces streamflow. Although the years 2015 and 2016 seem to have lowest runoff (drought years), however, there were much gaps on the streamflow data during these years, owing to instrument failure.

Table 5.1. Mean annual runoff, direct runoff and baseflow in the Two Streams catchment (January 2006 to 31 December 2017)

Year	**Total Runoff**	**Direct Runoff**	**Baseflow**	**Rainfall**	**Baseflow percentage**
	(m^3/d)	(m^3/d)	(m^3/d)	mm	%
2006	54653.23	11596.48	43056.75	1151	78.8
2007	46359.01	15639.00	30719.62	794	66.3
2008	27169.68	7039.93	20129.75	811	74.1
2009	24721.48	5170.51	19550.97	878	79.1
2010	10958.40	2537.51	8420.88	639	76.8
2011	16598.67	3800.55	12798.13	884	77.1
2012	21147.31	7515.00	13632.35	951	64.5
2013	24112.59	3384.56	20728.03	693	86.0
2014	9468.93	6760.67	2708.26	603	28.6
2015	2136.71	996.28	1140.42	618	53.4
2016	3131.94	1129.50	2002.44	633	63.9
2017	4191.04	1859.21	2331.80	743	55.6
Average	**20387.42**	**7013.52**	**14768.28**	**783.08**	**72.4**

The evidence from Figure 5.7 is that baseflow contribution to streamflow has continued to drop from 2007 when trees were only one year old. A significant reduction in baseflow contribution is observed from 2010, with lowest baseflow values observed in 2017. This is the period when *Acacia mearnsii* trees were 10 years old. These results suggest that as trees continue to grow, baseflow contribution to streamflow also continues to drop. Mainly because of reduction in rainfall infiltration as a result of increased evaporation rates. Furthermore, low baseflow observed in 2017 can also be attributed to delayed groundwater response resulting from draughts experienced in 2014, 2015 and 2016. These conclusions are in agreement with the stream hydrograph in Figure 5.4 and annual baseflow measurements in Table 5.1, which also indicate that as trees continue to grow, water flow in the stream gradually decreases irrespective of rainfall inputs, owing to the reduced baseflow contribution. This further suggests that the tree plantations in the study site are having a significant negative impacts on the water balance of the catchment by reducing baseflow that sustains streamflow in the study area, especially during dry season. This is an indication that the *Acacia mearnsii* trees have a direct impact on streamflow by reducing baseflow that sustains streamflow and are most likely to reduce available water for recharging the regional aquifer in the catchment.

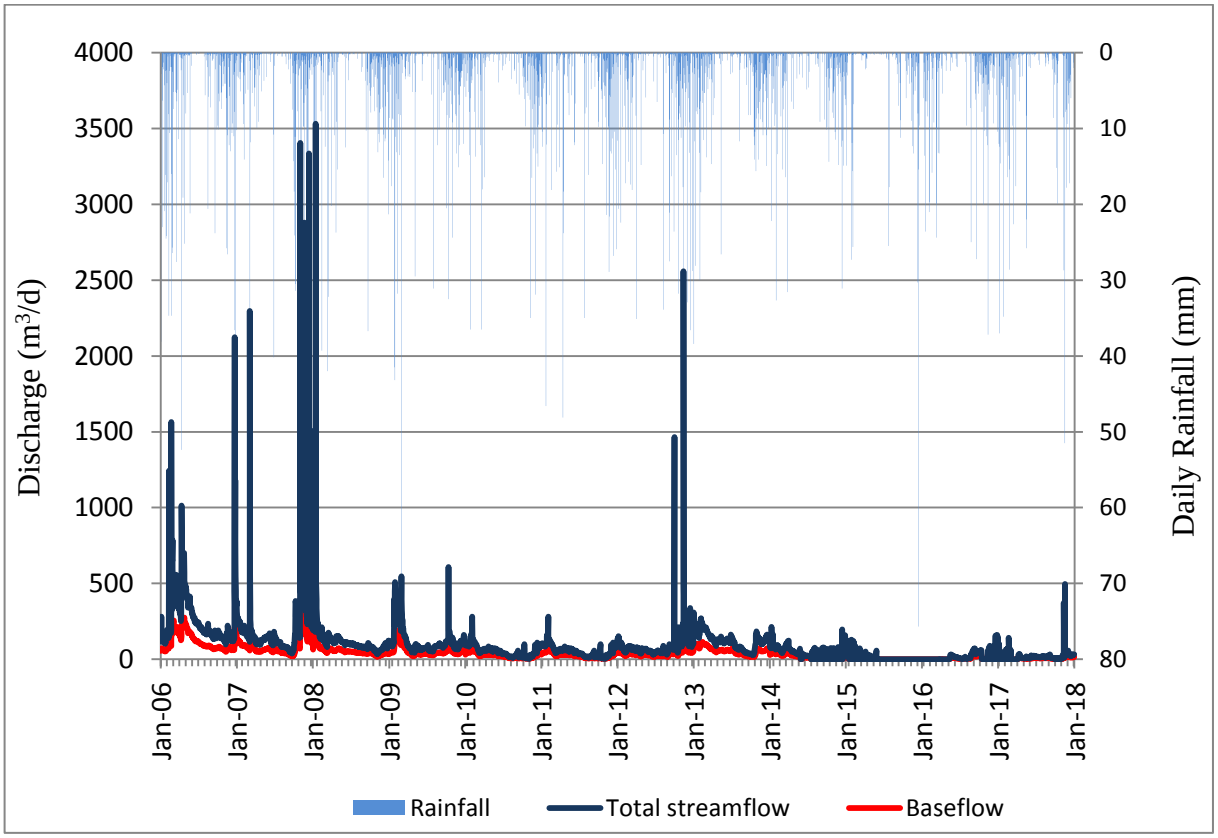

Figure 5.7. Daily streamflow discharge with corresponding daily rainfall in the Two-Streams catchment (January 2006 to December 2017).

5.3. Groundwater Level Characteristics

5.3.1. Groundwater flow direction

Accurate information on land-surface elevations and depth to groundwater level is needed to determine the accurate direction of groundwater flow in the area. In the present study, the direction of groundwater flow was determined using information obtained from the existing groundwater monitoring boreholes within the catchment as well as the hydrocensus boreholes located within a 10 km radius of the study site. The Bayesian correlation of surface altitude and groundwater level elevations were used to determine the correlation coefficient of the surface and groundwater level elevations as shown in Figure 5.8. A high correlation would indicate aquifers with a general flow behaviour following surface topography. A 100% correlation would indicate the presence of an entirely unconfined aquifer system with groundwater flow mimicking surface topography (Leketa, 2011). Based on the 53% correlation observed between surface and groundwater level elevations (Figure 5.8), it can be concluded that the groundwater around the Two Streams catchment occur in a confined to semi-aquifer conditions.

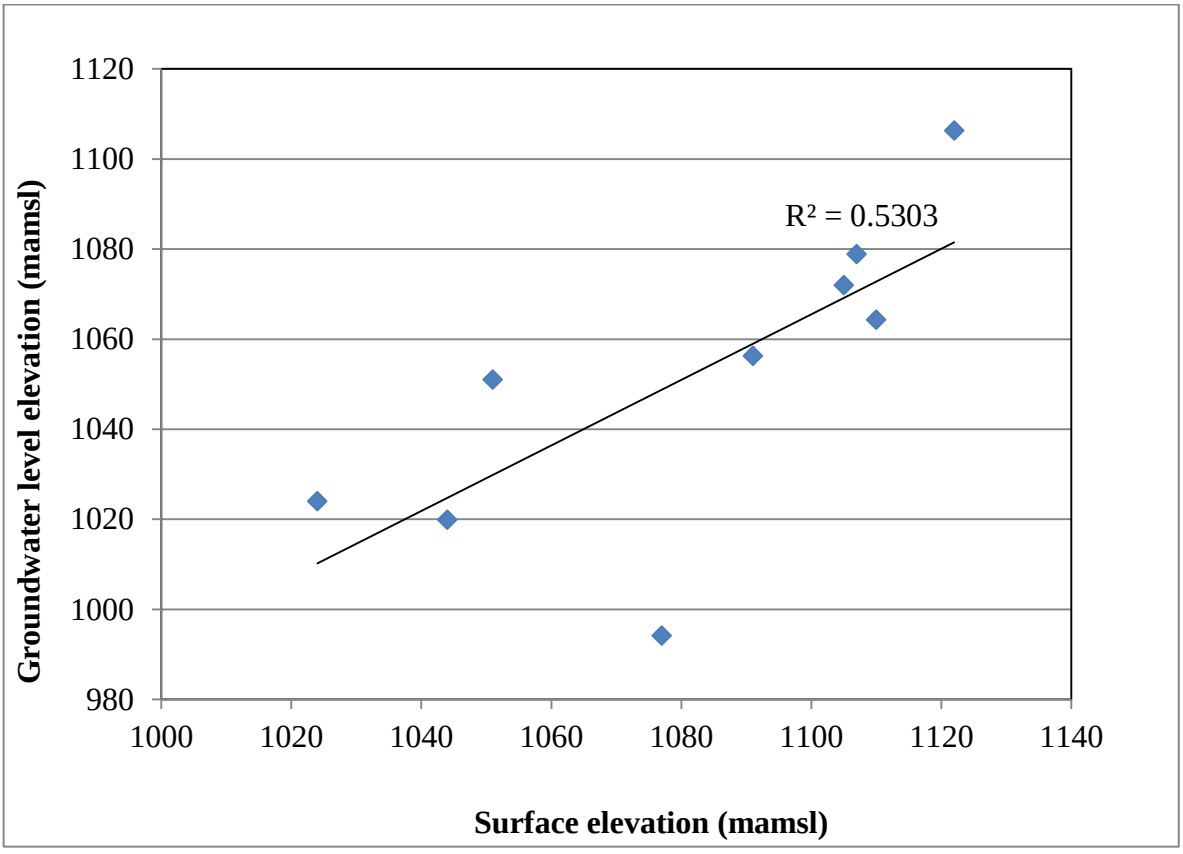

Figure 5.8. Bayesian correlation of groundwater level and surface elevation around the Two-Stream catchment.

Groundwater level contour map helps to define the groundwater flow direction, which is from highest contour lines to lowest ones, in a direction perpendicular to the contour lines and curves towards discharge points, such as spring discharge points, seepage zones, streams, wetlands, or pumping wells. The spacing of groundwater level contours provides a good indication of variations in aquifer transmissivity values. Contours that are close together would indicate low transmissivity values, because a steep hydraulic gradient would be needed to drive groundwater flow through an aquifer. Whereas, groundwater level contours that are more widely spaced indicate high transmissivity aquifer (Brassington, 2006). Based on the groundwater contour map of the study area (Figure 5.9), it can be concluded that the direction of regional groundwater flow around the Two-Streams catchment is towards an easterly and south easterly directions, following surface topography. The spacing of groundwater contours suggests that the aquifer is moderately transmissive in the northern section and southern section than in the central section.

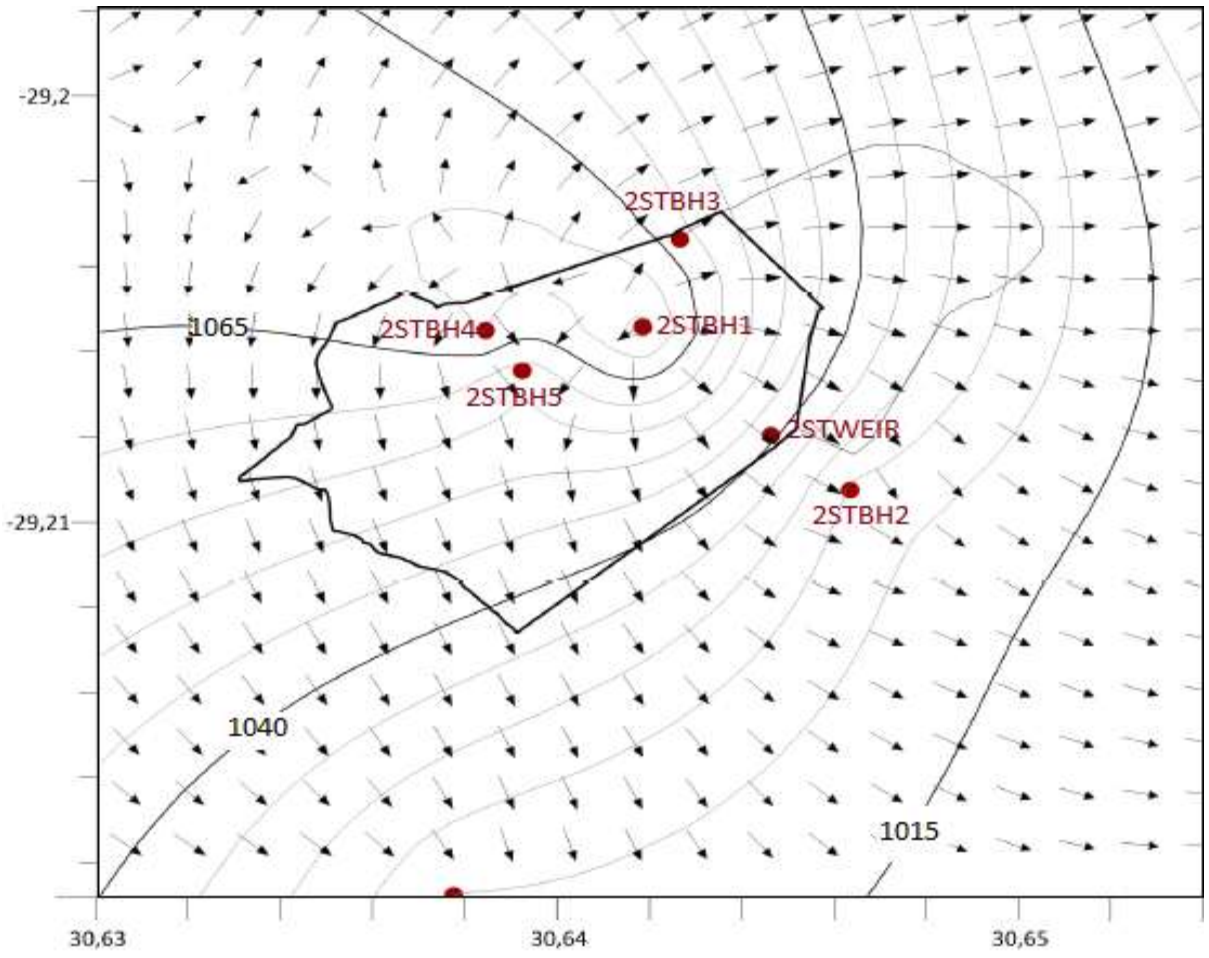

Figure 5.9. Groundwater level contour map showing groundwater flow direction within the Two-Streams catchment.

5.3.2. Changes in groundwater level over time

Generally, groundwater levels fluctuate according to the characteristics of precipitation events such as amount, duration and intensity that recharge the aquifer, as well as various hydrogeological variables such as thickness of the unsaturated zone and hydraulic characteristics of the aquifer. Borehole hydrographs given in Figure 5.10 show hourly groundwater level fluctuations in relation to daily rainfall. The rainfall data indicates the beginning of wet season in August, reaching maximum rainfall in December and ends in March. The dry season begins in April, reaching driest in June and ends in August. The groundwater level fluctuations observed in the borehole hydrographs vary between 8 m and 16 m with a mean fluctuation of 8 m for the centre (2STBH1) and north (2STBH3) boreholes. The mean groundwater level fluctuation for the west (2STBH4) and south (2STBH5) boreholes is 3 m. The response of the aquifer to recharge displays well-identified seasonal groundwater level fluctuations. Borehole hydrographs generally behave in a similar way as rainfall, rising with increasing rainfall and gradually dropping towards the dry season. Groundwater levels appear to start rising in August reaching peak in March, which is then followed by gradual recession into the dry season, reaching its lowest level in June.

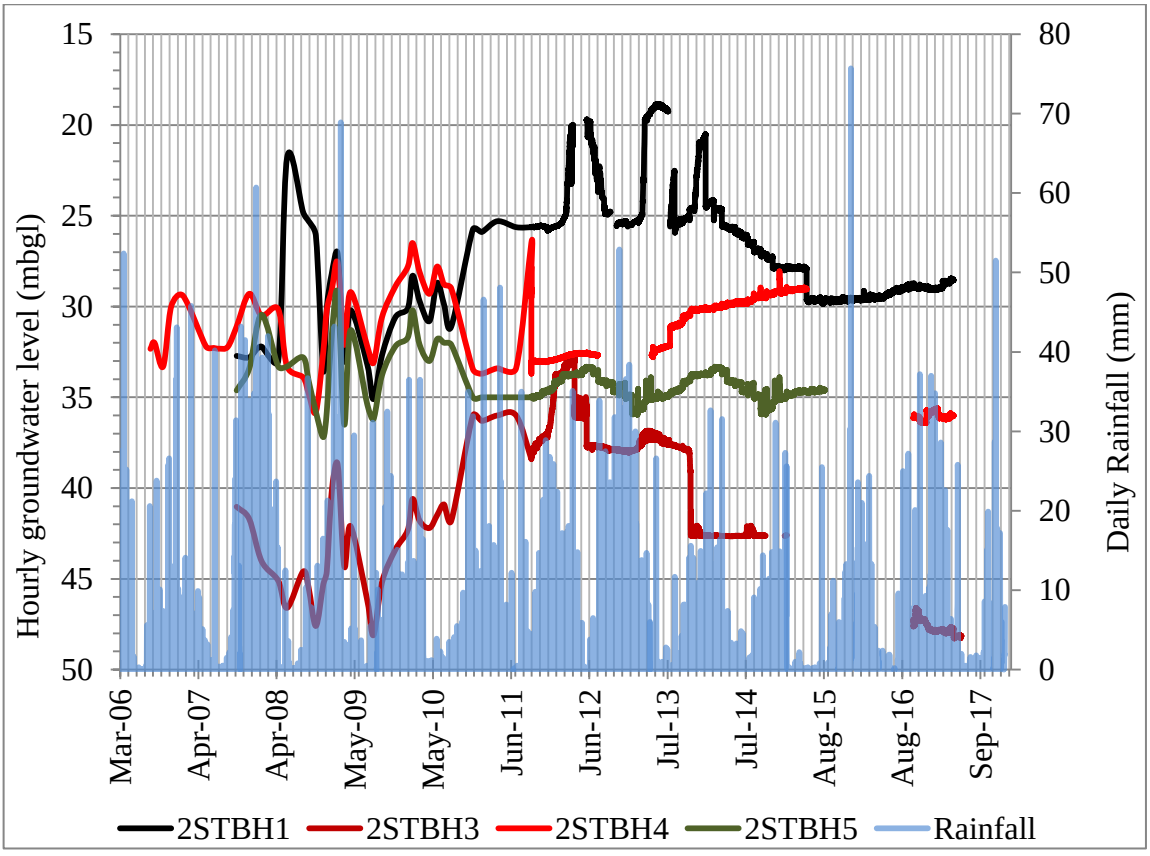

Figure 5.10. Response of groundwater level to daily rainfall in the Two Streams catchment.

Based on groundwater level fluctuation hydrographs given in Figure 5.10, the following conclusions can be drawn:

- Boreholes hydrographs show similar fluctuation trends in all boreholes, indicating that all boreholes are intercepting the same aquifer system, with higher groundwater levels mostly encountered during February or March, towards the end of the rainy season.
- Groundwater level responds significantly to storm events, suggesting a direct connection between hillslope processes and the underlying deep bedrock aquifer. The quick response of the groundwater table to rainfall events suggests the existence of preferential flow paths through plant roots and biological activities, which contributes significant amount of water to the bedrock surface.
- Groundwater levels have continued to drop and failed to reach original water levels measured in 2007 when trees were newly planted. This observation suggests that as trees continue to grow, less water become available for recharge into the regional aquifer system. This is in agreement with stream hydrograph analysis, which indicated that as trees continue to grow, the baseflow that sustains streamflow is also reduced, thus resulting in the reduction of streamflow in the catchment.
- Considering that the centre and north boreholes are located in the middle of the plantation, the 8 m mean groundwater level fluctuation may be as a result of the impact of trees on aquifer recharge rates. The west and south boreholes are located on the edge of the tree plantation, hence the 3 m groundwater level fluctuation suggests that the trees have less impact on groundwater recharge at the edge of the plantation.

Several conclusions have been established based on the observed groundwater level dynamics of the site. The similar trends in rising and dropping of water level in all boreholes suggest that all boreholes are drawing water from the same aquifer system. The response of the aquifer to recharge displays a well-identified seasonal water level fluctuation. Groundwater levels responds significantly to rainfall events, suggesting the existence of preferential flow paths through a direct connection between hillslope processes and the underlying bedrock aquifer. Groundwater levels in boreholes have continued to drop since 2007, when trees were re-planted. As trees continued to grow, groundwater levels also continue to drop. A groundwater level drop of 8 m and 3 m over the past decade was observed in the centre and north boreholes respectively. The continued drop of groundwater level indicates the impact of trees in reducing available water for recharging the regional aquifer in the catchment.

5.4. Aquifer Characterisation

Aquifer tests provide information on the type of flow that occurs in the aquifer and they are the simplest way to characterise aquifers in terms of parameters. The main purpose of conducting a pumping test in the present study was to obtain aquifer parameters of the study site, since hydraulic characterization of the aquifer has never been determined in the past. A simplified method of analysing constant discharge rate (CDR) tests proposed by Cooper and Jacob (1946) using semi-log plots of time-drawdown data was used to calculate the transmissivity (T) value of the aquifer from the pumping test. The Cooper-Jacob equation is given by:

$$T = \frac{2.30Q}{4\pi\Delta S} \quad (5.1)$$

Where,

T - is the transmissivity (m^2/d)

Q - is the discharge rate (m^3/d)

ΔS - slope of the straight line time-drawdown graph over one log cycle on the time axis.

The pumping test data was plotted on a semi-log scale as shown in Figure 5.11 with an approximate best-fit straight line. The full results of the CDR aquifer testing exercise are provided in Appendix I. The Cooper-Jacob equation was used to calculate the T value of the aquifer. Data inputs into the Cooper-Jacob equation are Q = 2.592 m^3/d and ΔS = 3.2 m. Solving Cooper-Jacob's equation provides an estimated aquifer transmissivity (T) value of 0.15 m^2 per day in the study site. The recovery data was analysed in a similar way to the pumping data. However, in the case of recovery analysis, residual drawdown is plotted against a ratio (t/t') of the time since pumping test started (t) to the time since the recovery test began (t'), both measured in minutes. The recovery equation is given by:

$$T = \frac{2.30Q}{4\pi\Delta S'} \quad (5.2)$$

Where,

T- transmissivity (m^2/d),

Q - discharge rate (m^3/d)

ΔS'- slope of the straight expressed as m/log cycle of t/t'.

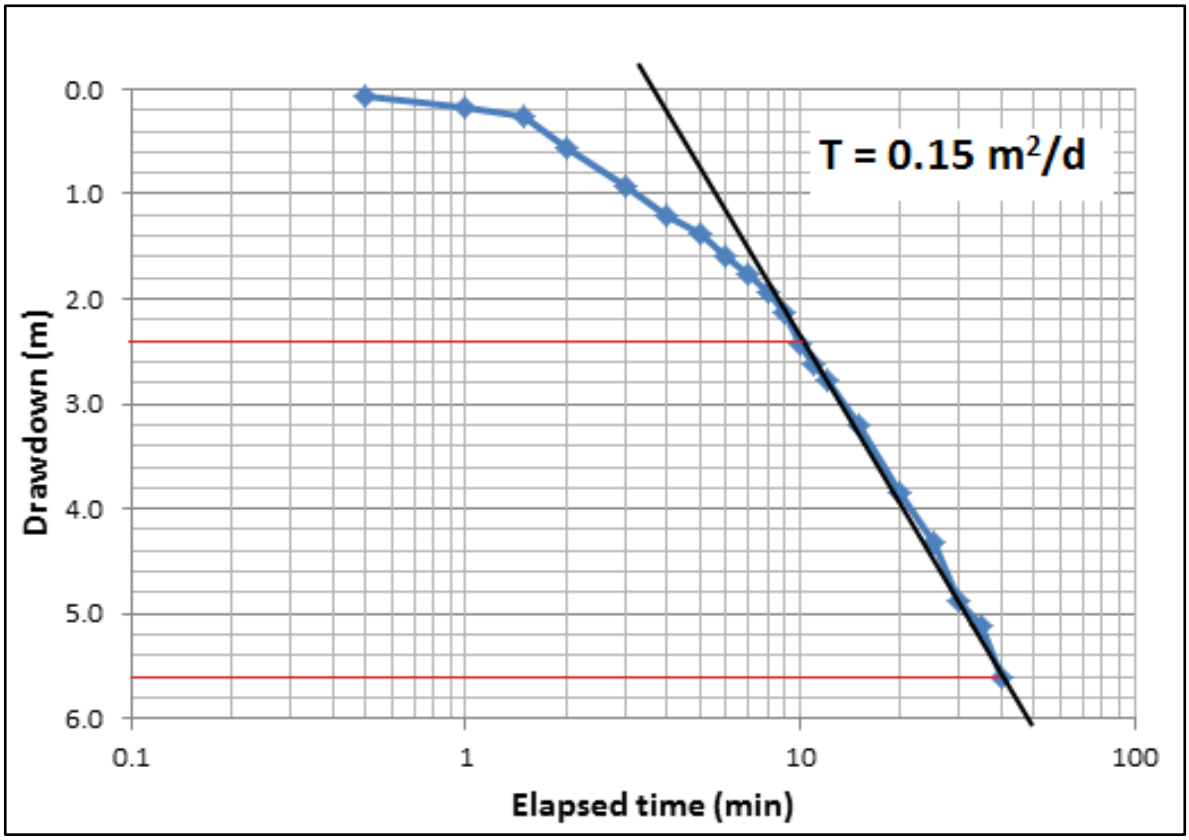

Figure 5.11. Semi-log plot used to solve Cooper-Jacob equation from a constant discharge rate pumping test.

The recovery test data was plotted on a semi-log scale as shown in Figure 5.12 with an approximate best-fit straight line. Data inputs into the Cooper-Jacob recovery equation are Q = 2.592 m^3/d, $\Delta S'$ = 0.093 m. Solving Cooper-Jacob's recovery equation provided an estimated aquifer transmissivity (T) value of 0.47 m^2 per day (m^2/d) in the study site. The two analyses provide a very low value for transmissivity. It can be estimated that the transmissivity of the aquifer ranges from 0.15 to 0.47 m^2 per day, indicating a poorly transmissive aquifer.

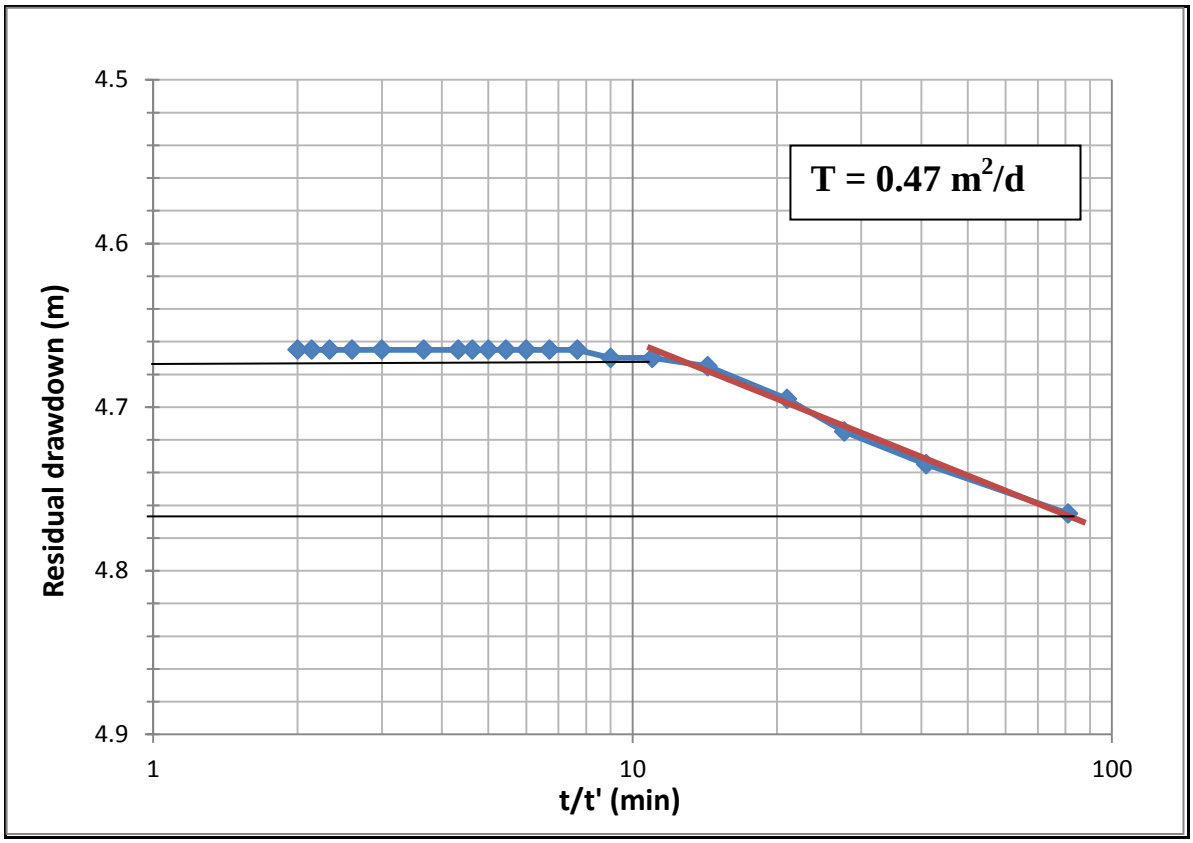

Figure 5.12. Semi-log plot used to solve Cooper-Jacob equation from the recovery test.

The FC program (Van Tonder *et al*. 2001) was also used to compare the transmissivity values obtained from the Cooper-Jacob equations and also to describe the type of flow through the aquifer formation. The best fit log-log plot used to describe the type of flow through the aquifer is given in Figure 5.13 and the basic FC Method recommendations are provided in Table 5.2. Using the log-log plot the following conclusions can be made about the type of flow through the aquifer:

- At an early time (2 min) the graph shows a liner flow in fracture, suggesting that this is a limited fracture and water is coming from the fracture and not the matrix.
- At medium time (3-40 minutes) the flow is now bilinear as the fracture has limited areal extent and water is now leaking from the matrix into the fracture.
- The shape of the graphs suggests that the aquifer concerned is a semi-confined aquifer.

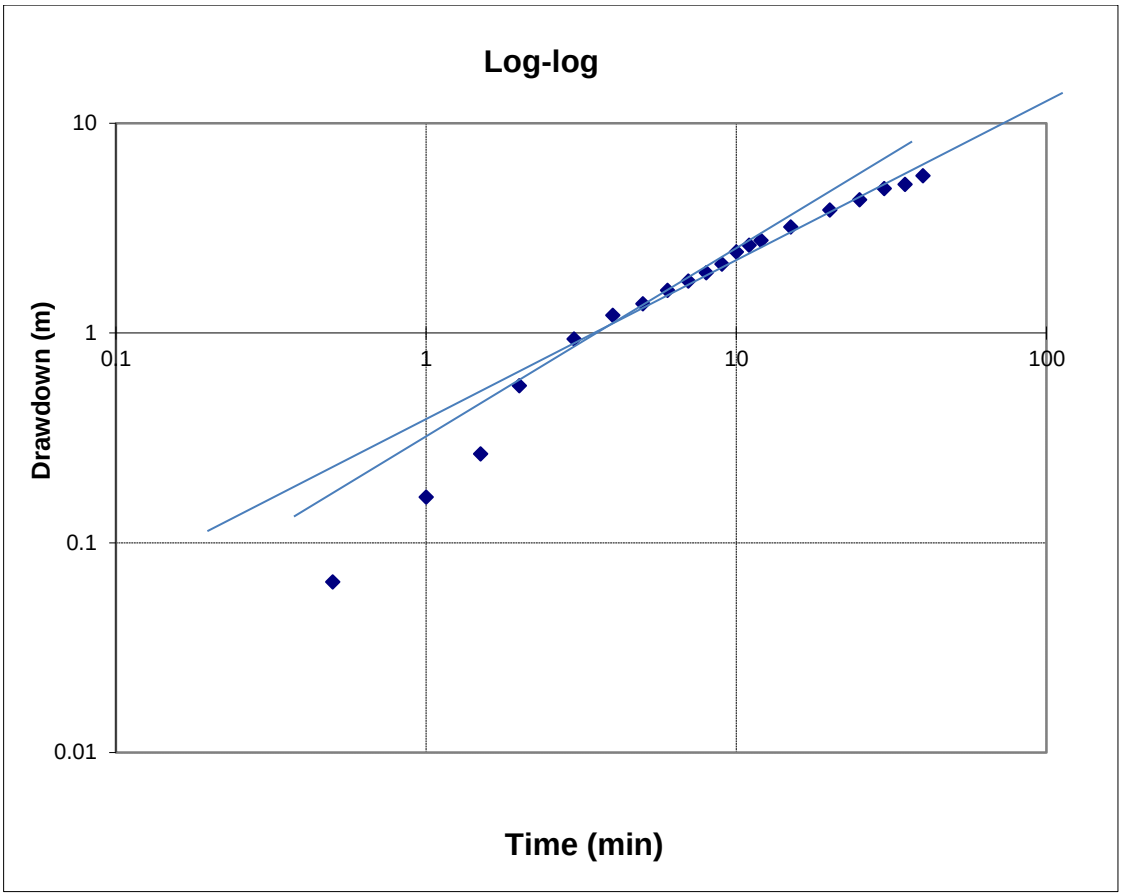

Figure 5.13. Log-log plot used to describe the type of flow through the aquifer.

Table 5.2. Basic FC method recommendations

Recommended abstraction rate (L/s)	0.03	24 hours per day
Hours of pumping per day	8	0.05 L/s for 8 h/d
Amount of water allowed to be abstracted per month	77.76	m^3
Borehole could satisfy the basic human need of	104	persons
Is the water suitable for domestic use		

The estimate of T-value can also be obtained from solving the Logan equation (van Tonder *et. al.*, 2001) given by:

$$T = \frac{1.22Q}{s} \qquad (5.3)$$

Where,

Q - abstraction rate in m^3/d,

S - drawdown (m) at the end of the test.

Inputs into the Logan's equation are Q = 2.592 m^3/d and s = 5.615 m. Solving Logan's equation provides an estimated transmissivity value of 2.03 m^2/d. This T value is way above the estimated values obtained from solving the Cooper-Jacobs equations and the FC program, thus indicating that the Logan's equation for pumping test analysis is not suitable for application in the study area. It is therefore concluded that the transmissivity of the aquifer in the study site would be close or within the range of 0.15 to 0.47 m^2 per day. These low transmissivity values are in close agreement with the groundwater contour map given in Figure 5.9, which shows contours that are close together. Groundwater contours that are close together tend to indicate low transmissivity values, because a steep hydraulic gradient would be required to drive water through the aquifer.

The hydraulic conductivity (K) defined as the volume of water that would move through a porous medium in a unit time under a unit hydraulic gradient through a unit area can be calculated by using aquifer thickness and transmissivity values. Taking into consideration that aquifer transmissivity (T) is given by the product of hydraulic conductivity (K) and the thickness of the saturated aquifer (equation 3.3), as discussed in Chapter 4. The hydraulic conductivity (K) may be estimated by solving equation 5.4 given by:

$$T = Kb$$

Therefore:

$$K = \frac{T}{b} \tag{5.4}$$

Where,

T – Transmissivity,

b – Saturated thickness of the aquifer.

Inputs into the equation are: T = 0.2 m^2/d and b = 5.615 m. Solving equation 5.4 provides an estimated aquifer hydraulic conductivity of 0.04 meters per day (m/d) for the study area. This indicates that the rock formations in the study area have low hydraulic conductivity. The common hydraulic conductivity for a weathered and fractured granite rock ranges from 0.0003 to 0.03 m/d as reported in Brassington (2006).

5.5. Groundwater Recharge Estimation

Groundwater recharge remains one of the critical parameters to determine in all hydrogeological studies and is one of the most difficult to quantify. Groundwater recharge estimation methods do not account for interception losses. As a result, all recharge estimation calculations must account for interception losses. In forestry catchment such as Two-Streams, interception can account for a large portion of rainfall. Bulcock and Jewitt (2012) measured canopy and litter interception of *Acacia mearnsii* and Eucalyptus grandis in the Two-Streams catchment research catchment and concluded that rainfall interception accounted for 57.7% of gross annual precipitation in the Two-Streams catchment. The mean annual rainfall in the Two-Streams catchment for January 2006 to December 2017 period is 778 mm. Therefore, subtracting 449 mm (57.7%) interception losses from the mean annual rainfall in the catchment becomes 329 mm. The RECHARGE spreadsheet program prepared by Van Tonder and Xu (2000) was used to provide an estimate of the recharge in the study site. Groundwater levels data from four boreholes (2STBH1, 2STBH3, 2STBH4 and 2STBH5) were used in the RECHARGE program as they are good representatives of the Two Streams catchment aquifer. The following recharge estimation methods included in the RECHARGE program were used to estimate groundwater recharge in the study area: Chloride mass balance (CMB), saturated volume flux (SVF), cumulative rainfall departure (CRD) and EARTH model. In addition to the RECHARGE program, the simple water balance and CMB methods were used to estimate groundwater recharge in the catchment.

5.5.1. Chloride mass balance (CMB) method

The CMB method is often used as a first approximation of recharge due to its simplicity and relatively low cost. Using the CMB method, the mean annual rainfall measured in the catchment from 1 January 2006 to 31 December 2017 is 778 and the mean annual effective rainfall after subtracting interception losses is 329 mm (57.7 %). The average chloride concentration in rainfall determined from rainfall samples collected during the present study is 0.53 mg/l. The minimum, maximum and average groundwater chloride values were analyzed from chloride samples collected from all boreholes in the study site during the present study. The estimated groundwater recharge values in the Two-Streams catchment calculated from the CMB method are presented in Table 5.3.

Table 5.3. Groundwater recharge estimation in the Two Streams catchment (CMB method)

	Chloride Concentration		**Recharge**	
Statistics	Groundwater (mg/l)	Rainfall (mg/l)	(mm/annum)	% MAP
Minimum	3.95	0.03	2.14	0.3
Maximum	8.71	1.11	42.40	5.4
Average	5.42	0.53	32.40	4.1
Mean annual Rainfall = 778 Effective precipitation = 329				

5.5.2. Simple water balance method

Groundwater water recharge can also be estimated using a simple water balance equation. Kok (1992) estimated groundwater recharge in Uitenhage springs successfully at 83% of average annual rainfall based on the following simple water balance equation:

$$\boldsymbol{Re}\ (\%) = \mathbf{100}\boldsymbol{x}\frac{\boldsymbol{Qs}}{\boldsymbol{Rf}*\boldsymbol{A}} \tag{5.5}$$

Where,

Q_s - is the average annual spring/stream flow (23938 m^3/annum)

R_f - is the average annual effective rainfall (329 mm/annum)

A - is the recharge area (A = 0.74 km^2).

Solving equation 5.5 of the water balance equation returns an estimated average groundwater recharge value of 9.8 % of mean annual precipitation (MAP) for the aquifer in the Two Streams catchment. This recharge value is over two times higher than the average recharge value of 4.1 % and also above the maximum recharge value of 5.4 % of MAP estimated from the CMB method.

5.5.3. Saturated volume fluctuation (SVF) method

The storage coefficient of an aquifer is defined as the volume of water that an aquifer releases or takes into storage per unit area of an aquifer per unit change in hydraulic head (Sophocleous, 1991). In the present study storativity values were obtained using the SVF method of the RECHARGE program. The S-value could not be obtained from pumping test data because there was no aquifer connectivity observed between the pumping and observation boreholes during pumping test data acquisition. Bredenkamp *et al.* (1995) caution against the use of S-values obtained from the pumping test data, as results can be unreliable in fractured rock environments due to problems associated with non-uniqueness, spacing of observation boreholes and the connectivity of observation boreholes with the pumping borehole. The S-value was estimated from the response of water level fluctuations using the recession period as per RECHARGE program. The rapid rise and drops in borehole water levels in the study area indicate a lower S-value that is mainly associated with fractures. According to Adams *et al.* (2004), rapid water level rises/drops indicate that the S-value is mainly associated with fractures, indicating lower S-values. Whereas slower water level rises/drops may indicate storage in the fractures and matrix, indicating high S-values. The SVF method from the RECHARGE program provided a recharge value of 40.1 mm per annum or 12.1% of MAP and a storativity value of 0.032.

5.5.4. Cumulative rainfall departure (CRD) method

The CRD method is a water balance approach and is based on the premise that groundwater level fluctuations are caused by rainfall events. The CRD method has been applied widely for estimating either effective recharge or aquifer storativity. The method uses the same data inputs as the SVF method. The recharge as observed from water level response (Figure 5.14) shows that water level responds significantly to rainfall events, indicating that recharge from the surface to groundwater is relatively fast. The recharge occurring in the study area was at maximum during the 2013 rainy season. In 2014 even when rainfall occurred, water levels did not respond to the high water levels as during the 2013 rainfall. This may be explained by the relative increase in storativity at shallow depth and since 2014 was relatively dry, storage at shallow depth may have been used by trees during the tree water uptake and evapotranspiration. The average groundwater recharge estimated from the CRD method is 39.9 mm per annum or 11.9 % of mean annual precipitation (MAP). This value is in close agreement with the recharge value of 12.1 % of MAP obtained from the SVF method.

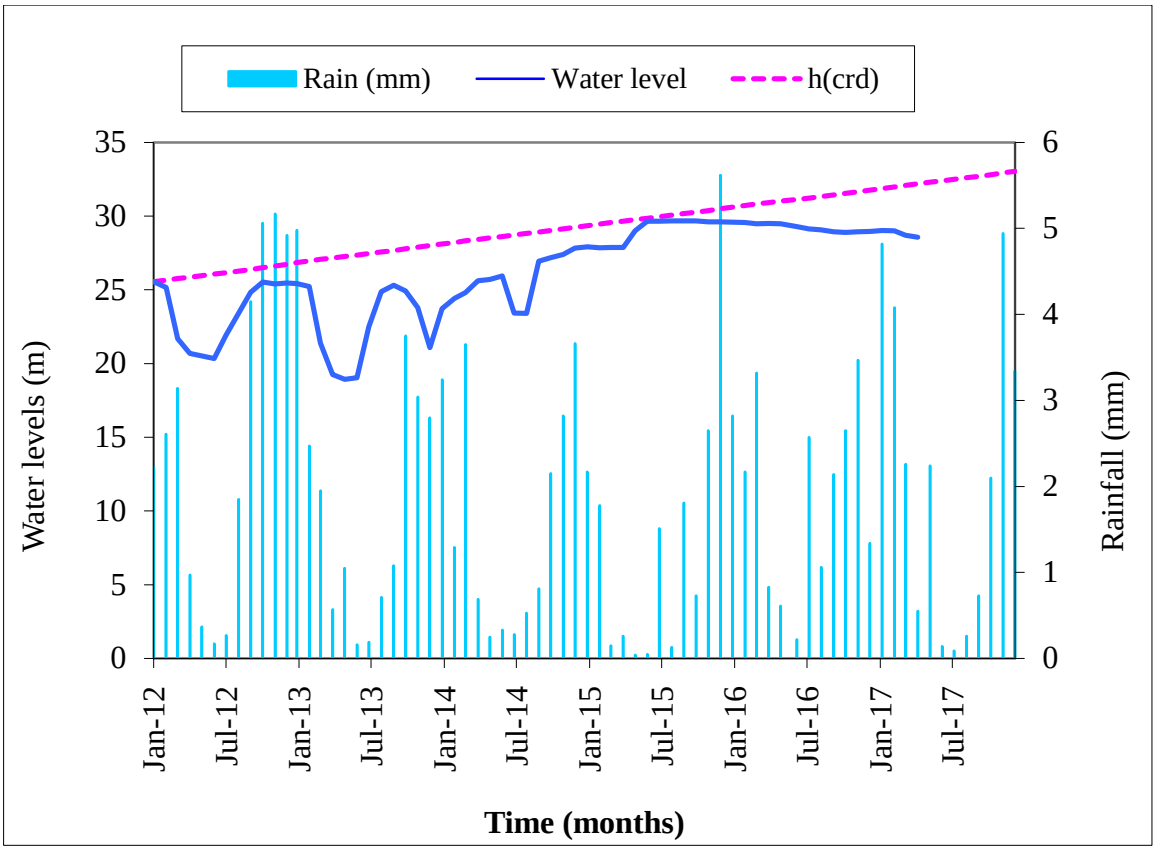

Figure 5.14. Borehole hydrograph used in the CRD method for estimating groundwater recharge in the catchment.

Table 5.4 presents a summary of groundwater recharge estimated for the study area using different recharge estimation methods associated with RECHARGE program. Data for the Qualified Guess methods were obtained by means of different maps included in the RECHARGE program. These maps are Vegter's Recharge Map (Vegter, 1995), the ACRU map (Schulze, 1997), the Harvest Potential Map (Baron J, 1998) and the groundwater component of river baseflow map (Vegter, 1995). Rainfall and groundwater chloride analyses data collected and analyzed during the present study were used for estimation of recharge using the chloride mass balance method (CMB). The soil information was a qualified guess according to the percentage area coverage with soil material in terms of percentage of clay. The geology information was also a qualified guess, indicated in brackets, according to the percentage of the area covered by sandstone, mudstone and siltstone (60%) and hard rock (40%). The results of the RECHARGE program indicate that the stream down-gradient of the catchment is perennial, effluent stream with an estimated baseflow of 100 mm per annum. The average groundwater recharge is estimated at 28.5 mm per annum or 8.6 % of MAP.

Table 5.4. Summary of groundwater recharge in the study area estimated using the RECHARGE program (Van Tonder and Xu (2000).

Method	**Groundwater recharge**		**Certainty**	
	(mm/a)	(% of rainfall)	1 = Low, 5 = Very High	
CMB	32.4	9.8	4	
SVF: Fit	40.1	12.1	4	
CRD	39.4	11.9	4	
Qualified Guesses				
Soil	13.7	4.1	3	
Geology	7.2	2.2	3	Area = 0.74 km^2
Vegter	32	9.7	3	
Acru	30	9.1	3	MAP = 329 mm
Harvest Potential	25.0	7.5	3	
Expert's guesses	16.6	5.0	3	
Base Flow (Min. Re)	100.0	30.2	1	
EARTH Model	106.7	32.2	1	
Average recharge	**28.5**	**8.6**		

The CMB method provided an estimated groundwater recharge values for the Two Streams catchment between 0.3 % (2.1 mm/a) and 5.4 % (42.4 mm/a), with an average recharge value of 4.1 % of MAP (32.2 mm/a). The recharge value obtained from the CMB method included in the RECHARGE program is 9.8 %, which is in agreement with the estimated recharge value of 9.8 obtained from solving the water balance equation of Kok (1992). The average groundwater recharge value obtained from the RECHARGE program is 8.6 % of MAP, this value is slightly higher than the maximum recharge value of 5.4 % of MAP obtained from the CMB method. This is expected as Van Tonder and Xu (2000) cautioned that the recharge values estimated with the RECHARGE program represents effective recharge and this value may be reduced by trees tapping water from the saturated zone in forested catchments.

5.6. Catchment Water Balance

The water-balance for the Two-Streams catchment was calculated based on rainfall, evapotranspiration, streamflow including baseflow using the water balance equation 4.6 and assuming that the groundwater contributing catchment to the stream gauging station is the same as the surface water contributing catchment. Rainfall, streamflow and plantation evapotranspiration (*Acacia mearnsii* and Eucalyptus) data are obtained from the database run by the Centre for Water Resources Research (CWRR) at the University of KwaZulu-Natal, Pietermaritzburg. Total streamflow was separated into direct runoff and baseflow components using the Web-based hydrograph analysis tool (WHAT) system.

The overall change in storage was calculated as the residual of the water-balance equation. Therefore, all errors inherent in each of the estimation and measurement of the water balance components is incorporated into the storage change term. The annual water balance results of the Two-Streams catchment for the period from 2007 to 2017 are presented in Table 5.6. In the water balance, the input parameter is rainfall (P), while output parameters are total evapotranspiration (ET), Direct Runoff (D_R) and groundwater outflow in the form of baseflow (G_{Bf}). A positive value for change in water storage indicates an increase in water storage, while a negative change equates to a decline in water storage. The calculated changes in water storage is indicated in Table 5.6 and shows a continuous groundwater storage reduction, responding to varying amount of water losses through evapotranspiration, direct runoff and groundwater discharge as baseflow. Annual storage changes are all negative over the entire 10 year period (2007 to 2017), except 2009 and 2012. This is expected, since 2012 recorded the highest rainfall over the 10 year period. The years with highest declines in storage are 2010, 2014 and 2015 which had -280, -268.8 and -217, respectively. These declines are expected as these years were relatively dry with their annual average rainfall lower than the 10 year average of 749 mm, whilst evapotranspiration continued to exceed rainfall inputs during these years. Baseflow and direct runoff were at the highest in the year 2007 with 63.2 mm/a direct runoff and 41.9 mm/a baseflow, respectively. This is expected as trees were newly planted (planted in August 2006) and were not expected to have significant impact on baseflow, instead direct runoff was expected to be favoured during this time. These results suggest that *Acacia mearnsii* trees display a significant impact in the water balance of the catchment, mainly by reducing baseflow and transpire significant amount of water into the atmosphere. The annual totals of four measured and calculated parameters show that evapotranspiration is the most dominant variable

which has almost always exceeded rainfall input into the catchment. These results are in agreement with stream and boreholes hydrographs presented in Figure 5.4 and Figure 5.10 respectively, which show that as trees continue to grow, stream level drops and groundwater levels in boreholes also continue to decline. Thus, indicating the impact of trees in reducing baseflow contribution to total streamflow, which subsequently result in a decline of streamflow and the groundwater level.

Table 5.5. Annual water balance components for the Two-Streams catchment from 2007 to 2017.

Year	**Rainfall**	**ET**	**Direct Runoff**	**Baseflow**	**Change in Water Storage**
	(mm)	(mm)	(mm)	(mm)	(mm)
2007	794	842	63.2	41.9	-153.7
2008	737	849	37.1	27.5	-176.3
2009	878	803	33.7	26.7	15.3
2010	639	893	14.9	11.5	-280.4
2011	909	872	22.6	17.5	-2.7
2012	951	850	28.8	18.6	53.2
2013	692	692	32.9	28.3	-61.0
2014	603	828	23.9	19.9	-268.8
2015	513	678	28.4	24.1	-217.0
2016	724	747	23.9	19.9	-67.2
2017	792	769	26.2	22.0	-25.1
Average	**748.40**	**802.08**	**30.52**	**23.42**	**-107.6**

5.7. Hydrochemical and Environmental Isotope Characterization

Hydrochemical and isotope analysis are important in aquifer characterization since they provide a picture of water chemistry and origin in the area. Water dissolves many inorganic materials of all three states and partially dissolves some inorganic substances. Because of this behaviour, water readily adopts the chemical behaviour of the environment that it interacts with. Hydrochemical and environmental isotope contents of various water sources were measured in the course of this research in order to understand the intricate relationship between rainfall, groundwater and surface water. The results are presented below.

5.7.1. Hydrochemical characterization

Hydrochemical information is important in aquifer characterization, since it supports the understanding of groundwater flow mechanisms as well as water quality for various uses (Leketa, 2011). The presentation of hydrochemical characteristics of the study area is divided into electrical conductivity profiling, hydrochemical composition and hydrochemical facies.

5.7.1.1. Electrical conductivity profile

The electrical conductivity (EC) of water is a measure of its ability to conduct an electric current and as such it is a direct indicator of the concentration of dissolved ions in water. Higher EC indicates the enrichment of dissolved matter in the water. EC is controlled mainly by the presence of major ions such as Sodium (Na^{+}), Calcium (Ca^{+2}), Potassium (K^{+}), Magnesium (Mg^{+2}), Chloride (Cl^{-}), Sulfate (SO_4^{-2}), Carbonate (CO_3^{-2}) and Bicarbonate (HCO_3^{-}) (CWT, 2004). EC profiles are plotted for four deep boreholes as shown in Figure 5.15 and Figure 5.16, respectively. EC profiles for 2STBH1 and 2STBH5 boreholes (Figure 5.15) indicate an increase in EC with increasing depth. The EC ranges between 53 mS/m and 65 mS/m from 25 m bgl to 40 m bgl for 2STBH1 (centre) and 30 mS/m 57 mS/m from 35 m bgl to 60 m bgl for 2STBH5 (south), respectively. A similar pattern is observed in the 2STBH3 (north) and 2STBH4 (west) boreholes as shown in Figure 5.16, which ranged between 26 mS/m to 34.6 mS/m from 31.5 m bgl to 60 m bgl and 20.1 mS/m to 27.2 mS/m from 33.5 m bgl to 60 m bgl respectively. The conductivity profiles show that groundwater in the catchment is having low conductivity, ranging between 20 mS/m to 65 mS/m for the water level measured between 25 m bgl and 60 m bgl. The low groundwater EC suggests the existence of rapid recharge into the aquifer and minimum residence time within the unsaturated zone and aquifer indicating local circulation rather than regional circulation.

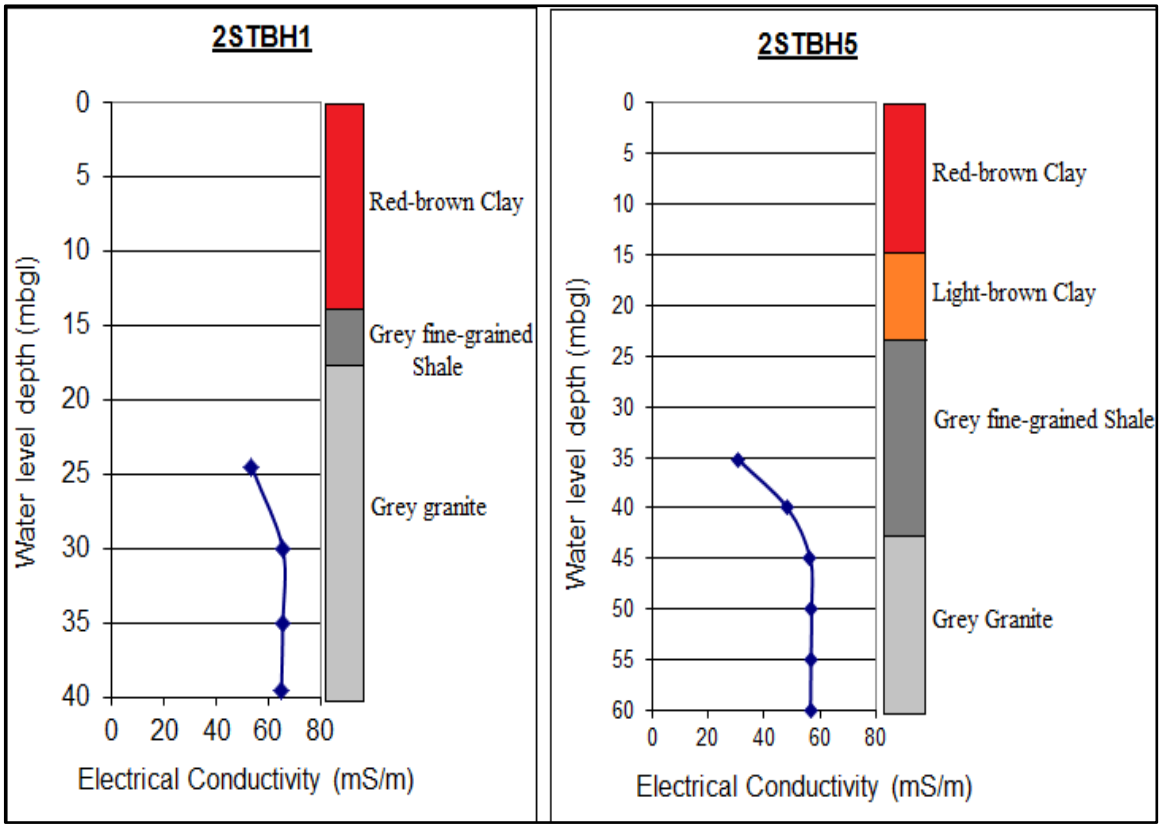

Figure 5.15. Electrical conductivity profiles for borehole 2STBH1 and 2STBH5

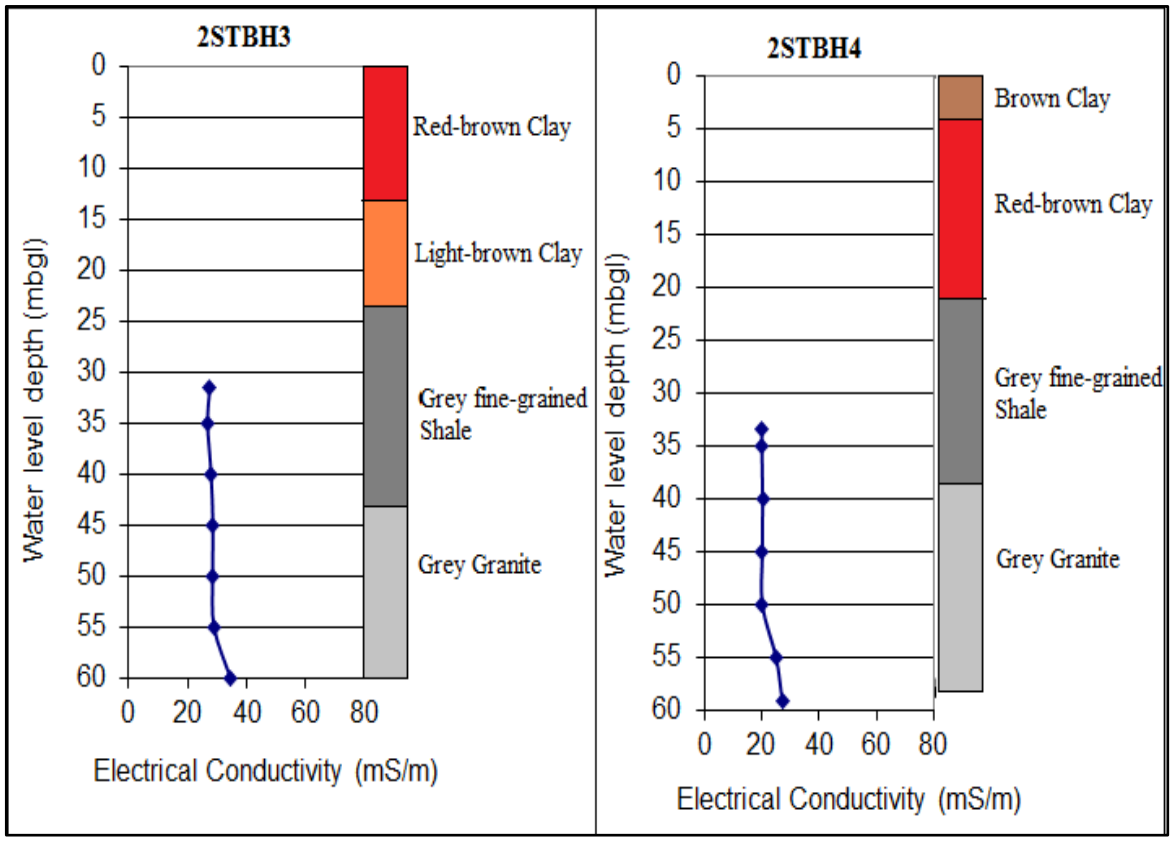

Figure 5.16. Electrical conductivity profiles for borehole 2STBH3 and 2STBH4

5.7.1.2. Hydrochemical composition

Hydrochemical information supports the understanding of groundwater flow mechanisms as well as water quality for various uses. The statistical summary table of hydrochemical data is presented in Table 5.6 and the entire data set is presented in appendix E. The pH of the stream and groundwater range from 5.8 to 8.0 with mean and median values of 6.8 and 6.7, respectively, indicating that water in the study area is mildly acidic to basic in nature. However, the water pH values fall within the natural water pH range. The mean and median values of electrical conductivity (EC) are 28.5 mS/m and 24 mS/m, respectively. The range is from a minimum of 17 mS/m to a maximum of 64 mS/m. The standard deviation of the EC is 10.8 mS/m, indicating small variation in the processes that affect surface and groundwater. Surface and groundwater samples are similar in chemical compositions as well, dominated by Na^+, K^+, Cl^- and HCO_3^-. The order of the relative abundances of cations and anions are $HCO_3^- > SO_4^{2-} > Cl^-$ and $Ca^{2+} > Mg^{2+} > Na^+ + K^+$, respectively. Calcium (Ca^{2+}) is the most abundant cation and bicarbonate (HCO_3) is the most abundant anion. The high concentration of HCO_3^- may be originating from the dissolution of carbonate minerals within the unsaturated zone or organic material decomposition in the rooting zone, which is characterised by low mineralisation as indicated by low electrical conductivity.

Table 5.6. Statistical summary of hydrochemical parameters of the study area

Parameter	**Unit**	**Min**	**Max**	**Mean**	**Median**	**Std. Dev.**
Temp	^0C	11.9	30.9	19.6	19.1	3.47
pH	units	5.82	8.00	6.84	6.82	0.43
EC	mS/m	17.0	64	28.51	24.00	10.86
TDS	mg/l	80	320	140.2	116.0	55.4
Na^+	mg/l	0.06	1.22	0.66	0.65	0.20
K^+	mg/l	0.0008	0.1085	0.0394	0.0439	0.0267
Mg^{2+}	mg/l	0.1823	1.3743	0.7813	0.7073	0.2432
Ca^{2+}	mg/l	0.2876	2.8707	1.1175	0.8505	0.6492
Cl^-	mg/l	0.1159	0.3731	0.1985	0.2003	0.0674
SO_4^{2-}	mg/l	0.3473	2.4934	1.3100	1.4674	0.5312
NO_3^-	mg/l	0.00003	0.03531	0.00601	0.00568	0.00631
HCO_3^-	mg/l	0.0154	2.6823	1.1342	1.0908	0.8822

The majority of the sampling points have EC values of less than 40 mS/m except for 2STBH1 (Centre borehole) which has EC values of between 44 mS/m and 64 mS/m. The EC of the stream and groundwater appear to vary with seasonal rainfall, rising with increasing rainfall and dropping towards the dry season (Figure 5.17). Based on the relationship between the rainfall and EC of the stream and groundwater, the following conclusions can be established:

- Stream and groundwater EC responds in a similar way to rainfall, both rising with increasing rainfall and dropping during periods of low rainfall. This relationship indicates a strong interaction between the stream and groundwater in the catchment.
- Low EC in groundwater samples suggested rapid (direct) recharge into the aquifer and minimum residence time within the unsaturated zone and the aquifer, which is an indication of local circulation rather than regional contribution. Thus indicating the existence of preferential flow paths that contributes significant amount of rainwater to groundwater, which in turn discharges into the stream and becomes streamflow.
- The low EC further suggests the fact that groundwater has undergone minimum mineralization, which can be attributed to recently recharged groundwater.

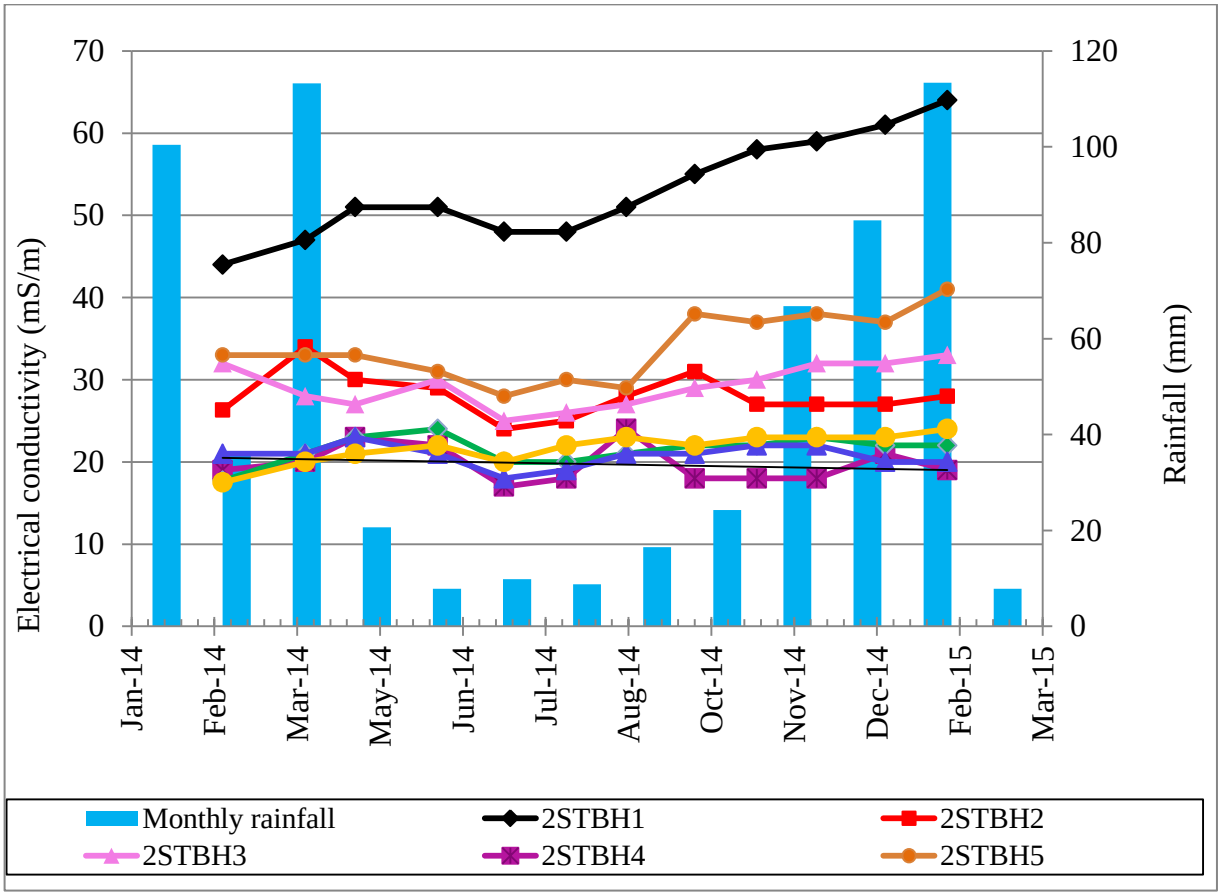

Figure 5.17. Relationship between rainfall and electrical conductivity of stream and groundwater over 12 months in the study area.

5.7.1.3. Sources of major ions

Soluble ions of surface and groundwater can originate from a variety of natural processes and sources including precipitation, evaporation and water-rock interaction (Zhang *et al.*, 2018). The functional sources of dissolved ions and dominant processes can also be broadly assessed by plotting a $HCO_3^- + SO_4^{2-}$ versus $(Ca^{2+} + Mg^{2+})$. Figure 5.18 shows that most groundwater samples plot on the 1:1 line, indicating that Ca^{2+}, Mg^{2+}, HCO_3^- and SO_4^{2-} are derived from the dissolution of carbonates and sulphate minerals. However, some samples of 2STBH1 plot below the 1:1 line, indicating the existence of reverse ion exchange as a minor process. The majority of stream and 2STBH2 (artesian borehole) samples plot above the 1:1 line, suggesting that $(Ca^{2+} + Mg^{2+})$ concentrations are slightly low compared with HCO_3^- and SO_4^-. As the dominant cation, Ca^{2+} is more preferably exchanged than Mg^{2+}. It can therefore be suggested that the low concentration of Ca^{2+} is due to ion exchange process that is a significant result from silicate weathering.

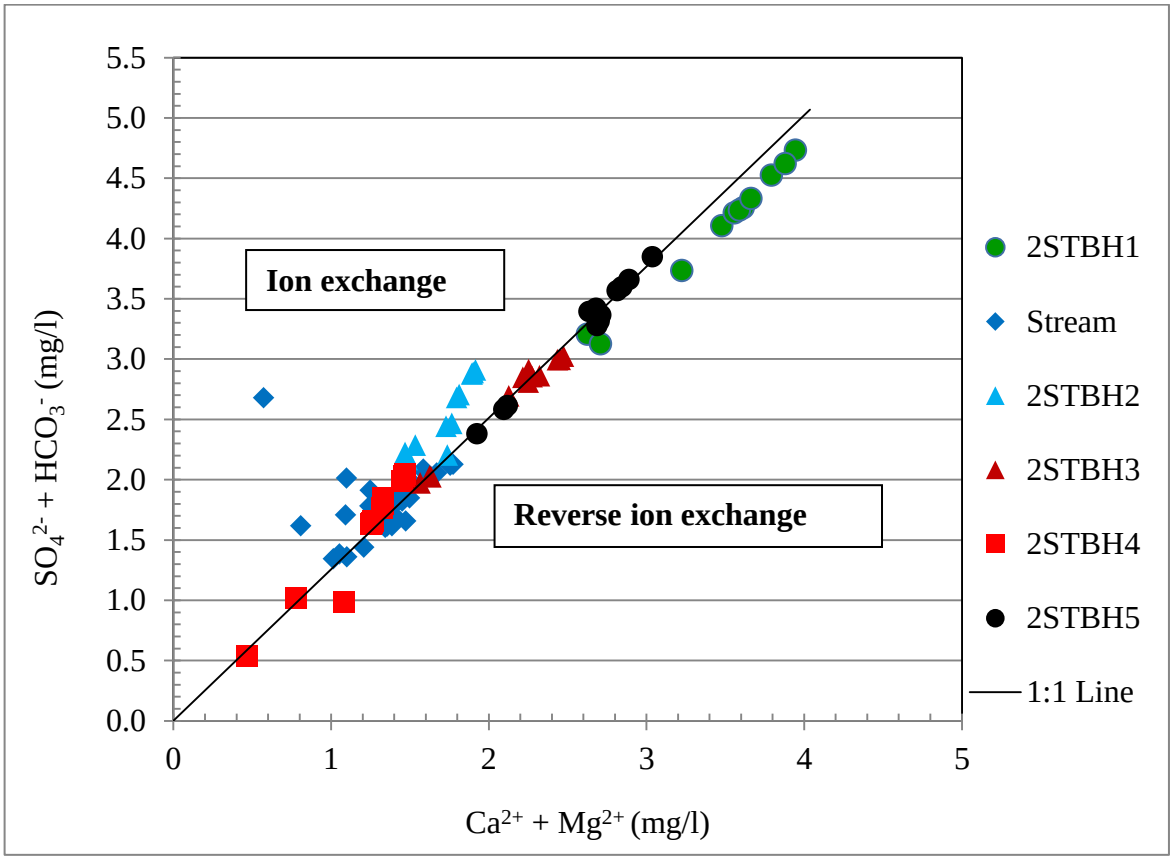

Figure 5.18. Relationship between $HCO_3^- + SO_4^{2-}$ and $Ca^{2+} + Mg^{2+}$ concentrations.

5.7.1.4. Hydrochemical facies

Hydrochemical facies are distinct hydrochemical signatures that cation and anion concentrations are described within defined compositional categories (Leketa, 2011). Graphical representation of major dissolved constituents in water helps in understanding its hydrochemical evolution, grouping and areal distribution. In this study, Piper trilinear diagram shown in Figures 5.19-21 were constructed to evaluate variations in hydrochemical facies of various sampling points, with Figure 5.20 and Figure 5.21 showing hydrochemical facies during wet and dry seasons, respectively. Distinctions could not be observed between shallow and deep groundwater samples. However, a slight variation could be observed between surface and groundwater chemical composition. Three hydrochemical facies were identified from the Piper trilinear diagram. The hydrochemical behaviour of water samples is almost similar between dry and wet season, with few shallow groundwater samples plotting in the same zone as stream samples. This is an indication of the existence of preferential paths that contribute significant amount of water to the shallow unconfined aquifer, which in turn discharges into the stream and becomes streamflow within minimum resident time. The hydrochemical facies in the Two-Streams catchment are described as follows:

- Facies 1: This hydrochemical facies is characterized by calcium and bicarbonate (HCO_3^-) ions as the most abundant ions giving rise to a Ca-HCO_3 type water. This is characteristic of freshly recharged groundwater that has equilibrated with CO_2 and soluble carbonate minerals under open system conditions in the soil zone. The dissolution of carbonate releases Ca^{2+} into solution made Ca-HCO_3 water type as a final product. Most groundwater samples falling in this zone are characterized by low mineralization as indicated by low electrical conductivity (EC) and relative enrichment in bicarbonate, attributed to recently recharged groundwater from rainfall.
- Facies 2: This facies has predominantly high concentration of calcium and chloride ions giving rise to a Ca-Cl hydrochemical water type and most stream samples fall into this zone. This zone provides an indication of water samples from an active discharge zone with a short residence time, where chloride is contributed from rainfall and shallow soil zones accumulated by evaporative processes.
- Facies 3: This hydrochemical facies indicate a mixed zone where water types cannot be identified by neither anion nor cation dominant. Some stream and groundwater samples fall into this zone indicating a strong inter-relationship between surface and groundwater in the study area.

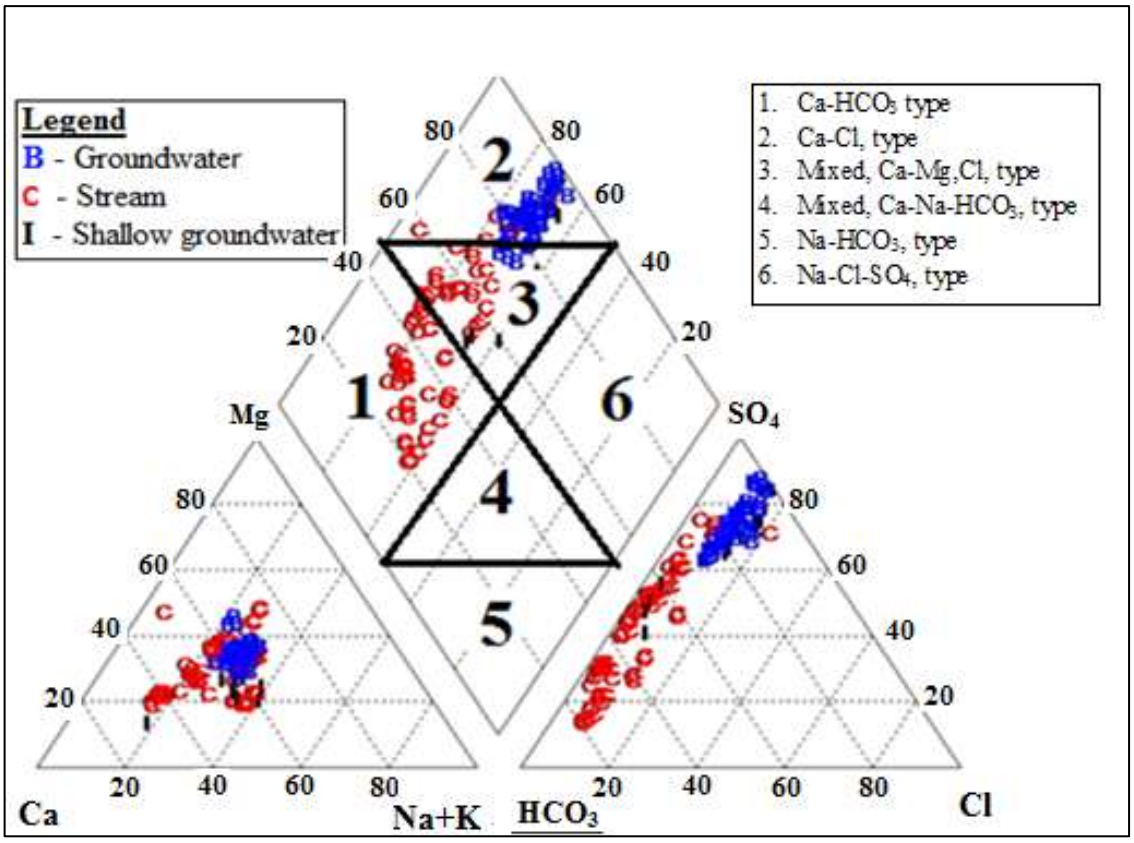

Figure 5.19. Piper diagram showing the relative proportions of major ions for three major groups of water samples in the Two Streams catchment.

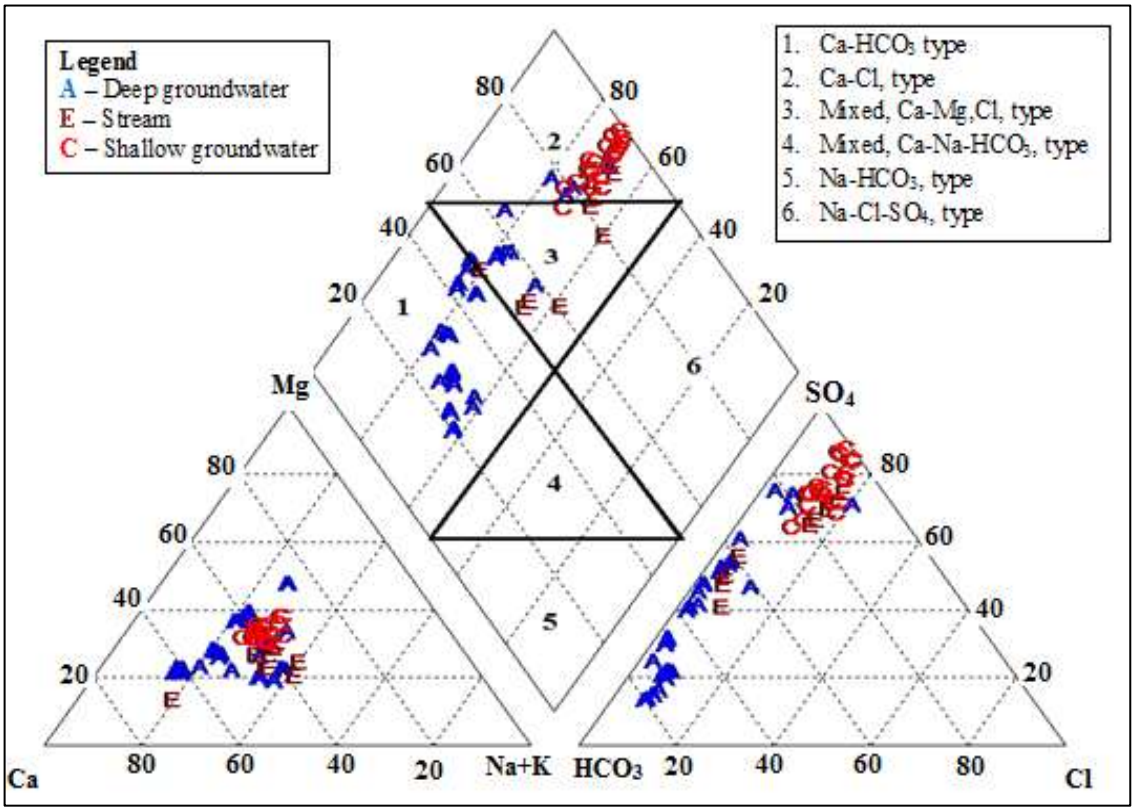

Figure 5.20. Piper diagram showing the relative proportions of major ions during wet season in the Two Streams catchment.

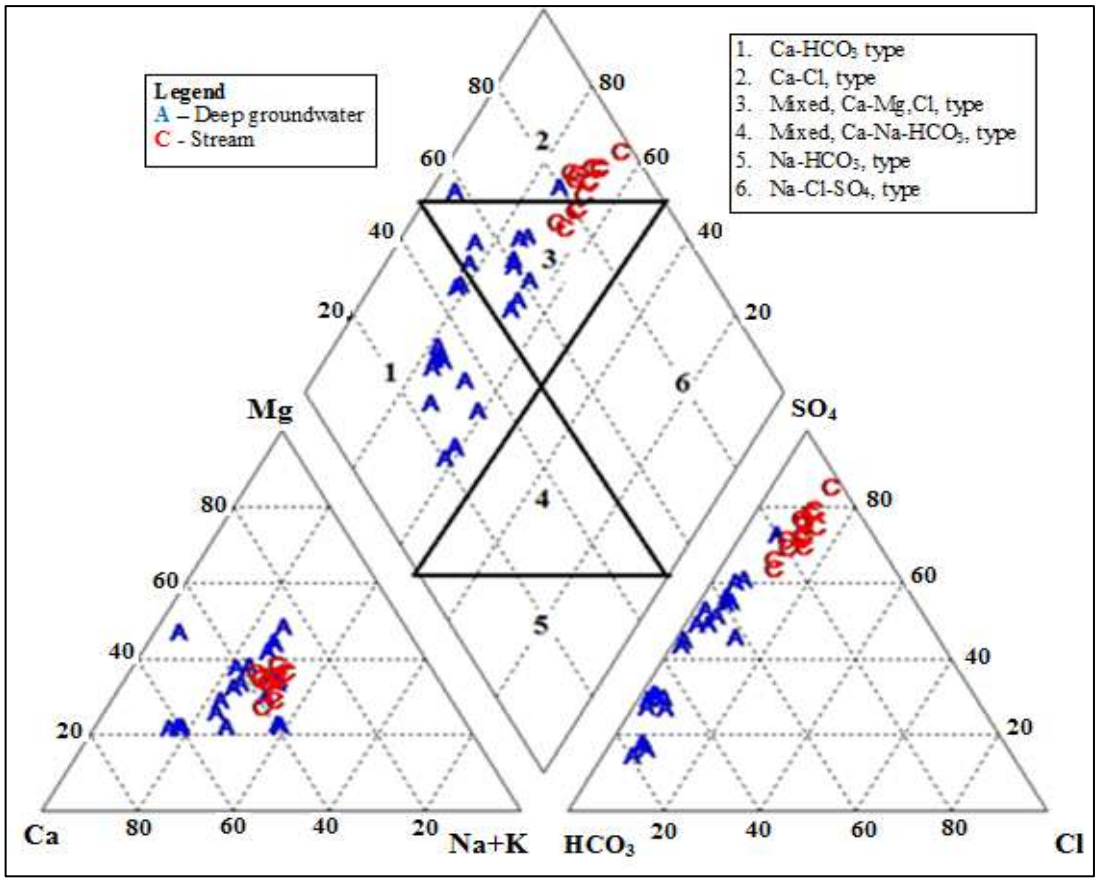

Figure 5.21. Piper diagram showing the relative proportions of major ions during dry season in the Two-Streams catchment.

All hydrochemical presentation tools reveal that the stream and groundwater in the study area have the same source. The stream and groundwater electrical conductivity (EC) responds in a similar way to rainfall, both rising with increasing rainfall and dropping during the dry season. The low EC in groundwater samples suggest the existence of direct recharge of the aquifer with minimum resident time on the surface. Thus, indicating the existence of preferential paths that contribute significant amount of rainwater to groundwater, which in turn discharges into the stream to form part of streamflow. The low EC also suggest that groundwater has undergone minimal mineralisation which can be attributed to recently recharged groundwater. The stream and groundwater samples are similar in chemical composition dominated by Ca^{2+}, Na^{2+}, K^{+}, Cl^{-} and HCO_3^{-}. Calcium is the most abundant cation and bicarbonate is the most abundance anion. The greater part of HCO_3^{-} may be originating from the dissolution of carbonate minerals. Groundwater samples are dominated by Ca-HCO_3 which is a characteristic of freshly, recently recharged groundwater from the infiltration of Ca-HCO_3 dominated rainwater, while stream samples are dominated by Ca-Cl type water, which is a characteristic of water from an active discharge zone.

5.7.2. Environmental isotope characteristics

Environmental isotopes have been proven to be important tools in hydrogeology for determining the origin of water, recharge and mixing processes, flow regime, residence time as well as changes in climatic conditions. Water samples collected from groundwater, stream and rainfall were analysed for stable environmental isotope signatures. The stable isotope plot in Figure 5.22 along with the local meteoric water line (LMWL) and global meteoric water (GMWL) lines indicate recharge from rainfall with insignificant evaporation during or prior to recharge. Most rainfall samples are relatively enriched in heavy isotope signal, while stream and groundwater samples are relatively depleted in heavy isotope signal (plot below LMWL). Stream and groundwater samples are close together, suggesting that groundwater is the primary source of streamflow in the study area. In this study, the signatures of hydrogen and oxygen isotopes for rainfall, stream and groundwater were also compared during dry and wet seasons. The results are illustrated in Figure 5.23 and Figure 5.24 for the wet and dry seasons, respectively. A significant difference is observed in hydrogen and oxygen isotope composition of rainwater. During the wet season, rainfall isotopes exhibit a depleted composition compared to that of dry season, suggesting different moisture sources due to the rainfall amount effect.

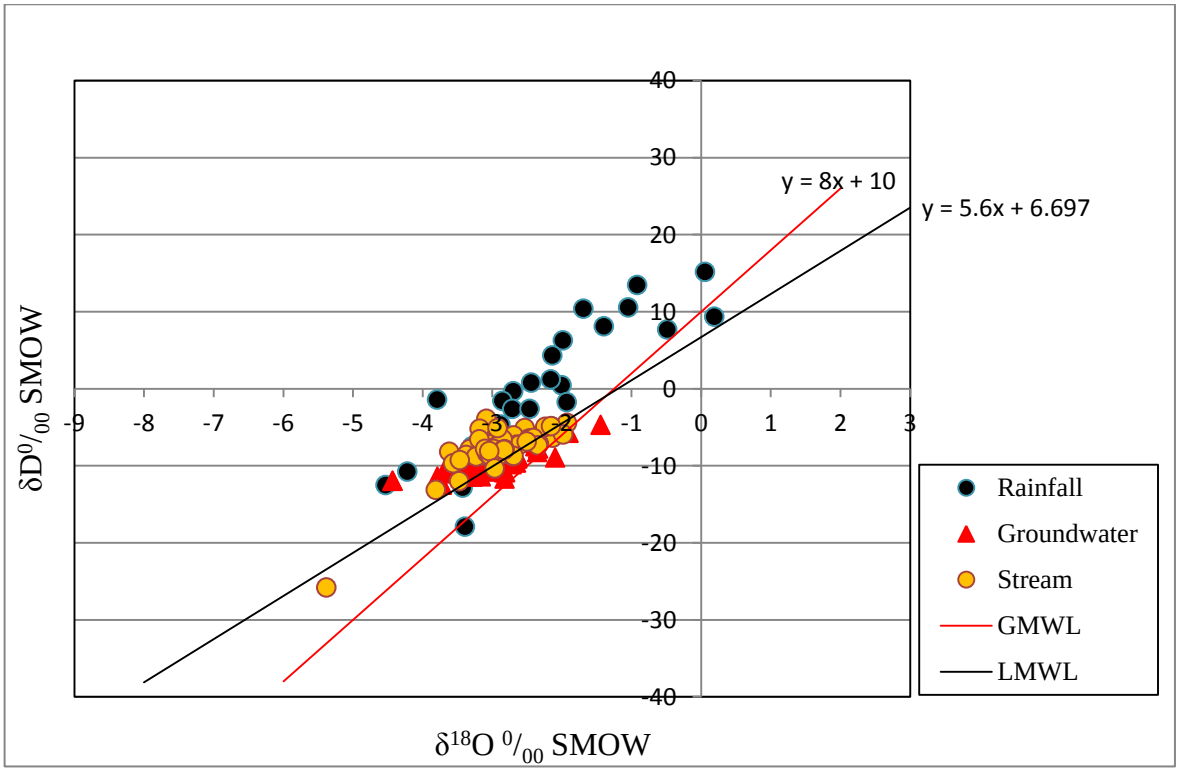

Figure 5.22. Isotope signatures of rainfall, stream and groundwater samples in the study area along with LMWL and GMWL.

5.7.2.1. Wet season isotope signals

The isotope signatures of rainfall, stream and groundwater during the wet season are similar and clustered together along the LMWL (Figure 5.23), indicating that the main source of stream and groundwater during the wet season is the rainfall. The isotopic composition of stream water is controlled by the mixing rates of surface runoff, interflow and baseflow. The difference between arrival times for interflow and surface runoff is in the order of hours, so they are both from recent rainfall and have similar isotopic composition. Therefore, from the isotopic composition point of view, stream water can be considered as being composed of groundwater and runoff during wet season. The groundwater composition is similar to those of rainwater and stream, indicating that the source of groundwater in the study area is rainwater which in turn discharges into the stream. The isotope data also suggests that groundwater recharge from the rainfall seems to take place rapidly, possibly via preferred pathways without undergoing significant evaporation. This is also supported by borehole hydrographs in Figure 5.8, which show a quick response of the groundwater to rainfall events. Given the fact that the isotope composition of all waters plot in the same zone, it can be concluded that rainfall which may have recently infiltrated and percolated without undergoing significant evaporation is the main contributor of water to the stream during the wet season.

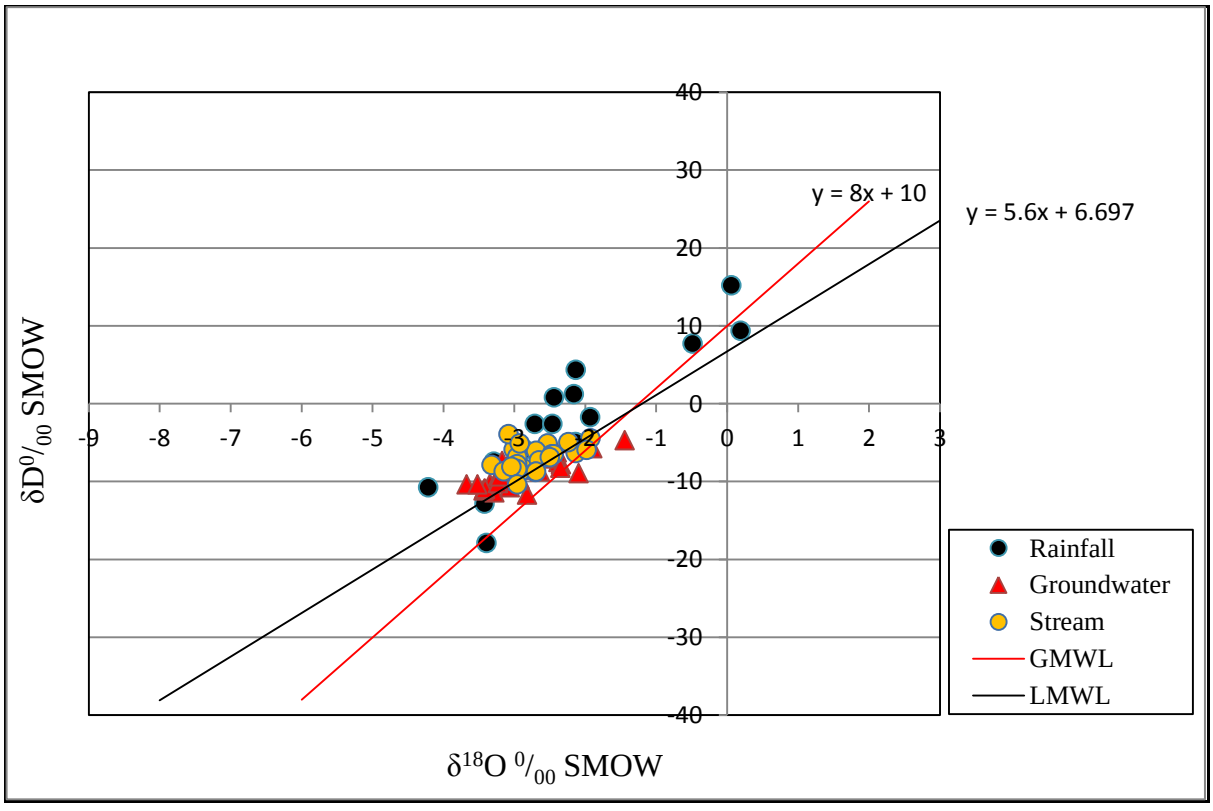

Figure 5.23. Isotope signatures of water samples during the wet season in the study area.

5.7.2.2. Dry season isotope analysis

During the dry season, rainfall isotope signatures are scattered along the LMWL (Figure 5.24) indicating that the rainfall moisture source has undergone some degree of isotopic modification during evaporation and condensation. The stream and groundwater samples are clustered together, suggesting that during dry season the main contributor of water flowing in the stream is groundwater discharge rather than rainfall.

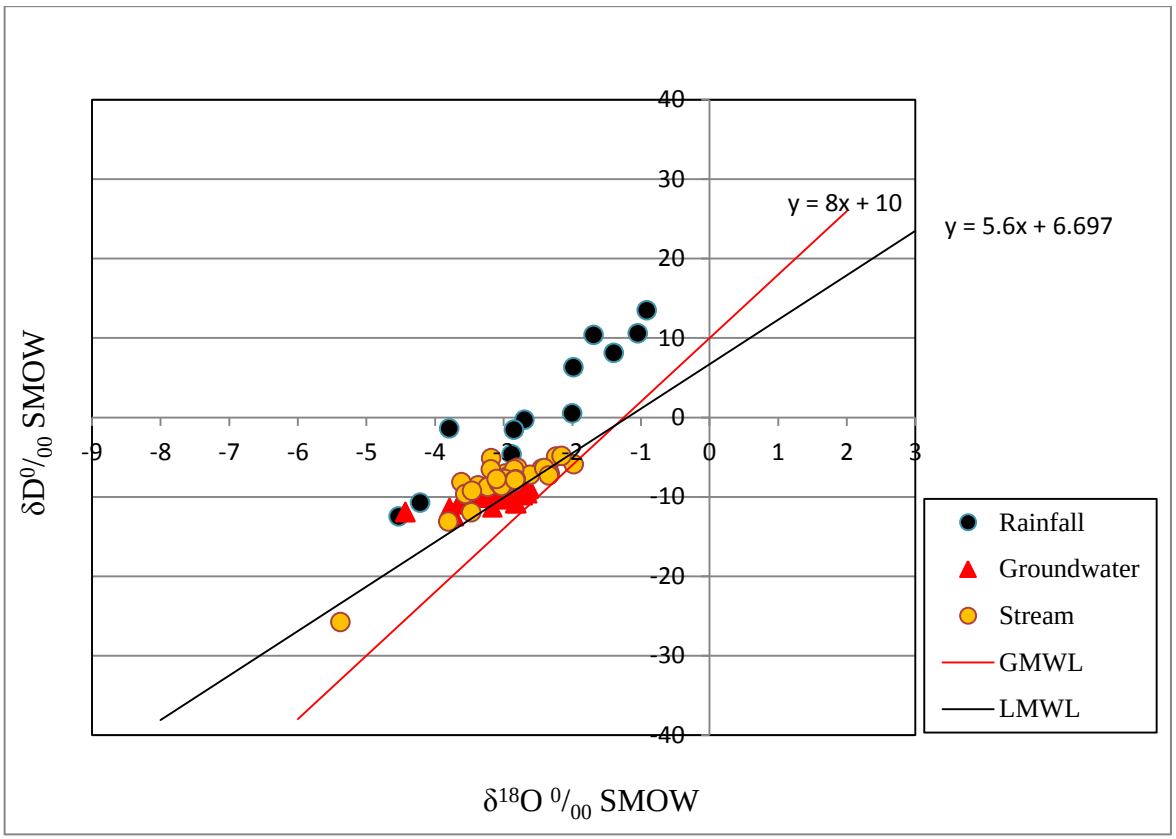

Figure 5.24. Isotope signatures of water samples during the dry season in the study area.

The stable isotope signatures indicate that the stream and groundwater in the study area are derived from local rainfall that has undergone insignificant evaporation and groundwater is the primary source of streamflow. The wet season rainfall isotope signatures exhibit a depleted composition compared to that of the dry season, suggesting different moisture sources. During wet season, groundwater composition is similar to those of rainwater and stream, indicating that the source of groundwater in the study area is rainwater, which in turn discharges into the stream. The isotope data also suggest that groundwater recharge from the rainfall takes place rapidly via preferential paths without undergoing significant evaporation. During the dry season, the main contributor of water flowing in the stream in the study area is groundwater discharge rather than rainfall.

5.8. Impacts of *Acacia Mearnsii* in Groundwater

The impacts of forests in the groundwater systems are usually inferred from changes in soil moisture, groundwater levels and stream discharges. Several reviews summarized the impacts of afforestation on groundwater (Peck and Williamson, 1987; Le Maitre *et al*., 1999; Smerdon *et al*., 2009). The key findings are that after the removal of forest in the catchment, wetter soil moisture contents and higher groundwater levels are expected due to reduced evapotranspiration rates. On the other hand, the planting of forests result in lower groundwater levels, reduced baseflow and consequently reduced streamflow. This is an indication that changes in forests can have significant impacts in groundwater recharge and consequently groundwater level and baseflow. Most studies regarding the impacts of forest on groundwater recharge or baseflow are conducted for a short period at small catchment scale. Direct and quantitative assessment on their long term and cumulative effects in large catchment scales are rare (Le Maitre *et al*., 1999; Smerdon *et al*., 2009). In this study, the impacts of *Acacia mearnsii* tree stand on the secondary groundwater system were studied over a 10 year period (2007 to 2017), by investigating the potential for direct groundwater uptake by roots, impacts of trees on groundwater levels as well as the impacts of trees on baseflow and consequently on streamflow.

5.8.1. Direct groundwater uptake

The primary factor affecting the pattern of water extraction by plants from the soil is rooting depth. Roots would penetrate as deep into the soil as required to reach available water, unless restricted by soil characteristics that prevent rooting or by permanent water table. Scott and Le Maitre (1998) reported that *Acacia mearnsii* roots can reach to a depth of 35 m and lateral roots can extend out to the radius greater than the height of the tree when not restricted by limiting growing space. In the Two-Streams catchment, *Acacia mearnsii* roots density has been reported to be increasing from 2006 when trees were planted. Roots were found up to a depth of 5 m in October 2012, six years after planting (Everson *et al*., 2014). Assuming the constant root depth growth rate of 5 m in 6 years, by 2017 tree roots would be approximately 10 m deep. According to Brunel *et al*. (1995), clay material formed from the weathering of shale can support a capillary fringe of up to 1.5 m. Therefore, considering the potential root depth of 10 m and maximum capillary fringe characteristics of 1.5 m in weathered shale material such as in the study area, the direct groundwater uptake by *Acacia mearnsii* tree roots would be possible for up to 11.5 m deep. Drilling and geophysical investigations identified three aquifer systems

that exist in the study area; namely, unconfined aquifer at the soil/bedrock interface ranging between 15 m mid-slope and 24 m bgl at the crest, a deep semi-confined aquifer made up of the weathered and fractured basement granite rocks at approximately 43 m bgl and pockets of scattered perched aquifer zones within the fine weathered zone above the thin unconfined aquifer which occur up to a depth of 24 m. The regional groundwater level measured from four boreholes in the study area ranged between 19 m bgl and 48 mbgl between 2006 and 2017. Given the possible direct groundwater uptake by tree roots of up to 11.5 m, the unconfined and semi-confined aquifers would not be available for extraction by *Acacia mearnsii* trees in the study area. The only possible available water for extraction by trees is the perched aquifer or pockets of water lenses located within the unsaturated zone and moisture in the unsaturated zone.

5.8.2. Impact of *Acacia mearnsii* on groundwater level and recharge

Acacia mearnsii stands were planted in August 2006. During the first few years of planting, groundwater level in boreholes (Figure 5.4 and Figure 5.25) showed a clearly defined seasonal water level fluctuation with water level rising during wet season and dropping during dry season. However, as trees continue to grow, groundwater levels in boreholes continued to decline and failed to rise to original water levels observed during the first few years after planting. The mean groundwater level graph (Figure 5.25) shows that groundwater levels in 2STBH1 and 2STBH3 boreholes declined by about eight (8) metres and six (6) metres between 2013 and 2017, respectively. This is in agreement with the study conducted by Bosch (1979) using Eucalyptus and Pinus, which demonstrated that afforestation causes reduction in baseflow and groundwater levels commencing some six to eight years after planting, irrespective of species. This is also in agreement with the calculated water balance of the Two-Stream catchment, which showed a gradual decrease in catchment water storage observed between 2007 and 2017. The highest storage change was observed in 2010 with annual change in storage of -280 followed by -268 in 2014 and -217 in 2015, with a 10 year average -107.6. These results indicate that the ten year old *Acacia mearnsii* stand has a significant impact on groundwater levels by extracting water from within the unsaturated zone to meet demands, thus reducing water available for recharging the regional aquifer. The indication that the decline in groundwater levels is a result of reduced available water for recharging the regional aquifer is in agreement with the results of groundwater recharge estimation undertaken in the present study. The CMB method provided an estimated minimum recharge value of 0.3 %, maximum

value of 5.4 % and an average recharge value of 4.1 % of MAP. These values are less than half of the recharge values of 9.8 % of MAP estimated using simple water balance method (Kok, 1992) and RECHARGE program (Van Tonder and Xu, 2000). This is an indication that *Acacia mearnsii* trees are reducing groundwater recharge by extracting water from the perched aquifer within the unsaturated zone, thus reducing water available for recharging the regional aquifer. This is in agreement with Kok (1976) who found that groundwater recharge was reduced from the expected 10 % of MAP under grassland to nil at 5 to 8 years after planting trees, due to water extraction from the unsaturated zone and increased transpiration rates. Van Tonder and Xu (2000) cautioned that recharge values obtained from the RECHARGE program may be reduced in forested catchments due to trees extracting water from either saturated or unsaturated zones. The study conducted by Kelbe *et al*. (1995) in the Zululand coastal plain concluded that the impacts of trees on groundwater is through the extraction of water from the unsaturated zone and shallow groundwater, thus reducing the proportion of rainfall that eventually recharges groundwater. These results imply that where there are deep soils, deeply fractured or decomposed rock, *Acacia mearnsii* trees can have a large impact on groundwater by dropping groundwater levels through extracting water from the unsaturated zone, thus reducing water available for groundwater recharge without necessarily having direct access to the groundwater.

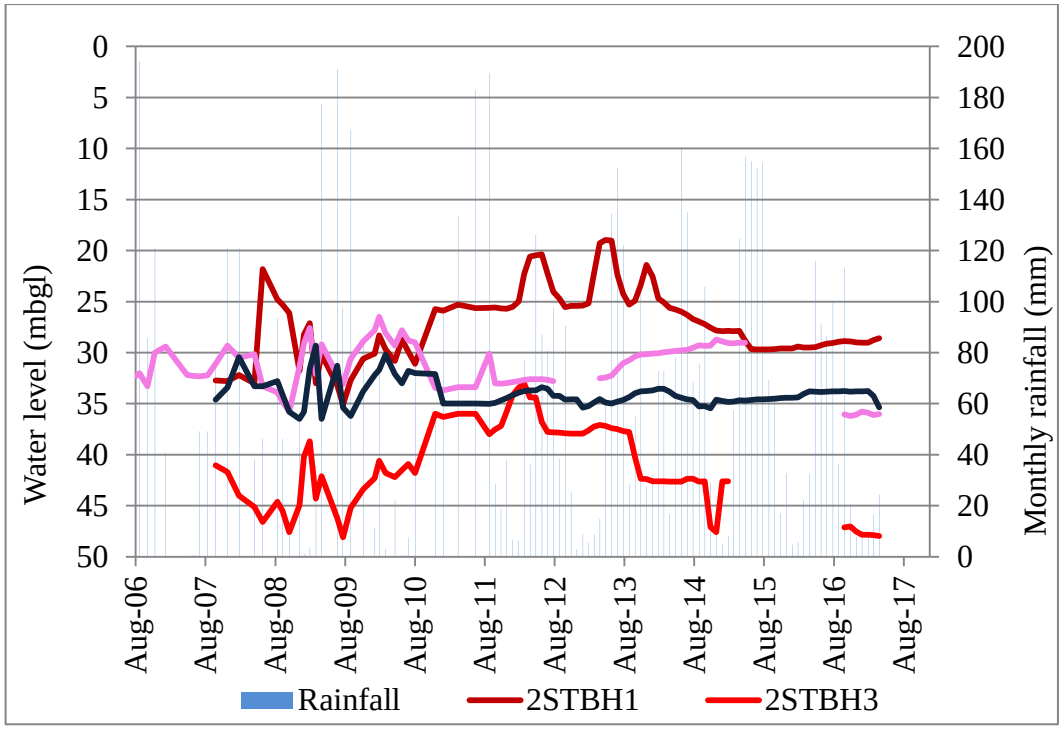

Figure 5.25. Mean groundwater level in relation to monthly rainfall from 2006 and 2017 in the Two Streams catchment.

5.8.3. Impact of *Acacia mearnsii* trees on baseflow

Baseflow is an important component of streamflow which comes from groundwater storage or other delayed sources, such as shallow subsurface storage. Baseflow separation techniques indicated that 57 % of total streamflow in the study area is attributed to baseflow. As expected, the baseflow (Figure 5.26) decreases drastically during the first five years of afforestation with *Acacia mearnsii* trees. There was an increase in baseflow in response to good rainfall recorded between 2011 and 2013, which was then followed by a decline in baseflow and levelling off between 2014 and 2017. These results are in agreement with the study conducted by Bosch (1979) which indicated that afforestation causes reduction in baseflow commencing some six to eight years after planting and levelling off at around 50 %. The maximum baseflow value of 43056.7 m^3/annum occurred in 2006, minimum value of 8420.88 m^3/annum occurred in 2010 with an average annual value of 19329.2 m^3. This is an indication that *Acacia mearnsii* trees affect baseflow by extracting water from the unsaturated zone, which then reduces the amount of water available for baseflow, hence the observed reduced baseflow contribution and subsequently reduced streamflow.

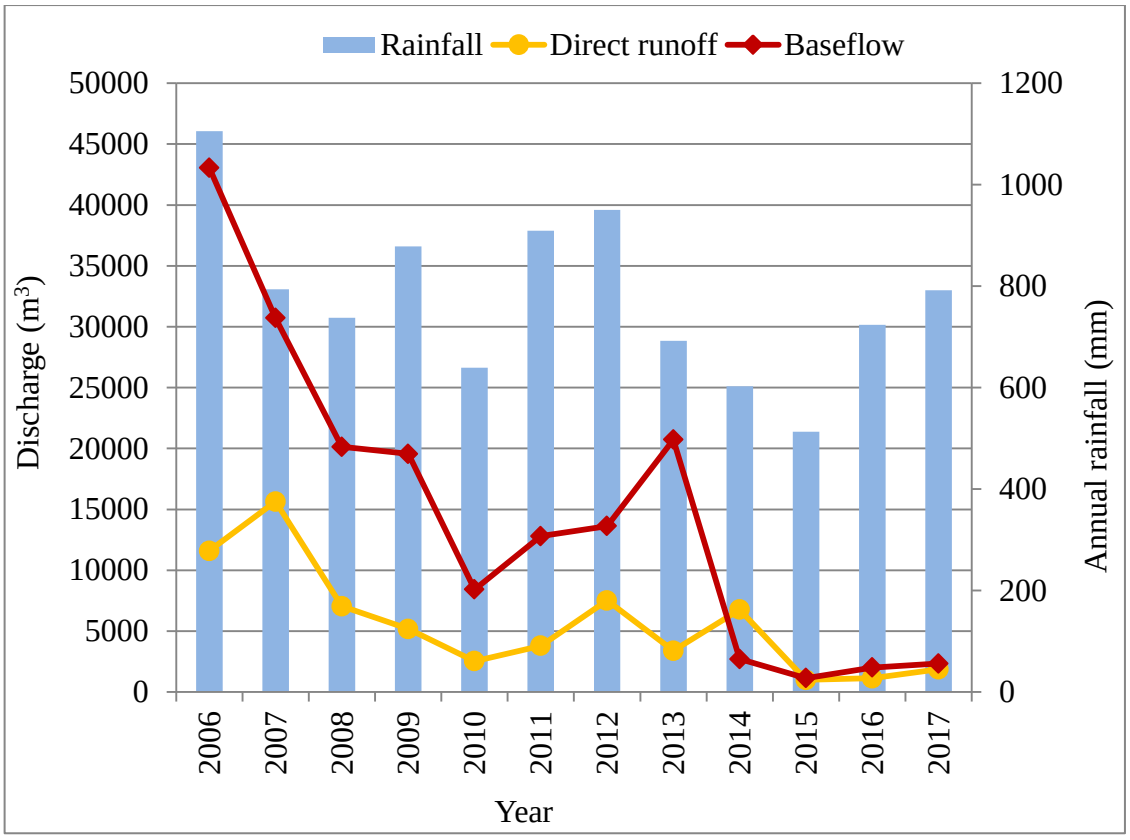

Figure 5.26. Annual baseflow and direct runoff with corresponding rainfall in the Two-Streams catchment.

5.7 Hydrogeological Conceptual Model

The foundation of all hydrogeological investigations is to gather sufficient reliable information to develop an understanding of a particular groundwater system. Such an understanding is usually presented in the form of a conceptual model of the study area and comprises a simplified but quantified description encompassing all aspects of the local hydrogeology of the area including aquifer physical framework, hydrostratigraphic units, hydraulic characteristics of aquifers, groundwater recharge, groundwater flow dynamics, groundwater storage changes and hydrogeochemistry, amongst others. The hydrogeological conceptual model of the Two-Stream catchment study site was developed by integrating and interpreting all geological, geophysical, hydrological, hydrogeological, hydrochemical and environmental isotope data that describe the hydrogeological conditions of the catchment. The conceptual model is based on the original data (chemical and isotope data, water level measurements, borehole logs, geophysical measurements, climatological data and hydraulic properties) determined from aquifer tests as well as information based on field observations undertaken from the current study and complemented by data from previous studies. The proposed hydrogeological conceptual model for the Two-Stream catchment is presented in Figure 5.27.

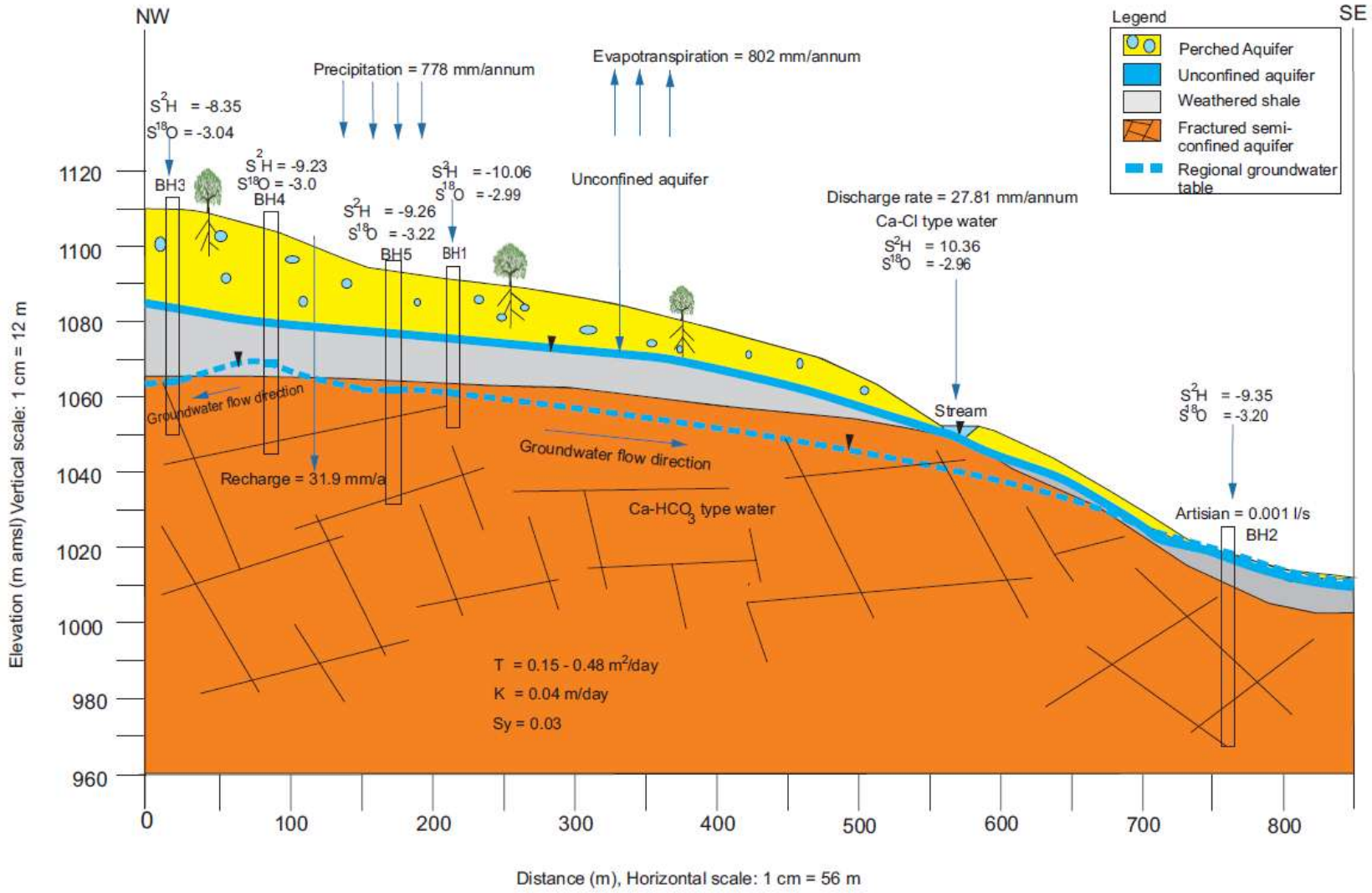

Figure 5.27. Hydrogeological conceptual model of the Two Streams catchment study site.

CHAPTER SIX: CONCLUSIONS AND RECOMMENDATIONS

6.1 Conclusions

The Two-Streams catchment has been used as an experimental catchment over the past decade to investigate the impacts of *Acacia mearnsii* on hydrological processes. These studies have focused mainly on evaporation and soil hydrological processes. Little attention was given into characterizing the hydrogeology of the catchment and investigating the impacts of deep-rooted plantations on the secondary aquifer system. Hence, this thesis investigates the site specific factors of the catchment such as aquifer characteristics, preferential flow paths and groundwater recharge, which are interpreted to understand the impacts of *Acacia mearnsii* trees on the secondary aquifer system.

The study area is located in the Seven Oaks district, within uMvoti local municipality in the KwaZulu-Natal midlands, South Africa and covers an area of about 0.74 km^2. It lies in the warm sub-tropical climate of South Africa, where summers are hot, humid and it is the main rainy season, whilst winters are cold and dry. The mean annual precipitation from 2006 to 2017 is 778 mm, average minimum temperature occurring in July is 4.5 ^{0}C, average maximum temperature occurring in March is 31.7 ^{0}C and the average mean temperature is 18.1 ^{0}C. The average annual evapotranspiration is 802 mm. The average annual stream discharge is 20387.40 m^3 of which 5619.10 m^3 is direct runoff and 14768.28 m^3 is the baseflow component. Geologically, the study area is underlain by red-brown clayey material with thickness ranging between 24 m at the crest, 15 m mid-slope and decreases towards zero at the toe of the hillslope. Deeper soil represents the deep weathering of the bedrock surface which is a dominant factor governing subsurface water flow paths in the catchment. There are lateral variations in water content distribution from wet to dry material in this formation, which gives rise to perched water table or pockets of water bearing material. The clayey layer is underlain by weathered shale with lateral changes in layer thickness, decreasing towards the toe of hillslope. The base of this layer is located at approximately 43 m bgl up-gradient and 25 m bgl down-gradient with an approximate thickness of 22 m. The interface between clayey material and weathered shale is saturated giving rise to a thin unconfined aquifer. Groundwater moves horizontally through this weathered unconfined aquifer and discharges into the stream. The water that does not move on top of bedrock moves laterally and vertically through fractures to recharge the underlying regional semi-confined aquifer. The shale layer is

in turn underlain by a deep fractured basement granite rock from 44 m bgl. The main weathered and fractured granitic basement aquifer occurs in a semi-confined conditions. However, artesian condition is encountered at a borehole located at the downstream end of the catchment. The regional groundwater flow direction around the study area is in an easterly to south easterly direction, mimicking surface topography. The aquifer is characterised by a transmissivity (T) of 0.15 to 0.48 m^2/d, hydraulic conductivity (K) of 0.04 m/d and a specific yield of 0.03. The dominant groundwater recharge mechanism is direct recharge at an average rate of 4.1 % of MAP.

Groundwater and stream samples are characterized by low mean specific electrical conductivity (EC) of 28.5 mS/m, indicating the existence of direct recharge and minimum resident time within the unsaturated zone and aquifer. The stream and groundwater systems are similar in hydrochemical composition, dominated by calcium (Ca^{2+}), sodium (Na^{+}), potassium (K^{+}), chloride (Cl^{-}) and bicarbonate (HCO_3^{-}). Ca^{2+} is the most abundant cation and HCO_3^{-} is the most abundant anion. Three main hydrochemical facies were identified: (1) Ca-HCO_3 type water, characterized by low mineralization and relative high concentration of HCO_3^{-} attributed to an active young and flushed groundwater system; (2) Ca-Cl water type, which is a characteristic of water from an active discharge zone with short residence time, where chloride is contributed from rainfall and shallow soil zones accumulated by evaporative processes; (3) mixed zone type water, where water types cannot be identified by neither any anion nor any dominant cation. All samples have δD and $\delta^{18}O$ isotopic values that plot on or above the local and global meteoric water lines, indicating recharge from rainfall with insignificant evaporation during or prior to recharge. Most stream and groundwater samples plot together indicating that groundwater is the primary source of streamflow in the study area. Seasonal isotope analysis indicates that the main source of stream and groundwater in the study area is wet-season rainfall. The isotope composition of stream water is controlled by mixing rates of surface runoff, interflow and baseflow. The difference between arrival times for interflow and surface runoff is in the order of hours, thus they are both from recent storms and have a similar isotopic composition. The main contributor of streamflow during dry season is groundwater discharge rather than rainfall. The impacts of forests in groundwater are usually inferred from the changes in soil moisture, groundwater levels and stream discharges. The key findings of forests impacts in groundwater are that after the removal of forests, wetter soil moisture contents and higher groundwater levels are expected due to reduced evapotranspiration rates. Whilst afforestation results in reduced recharge, lower

groundwater levels, decline in baseflow and consequently declined in streamflow. In this study, the impacts of *Acacia mearnsii* tree stand on the secondary aquifer system were studied by investigating potential for direct groundwater uptake by tree roots, impacts of trees on groundwater recharge and groundwater levels as well as the impacts of trees on baseflow. Assuming the potential root depth of 10 m and maximum capillary fringe characteristics of 1.5 m, direct groundwater uptake by *Acacia mearnsii* tree roots would be possible for the depth of up to 11.5 m. Therefore, unconfined and semi-confined aquifers would not be available for direct extraction by *Acacia mearnsii* trees in the study area. The only possible available water for extraction by *Acacia mearnsii* trees is the perched aquifer and soil moisture within the unsaturated zone. The impact of *Acacia mearnsii* trees on groundwater levels show that as trees continue to grow, groundwater levels in boreholes continued to decline and failed to rise to original water levels, observed during the first few years after planting irrespective of rainfall inputs. The groundwater level decline of six to eight metres was observed in the north and centre boreholes between 2013 and 2017 respectively. This is an indication that afforestation causes decline in groundwater levels commencing some six to eight years after planting. The results indicate that *Acacia mearnsii* stands can have significant impact on groundwater by extracting water from within the unsaturated zone, thus reducing the amount of water available for recharging the regional aquifer and subsequently inducing regional groundwater level decline. Baseflow is an important component of streamflow as about 57 % of total streamflow in the study area is attributed to baseflow. Unlike groundwater levels, which showed five years lag time prior to declines in groundwater levels after afforestation, baseflow declined drastically during the first five years of afforestation. There was an increase in baseflow during 2011 to 2013 probably in response to good rainfall recorded during these years, which was then followed by a decline in baseflow and levelling off between 2014 and 2017 due to drought spells. This is an indication that *Acacia mearnsii* trees affect baseflow as well by extracting water from within the unsaturated zone, which than reduces the amount of water available for baseflow contribution, hence the observed declines in baseflow contribution to total streamflow. The results of this study show that direct groundwater uptake by tree roots from the saturated zone at Two-Streams would not be possible due to limiting root depth. Thus, in instances where the regional groundwater table is not available for direct abstraction by tree roots, *Acacia mearnsii* trees can have a large impact on groundwater through extracting water from within the unsaturated zone, reducing the proportion of rainfall that eventually contributes recharge to the aquifers and baseflow, without necessarily having direct access to the groundwater proper.

6.2 Recommendations

- *Acacia mearnsii* trees have been replaced by Eucalyptus trees in the catchment. It has been noted during this study that some of the groundwater monitoring equipments have not been in good working order lately. It is therefore recommended that all water balance measurements (including groundwater level measurements) be continuous measured to determine the influence of these fast-growing trees on the hydrological processes of the catchment and to provide calibration data for simulation models.
- The effects of afforestation on secondary aquifer system have been investigated to a certain extent during the course of this study and the results have been very promising. In the future more pressure will be placed on forestry companies and the government to provide answers to questions around the effect of afforestation on water resources. It is recommended that groundwater recharge studies that that have been conducted during the course of this study be continued to investigate the effects of Eucalyptus trees on the groundwater system in the catchment.
- Surface energy balance models using remote sensing data can provide estimates of plant water-use over wide areas, but require validation for South African conditions. The evaporation measurements existing in the site provides a good opportunity for testing these techniques in afforested catchments. These will in the future provide water resource managers with catchment wide water use estimates and assist researchers in monitoring the impacts and changes associated with global climate change.

REFERENCES

Adams, S. Titus, R. & Xu, Y. (2004). Groundwater recharge assessment of the basement aquifers of central Namaqualand. WRC Report No 1093/1/04. Pretoria, South Africa, 31-35.

Allison, G. B., Barnes, C. J., Hughes, W. M. & Leany, F .W. J. (1984). Effect of climate and vegetation on oxygen-18 and deuterium profiles in soils. Isotope Hydrology 1983. Proc. Symposium, Vienna, IAEA, 105-123.

Allison, G. B. & Hughes, M. W. (1972). Comparison of recharge to groundwater under pasture and forest using environmental tritium. *Journal of Hydrology 17*, 81-95.

Baldocchi, D. D. & Xu, L. (2007). What limits evaporation from Meditererranean oak woodlands- the supply of moisture in the soil, physiological control by plants or the demand by the atmosphere?. Ecosystem Science Division, University of California, Berkeley, United States. 2114-2120.

Baron, J., Seward, P. & Seymour, A. (1998). The groundwater harvest potential map of the Republic of South Africa. Department of Water Affairs and Forestry, Pretoria, South Africa, Gh, 3917.

Benyon, R. G., Theiveyanathan, S. & Doody, T. M. (2006). Impacts of tree plantations on groundwater in South-Eastern Australia. Kingston, Australia. *Australian Journal of Botany 54*, 181-192.

Berman, E. S., Gupta, M., Gabrielli, C., Garland, T. & McDonnell, J. J. (2009). High-frequency field-deployable isotope analyzer for hydrological applications. *Water Resources Research*, *45*(10).

Bosch, J. M. (1979). Treatment effects on annual and dry period streamflow at Cathedral Peak. S. Afr. For. J. 108, 29–38.

Bosch, J. M. & Hewlett, J. D. (1982). A review of catchment experiments to determine the effects of vegetation changes on water yield and evaporation. *Journal of Hydrology* 55, 3-23.

Brassington, R. (2006). Field Hydrogeology. London: Geological society of London hand book series, Open University Press.

Bredenkamp, D. B., Botha, L. J., Van Tonder, G. J. & Van Rensburg, H. J. (1995). Manual on quantitative estimation of groundwater recharge and aquifer storativity. WRC Report TT 73/95. Pretoria, South Africa.

Bronstert, A., Glusing, B. & Plate, E. (1998). Physically-based hydrological modeling on the hillslope and micro-catchment scale: examples of capabilities and limitations. Hydrology, Water Resources and Ecology in headwaters. Italy. IAHS Publ. No. 248, 207-215.

Brunel, J. P., Walker, G. R. & Kennett-Smith, A. K. (1995). Field validation of isotopic procedures for determining sources of water used by plants in a semi-and environment. *Journal of Hydrology 167*: 351-368.

Bulcock, H. H. & Jewitt, G. P. W. (2012). Field data collection and analysis of canopy and litter interception in commercial forest plantation in the KwaZulu-Natal Midlands. *Hydrology and Earth systems Science, 16*, 3717-3728.

Burger, C. (1999). Comparative evaporation measurements above commercial forestry and sugarcane canopies in the KwaZulu-Natal Midlands. MSc. Agric. thesis, University of KwaZulu-Natal, Pietermaritzburg, South Africa.

Cannon, W. A. (1949). A tentative classification of root systems. *Ecology* 30, 544-548

Clark, I. & Fritz, P. (1997). Environmental isotopes in Hydrogeology. Lewis Publishers. New York. 80-92.

Clulow, A. D, Everson, C. S, & Gush, M. B. (2011). The long-term impact of *Acacia Mearnsii* trees on evaporation, streamflow and groundwater resources. WRC Report No. TT 505/11. Pretoria, South Africa. 2-90.

Colville, J. S. & Holmes, J. W. (1972). Water table fluctuations under forest and pasture in a karstic region of southern Australia. *Journal of Hydrology 17,* 61-80.

Cooper, H. H. & Jacob, C. E. (1946). A generalized graphical method for evaluating formation constants and summarizing well-field history. *Eos, Transactions American Geophysical Union*, *27*(4), 526-534.

Council for Geoscience (1992). 1:250 000 Geological Map Series, 2930 Durban.

De Beer, H. (1986). Black Wattle. Farming in South Africa, Weeds. Department of Agriculture and Water Supply, Pretoria, South Africa.

Delta Mine Training Centre, Alaska, USA. Available from: http://www.dmtcalaska.org/exploration/ISU/unit3/u3lesson3html. [Accessed 1 March 2019].

De Wit, M. P., Crookes, D. J. & Wilgen, B. W. (2001). Conflicts of interest in environmental management: Estimating the cost and benefits of tree invasion.

CSIR Division of Water, Environment and Forestry Technology, Pretoria, South Africa.

Du Preeze, J. (2007). Hydrogeological investigation of Eshane bulk water supply, uMzinyathi district municipality, uThukela water. Pietermaritzburg, South Africa. 5-7.

DWAF, (1995). Characterization and Mapping of the groundwater resources KwaZulu-Natal Province. Pretoria, South Africa. 40-60.

DWAF, (1998). Hydrogeological map series 1:500 000, 2928 Durban.

Dye, P. J. & Poulter, A. G. (1995): A field demonstration of the effect on streamflow of clearing Invasive pine and wattle trees from a riparian zone. *South African Forestry Journal, 173*, 27-30.

Eckhardt, K. (2005). How to construct recursive digital filters for baseflow separation, Hydrol. Processes, 19, 507-515.

Edmunds, W. M. & Gaye, C. B. (1994). Estimating the special variability of groundwater recharge in the Sahel using chloride. *Journal of Hydrology, 156,* 47-59.

Eriksson, E. & Khunakasem, V. (1969). Chloride concentration in groundwater recharge rate of chloride deposition in the Israel coastal plain. *Journal of Hydrology, 7,* 178-197.

Everson, C. S., Clulow, A. D., Becker, M., Watson, A., Lorentz, S., Bulcock, H., Ngubo, C. & Mengistu, M. (2014). The long term impacts of *Acacia mearnsii* trees on evaporation, streamflow, low flows and groundwater resources. Phase ii: Understanding the controlling environmental variables and soil water processes over a full crop rotation. WRC Report K5/2022. Pretoria, South Africa. 19-164.

Famiglietti, J. S., Rudnicki, J.W. & Rodell, M. (1998). Variability in surface moisture content along a hillslope transect: Rattlesnake Hill, Texas. *Journal of Hydrology 210,* 259-281.

Fanning, D. S. & Fanning, M. C. B. (1989). Soil: Morphology, Genesis and Classification. Wiley and Sons, New York. 360–369.

Fette, M. W. (2005). Tracer studies of river-groundwater interaction under hydropeaking conditions. Swiss Federal Institute of Technology Zuric. Phd dissertation. Germany. 22-52.

Freeze, R. A. & Cherry, J. A. (1979). Groundwater. Prentice-Hall, Inc. Englewood Cliffs, New Jersey. 47-49.

Gat, J. R. (1996). Oxygen and hydrogen isotopes in the hydrologic cycle. Annu. Rev. Earth Planet. Department of Environmental Sciences and Energy Research, Weizmann, Israel. 24, 225-62.

Gat, J & Tzur, Y. (1967). Modification of the isotopic composition of rainwater by processes which occur before groundwater recharge. *Proceedings of the Symposium on Isotopes in Hydrology,* International Atomic Energy Agency, Vienna, 49-60.

Gat, J. G. (2010). Isotope hydrology. A study of the water cycle. *Series on environmental science and management Vol.6*. Weizmann institute of Science, Israel. 58-140.

Gorgens, A. H. M. & Van Wilgen, B. W., (2004). Invasive alien plants and water resources in South Africa: current understanding, predictive ability and research challenges: Working for Water. *South African Journal of Science, 100* (1-2), 27-33.

Groundwater Primer. (1997). Agricultural and Biological engineering, Purdue University, United States Environmental Protection Agency. USA. Available from: http://mikeb203.tripod.com/water/src/geo2.htm. [Accessed 04 March 2019].

Healy, R. W. (2010). Estimating groundwater recharge. Published by Cambridge University Press, Cambridge. 245.

Hibbert, A. R. (1967). Forest treatment effects on water yield. International symposium on forest hydrology. Pergamon, Oxford. 527-543.

Hiscock, K. (2005). Hydrogeology: Principles and Practice. Blackwell Publishing, Oxford. 26-34.

Holmes, J. W. & Colville, J. S. (1970b). Forest hydrology in karstic region of Southern Australia. *Journal of Hydrology 10*, 59-74.

Holmes, J. W. & Sinclair, J. A. (1986). Water yield from some afforested catchments in Victoria. Hydrology and water resources symposium, Griffith University, Brisbane, 25-27 November 1986. The Institute of Engineers Australia: Barton. 214-218.

Jarmain, C. & Everson, C. S. (2002). Comparative evaporation measurements above commercial forestry and sugarcane canopies in the KwaZulu-Natal Midlands. Final report to the Department of Water Affairs and Forestry.

Johansson, P. (1987). Methods for estimation of direct natural groundwater recharge in humid climates. Royal Institute of Technology. Department of Land Improvement and Drainage, Stockholm.

Kelbe, B. E., Rawlins, B. R. & Nomquphu, W. (1995). Geohydrological modelling of St. Lucia. Technical Report of Department of Hydrology, University of Zululand, South Africa.

Kelly, E. F., Chadwick, O. A., Hilinski, T. E. (1998). The effects of plants on mineral weathering. Biogeochemistry. 21-42.

Kendal, C. & MacDonnell, J. J. (1998). Isotope tracers in Catchment Hydrology. Amsterdam.

Kok, T. S. (1992). Recharge of springs in South Africa. Technical report GH 3748. Department of Water Affairs, Pretoria, South Africa.

Kok, T. S. (1976). Die geohidrologie van die Bloemendalbasboompiaas, distrik Pietermaritzburg, Natal. Internal report GH 2924 of the Geohydrology Directorate of the Department of Water Affairs and Forestry, Pretoria, South Africa.

Kotze, D. J. C. (2001). Hydrogeology of the Table Mountain sandstone aquifer-Klein Karoo. Un-published PhD Thesis. University of the Free State, Institute for Groundwater Studies Bloemfontein, South Africa. 41-70.

Kruseman, G. P. N. and De Ridder, A. (1994). Analysis and evaluation of pumping test data (2nd Ed.). Amsterdam. International Institute for Land Reclamation and Improvement, 6700 AA Wageningen, The Netherlands. 1-128.

Ladouche, B., Probst, A., Viville, D., Idir, S., Baqué, D., Loubet, M., Probst, J. & Bariac, T. (2001). *Hydrograph separation using isotopic, chemical and hydrological approaches (Strengbach catchment, France).* Journal of Hydrology, vol. 242 (3-4). 255-274.

Leketa, K. C. (2011). Flow characteristics of groundwater systems: An investigation of hydraulic parameters. MSc. Report for University of the Free State. Institute for Groundwater Studies, Bloemfontein, South Africa. 5-92.

Le Maitre, D. E., Scott, D. F. & Colvin, C. (1999). A review of information on interactions between vegetation and groundwater. CSIR division of Water, Environment and Forestry Technology, Stellenbosch, South Africa. 137-140.

Le Maitre, D. E., Van Wilgen, B. W., Chapman, R. A. & Mckelly, D. H. (1996). Invasive plants and water resources in the Western Cape Province, South Africa: Modeling the consequences of a lack of management. *Journal of Applied Ecology*, *33*, 161-172.

Lerner, D. N., Issar, A. S. & Simmers I. (1990). A guide to understanding and estimating natural recharge, Int. contribution to hydrogeology, I.A.H. Publ., Vol. 8, Verlag Heinz Heise. Hanover. 345.

Lim, K. J., Engel, B. A., Tang, Z., Choi, J., kim, k. S., muthukrishnan, D. T. (2005). Automated Web GIS Based Hydrograph Analysis Tool, WHAT. JAWRA Journal of the American Water Resources Association 41 (6), 61-80.

Lin, H. S., Kogelmann, W., Walker, C., & Bruns, M. A. (2006). Soil moisture in a forested catchment: A hydropedological perspective. *Geoderma*. 131, 345-368.

Lloyd, J. W. (1986). A review of aridity and groundwater. *Hydrological processes*, *1*(1), 63-78.

Lloyd, J. (2010). Water to people, or people to water?, Groundwater, 48 (6), 929-931.

Loke, M. H., (2000). Electrical imaging surveys for environmental and engineering studies: A practical guide to 2-D and 3-D surveys. *Electronic version available from http://www.terra plus.com*.

Lorentz, S. A., Bursey, K., Idowu, O., Pretorius, C. & Ngeleka, K. (2007). Definition and up-scaling of key hydrological processes for application in models. Report No. K5/1320. Water Research Commission, Pretoria, South Africa.

McElrone, A. J., Choat, B., Gambetta, G. A. & Brodersen, C. R. (2013). Water uptake and transport in vascular plants. Nature Education Knowledge. 4(5), 2-9.

McGuire, K. J. & McDonnell, J. J. (2006). A review and evaluation of catchment transit time modelling. *Journal of Hydrology 330*, 543-563.

Mosley, M. P. (1982). Surface flow velocities through selected forest soils South Island, New Zealand. *Journal of Hydrology 55*, 65-92.

Nahar, N., Govindaraju, R. S., Corradini, C. & Morbidelli, R. (2004). Role of run-on for describing field-scale infiltration and overland flow over spatially variable soils. *Journal of Hydrology 286*, 36-51.

Nepstad, D. C., de Carvaiho, C. R., Davidson, E. A., Jipp, P. R., Lefebvre, P. A., Negreiros, G. H., da Silva, E. D., Stone, T. A., Trumbore, S. E. & Veira, S. (1994). The role of deep roots in the hydrological and carbon cycles of Amazonian Forests. *Mature* 372, 666-669.

Nieber, J. L., Steennhuis, T. S., Walter, T. & Bakker, M. (2006). Enhancement of seepage and lateral preferential flow by biopores on hillslopes. *Biologia, Bratislava, Suppl. 61*, 225-228.

Nuberg, I., George, B. & Reid, R. (2009). Agroforestry for natural resource management. CSiro publishing, Cooling wood VIC, Australia.

Parsons, R. (2004). Surface water: groundwater interaction in a South African context. Report No. TT218/03. Water Research Commission, Pretoria, South Africa. 4-13.

Peck, A. J. & Williamson, D. R. (1987). Effects of forest clearing on groundwater. *Journal of Hydrology 94*, 47–65.

Pinder, G. F. & Celia, M. A. (2006). Subsurface Hydrology. John Wiley & Sons, Inc. Hoboken, New Jersey. 343-366.

Poulter, A. G., Soko, S. & Maphanga, D. (1994). A Comparative Study of Water Use by Invasive and Indigenous Species Found in Riparian Zones. Report for Department of Environmental Affairs and Forestry, Pretoria, South Africa. 790.

Pretorius, C. (2014). Isotope analysis report, Centre for water resources research, University of KwaZulu-Natal, Pietermaritzburg, South Africa. Unpublished.

Schulze, R. E. (1997). South African Atlas of Agrohydrology and Climatology: Contribution Towards a Final Report to the Water Research Commission on Project 492: Modelling Impacts of the Agricultural Environment on Water Resources: TT82-96. Water Research Commission (WRC). Pretoria, South Africa.

Scott, D. F. & Le Maitre, L. E. (1998). The interaction between vegetation and groundwater: Research priorities for South Africa. CSIR report No ENV/S-C 97161. Pretoria, South Africa. 1-60.

Scott, D. F. & Lesch, W. (1997). Streamflow responses to afforestation with Eucalyptus grandis and Pinus patula and to felling in the Mokobulaan experimental catchments, South Africa. *Journal of Hydrology, 199,* 360-377.

Scott, D. F. & Lesch, W. (1996). The Effects of Riparian Clearing and Clear Felling of an Indigenous Forest on Streamflow, Stormflow and Water Quality. *South African Forestry Journal, 175*, 1-14.

Scott, D. F. & Lesch, W. (1995). The Water Yield Gains Obtained From Clear Felling Riparian Zone Vegetation. Paper presented at the SANCIAHS 7th National Hydrology Symposium, Grahamstown, South Africa.

Scott, D. F. & Smith, R. E. (1997). Preliminary empirical models to predict reduction in annual and low flows resulting from afforestation. Water SA (23), 135-140.

Scott, D. F., Versfeld, D.B. & Lesch, W. (1998). Erosion and sediment yield in relation to afforestation and fire in the mountains of the Western Cape Province, South Africa, *South African Geographical Journal, 80*, 52-59.

Sherry, S. P. (1971). The black wattle *(Acacia mearnsii* De Wild.). University of Natal Press, Pietermaritzburg.

Sidle, R. C., Noguchi, S., Tsuboyama, Y. & Laursen, K. (2001). A conceptual model of preferential flow systems in forested hillslopes: Evidence of seld-organization. *Hydrol. Process. 15*, 1675-1692.

Simmers, I. (1998). Groundwater recharge: an overview of estimation problems and recent developments. In: Robins, N.S. (ed) Groundwater Pollution, Aquifer Recharge and Vulnerability. Geological Society, London, Special Publications. 130, 107-115.

Singh, B. & Kumar, B. (2005). Isotopes in Hydrology, Hydrogeology and Water Resources. Narosa publishing house. Delhi, India.

Smerdon, B. D., Redding, T. & Beckers, J., (2009). An overview of the effects of forest management on groundwater hydrology. *Journal of Ecosystems and Management*, *10*(1), 22-44.

Smith, R. E., Moses, G. & Versfeld, D. E. (1992). Verification of heat pulse velocity technique for *Acacia mearnsii*. *South African Forestry Journal*. 163, 1-4.

Sophocleous, M. (1991). Combining the soilwater balance and water level fluctuation methods to estimate natural groundwater recharge: Practical aspects. *Journal of hydrology, 124*, 229-241.

Stirton, C. H. (1987). Plant Invaders-beautiful but dangerous, 5th Edition. The Department of Nature and Environmental Conservation of the Cape Provincial Administration. South Africa.

Stone, E. L. & Comerford, N. B. (1994). Plant and animal activity below the solum. Whole regolith pedology: Proceedings of a symposium, Minneapolis, Minnesota. 57-74.

Stone, E. L. & Kalisz, P. J. (1991). Maximum extent of roots. *Forest Ecology and Management*, 46, 59-102.

Thermo Fisher Scientific, (2011). Operation Manual Gallery Discrete Analyzer. Vantaa, Finland.

Ticehurst, J. L., Cresswell, H. P., Mckenzie, N. J. & Clover, M. R.(2007). Interpreting soil and topographic properties to conceptualise hillslope hydrology. Geoderma 137, 279-292.

Todd, D. K. & Mays, L.W. (2005). Groundwater Hydrology. Willy & Sons Inc., New York. 162-163.

Van Der Zel, D. W. (1987). Hydrological Implications of the Changing Role of Forestry in A Catchment Context. *Hydrological Sciences Symposium Proceedings, 2*, 671-679.

Van Tol, J. J., Le Roux, P., Hensley, M. & Lorentz, S. A. (2008). Soil as indicator of hillslope hydrological behaviour in the Weatherly catchment, Eastern Cape, South Africa Bloemfontein, South Africa. 513-518.

Van Tonder, G. J, Kunstmann, H., Xu, Y. (2001). FC Program. Software developed for DWAF by the Institute for Groundwater Studies. IGS, University of the Free State, Bloemfontein, South Africa.

Van Tonder, G & Xu, Y. (2000). A guide for the estimation of groundwater recharge in South Africa. Project conducted for DWAF under the supervision of Eddie van Wyk. 3-11. Pretoria, South Africa. Unpublished.

Van Tonder, G. J. & Vermeulen, P. D. (2005). The applicability of slug tests in fractured rock formations. *Water SA, Vol. 31*(2), 157.

Van Tonder, G. J. & Xu, Y. (2000). Excel based software to quantify recharge. Department of Water Affairs and Forestry, Pretoria, South Africa. Unpublished.

Van Wyk, E., Van Tonder, G. J. & Vermeulen, D. (2011). Characteristics of local groundwater recharge cycles in South African semi-arid hard rock terrains – rainwater input. Water SA 37 (2) 147–154.

Vegter, J. R. (1995). An explanation of a set of national groundwater maps. Report to the Water Research Commission, Report Number TT74/95. Pretoria, South Africa. A1-A26.

Versveld, D. B., Le Maitre, D. C. & Chapman, R. A. (1998). Alien invading plants and water resources in South Africa: A preliminary assessment. Report to the Water Resource commission. WRC Report No. TT 99/98, Pretoria, South Africa.

Vivier, J. J. P., van Tonder, G. J. & Botha, J. F. (1995). The use of slug tests to predict borehole yields: correlation between the recession time of slug tests and borehole yields. Groundwater Recharge and Rural Water Supply, Midrand, South Africa. 157-160.

Weaver, J. M. C., Cave, L. & Talma, S. (2007). Groundwater sampling a comprehensive guide for sampling methods guide. WRC Report No TT 303/07. Pretoria, South Africa. 5-158.

Wentzel, L. K., (1936). Several methods of studying groundwater levels. Trans. Amer. Geophysical Union. Vol.17.

Wilding, L. P., Smeck, N. E. & Hall, G.F. (1983). Pedogenesis and Soil Taxonomy: concepts and Interactions. Amsterdam. 117-136.

Woodford, A., & Chevallier, L. (2002). Hydrogeology of the Main Karoo Basin: Current knowledge and future research needs. WRC report no TT179/02.Pretoria South Africa.

Xu, Y. & Beekman, H. E. (Eds). (2003). Groundwater recharge estimation in Southern Africa. UNESCO IHP Series No. 64. UNESCO Paris. ISBN 92-9220-000-3. 8-16.

Zhang, L., Dawes, W. R. & Walker, G. R. (1999). Predicting the effect of vegetation changes on catchment average water balance. (Co-operative Research Centre for Catchment Hydrology: Canberra).

Zhang, Y., Xu, M., Li, X., Qi, J., Zhang, Q., Guo, J., Yu, L. and Zhao, R. (2018). Hydrochemical characteristics and multivariate statistical analysis of natural water system: A case study in Kangding county, Southern China. Water, 10(1), 80.

APPENDICES

Appendix A: Two-Streams rainfall and temperature measured from the automatic weather station in the catchment (CWRR, 2017).

Month	Monthly Rainfall (mm)	Mean monthly temperature (^{0}C)	Average min temperature (^{0}C)	Average max temperature (^{0}C)
Mar-07	93.3	18.80	14.23	25.41
Apr-07	46.1	17.10	11.95	24.16
May-07	8.5	14.70	7.79	24.16
Jun-07	55	12.20	6.07	20.65
Jul-07	1.1	12.10	5.21	21.57
Aug-07	3.7	14.00	6.98	23.28
Sep-07	35.6	17.00	11.19	25.60
Oct-07	177.4	15.20	11.17	21.46
Nov-07	191.1	16.80	12.29	23.57
Dec-07	97.5	18.10	13.45	24.73
Jan-08	167.3	19.90	15.36	26.51
Feb-08	84.5	19.90	15.51	26.61
Mar-08	111.4	18.60	13.97	25.47
Apr-08	74.2	15.40	10.38	22.99
May-08	3.1	15.30	9.62	23.64
Jun-08	22.2	12.40	7.05	20.33
Jul-08	0.7	12.50	5.91	22.50
Aug-08	7.5	14.70	7.85	23.63
Sep-08	79.3	15.10	7.37	24.03
Oct-08	56.4	16.50	11.61	23.41
Nov-08	97.2	19.10	14.53	26.47
Dec-08	133.6	21.00	16.20	28.47
Jan-09	183	21.20	16.81	28.25
Feb-09	189.4	21.40	16.81	28.53
Mar-09	28.6	20.30	15.62	28.01
Apr-09	18.9	18.80	13.49	26.98
May-09	38.1	16.60	11.39	24.86
Jun-09	6.7	14.30	8.72	22.62
Jul-09	6.5	12.80	6.42	22.50
Aug-09	77	14.90	8.64	23.42
Sep-09	36.2	17.20	11.12	25.53
Oct-09	126.2	17.70	13.31	24.50
Nov-09	87	18.50	13.77	24.81
Dec-09	80.8	20.40	15.95	26.86
Jan-10	97.7	21.90	17.62	28.34
Feb-10	38.4	23.80	18.72	31.33
Mar-10	90.5	21.80	16.64	29.50

Apr-10	25.3	19.90	15.19	27.63
May-10	3	18.60	12.44	27.92
Jun-10	8.9	14.20	7.77	25.13
Jul-10	5.6	14.70	8.44	24.18
Aug-10	8.7	15.70	8.65	24.91
Sep-10	14.9	18.80	12.53	27.79
Oct-10	59.5	18.70	13.38	27.34
Nov-10	134.5	20.20	14.90	27.56
Dec-10	152.2	20.20	15.89	26.90
Jan-11	122.1	21.60	17.66	27.72
Feb-11	28.3	22.30	17.78	29.19
Mar-11	55.3	23.60	18.21	31.78
Apr-11	108.3	18.66	13.94	25.95
May-11	27.6	16.53	11.48	23.89
Jun-11	32	12.67	7.06	18.28
Jul-11	72.8	11.44	6.12	24.18
Aug-11	72.8	14.74	8.34	22.60
Sep-11	16.8	15.91	10.09	24.11
Oct-11	78.1	16.41	11.11	23.76
Nov-11	160.2	16.04	11.76	22.55
Dec-11	135.1	18.85	14.33	25.12
Jan-12	68.8	19.85	15.57	25.84
Feb-12	75.7	20.32	15.57	27.05
Mar-12	105.7	18.68	14.21	25.57
Apr-12	29.2	15.03	9.81	22.58
May-12	11.4	15.45	9.62	13.82
Jun-12	5.2	11.75	5.44	19.93
Jul-12	8.3	11.94	5.90	20.47
Aug-12	57.4	14.17	7.86	22.16
Sep-12	124.6	14.29	9.38	21.09
Oct-12	156.8	15.50	11.29	21.66
Nov-12	155	16.22	12.01	22.28
Dec-12	152.5	18.96	14.46	25.23
Jan-13	154.4	20.00	15.65	26.30
Feb-13	69.2	20.06	15.76	26.72
Mar-13	60.4	18.39	14.17	24.88
Apr-13	17	16.44	11.20	23.75
May-13	32.7	14.49	9.38	21.09
Jun-13	4.7	13.00	6.91	20.67
Jul-13	5.7	12.38	7.10	20.33
Aug-13	22	13.58	7.26	21.52
Sep-13	32.4	14.76	8.44	23.20
Oct-13	116.1	15.88	10.34	22.87
Nov-13	91.2	19.66	12.78	26.53
Dec-13	86.7	19.54	14.15	24.93
Jan-14	100.4	20.23	15.61	26.59

Feb-14	36.25	19.83	15.43	26.33
Mar-14	113.25	18.72	14.58	25.42
Apr-14	20.65	16.05	10.78	23.64
May-14	7.85	15.05	9.15	23.47
Jun-14	9.8	12.58	5.89	21.33
Jul-14	8.75	11.47	5.01	19.91
Aug-14	16.5	14.46	8.67	22.86
Sep-14	24.25	16.88	9.76	26.18
Oct-14	66.8	14.45	9.44	21.25
Nov-14	84.65	15.84	11.93	21.61
Dec-14	113.4	18.07	13.90	24.46
Jan-15	67.4	19.57	14.90	26.20
Feb-15	49.9	18.96	14.56	25.78
Mar-15	4.5	18.94	14.52	25.89
Apr-15	7.8	15.65	11.29	22.59
May-15	1.1	16.42	8.62	25.42
Jun-15	1.5	11.94	5.74	20.70
Jul-15	46.7	13.51	6.79	20.69
Aug-15	3.9	15.26	8.64	23.01
Sep-15	54.4	16.48	10.64	22.33
Oct-15	22.5	19.00	12.12	27.53
Nov-15	79.4	16.85	11.27	25.07
Dec-15	174.1	21.98	16.19	28.96
Jan-16	87.4	19.93	15.49	26.24
Feb-16	78.5	20.11	12.66	27.65
Mar-16	102.9	19.83	13.96	26.87
Apr-16	24.9	17.77	12.66	25.03
May-16	19	14.26	7.81	22.05
Jun-16	6.5	13.01	7.16	20.64
Jul-16	79.8	11.31	4.53	19.01
Aug-16	32.8	14.24	7.44	22.77
Sep-16	64.1	15.88	10.29	23.71
Oct-16	82.3	15.13	10.82	21.85
Nov-16	104.1	17.01	13.05	23.15
Dec-16	41.4	19.95	14.70	26.97
Jan-17	149.4	19.05	14.55	25.43
Feb-17	126.6	19.36	15.20	24.98
Mar-17	70	18.76	13.96	25.92
Apr-17	17	16.74	11.28	24.36
May-17	69.3	14.73	9.83	22.50
Jun-17	4.4	13.11	7.04	21.43
Jul-17	2.7	12.75	7.10	20.76
Aug-17	8	12.75	7.37	20.77
Sep-17	22.7	15.82	9.59	24.62
Oct-17	65.1	15.88	9.76	23.58
Nov-17	153.1	16.88	10.95	24.68

Appendix B: Comparison of methods for recharge estimation (Adapted from Api, 1997).

Estimation technique	**Data Requirements**	**Optimal site characteristics**	**Relative accuracy**	**Relative cost**	**comments**
Soil water balance	1. Precipitation 2. Runoff 3. Evapotranspiration 4. storage	Humid/temperature climate (P>ET); flat topography with negligible runoff; short uniform vegetation; small scale	low	High to low	Commonly used technique for arid climate where ET > P; uncertainty varies by a factor of 3 to 10 or more
Lysimetry	Water volume	Applied under any site conditions; construction results in devegetation	High	High	Direct, precise measurement of deep drainage; precision +/- mm/yr; long term monitoring and maintenance required; when combined with soil-water balance is very reliable for arid site
Darcy flux	1.Hydraulic gradient 2.Unsaturated hydraulic conductivity	Applied under any site conditions	Low to moderate	Low to moderate	Results rely on measurement of unsaturated hydraulic conductivity; accurate with a factor of +/- 10 or more
Plane of zero flux	1. Soil water potential profile 2. water content changes with time	Temperature, semi-arid or arid climate (ET > P); any soil type	Moderate	Moderate to high	Accuracy of +/- 15% or 20 mm/yr; requires weekly monitoring; fails during periods when rainfall exceeds K saturated
Soil temperature gradient	Soil water potential profile from saturated zone	Deep aquifers with upward temperature gradient	Low	Low	Provides regionally averaged recharge estimation with accuracy similar to basin water balance
Electromagnetic resistivity	1. Electrical conductivity data 2. Independent recharge estimation for comparison	Non-quantitative	Low to moderate	Low to moderate	Provides reconnaissance level, qualitative results that identify areas of recharge
Basin outflow	1. Aquifer transmissivity 2. Aquifer hydraulic gradient basin boundaries 3. Upstream catchment surface	Any unconfined aquifer with a well characterised flow regime and well defined recharge areas	Low	Low to high	Provides regionally averaged recharge estimate with accuracy similar to basin water balance; can often rely on existing data. Low cost provided data already exist, high cost if data collection is required

	area 4. Specific yield Transient hydraulic change				
Water level fluctuation (incl. CRD, SVF)	1. Water table hydrograph 2. Specific yield 3. Rainfall 4. Area	Any unconfined aquifer with a well characterised flow regime and recharge areas	Low to high	Low	Provides regionally averaged recharge estimate with accuracy similar to basin water balance; can often rely on existing data
Stream gauging	Streamflow hydrograph	Humid/temperature climate; well-developed unmanaged watershed with perennial streams; stream connected shallow aquifer; minimal snowmelt	Moderate	Low	Avoids need to measure climatic parameters; provides regionally averaged recharge estimate for watershed with better accuracy than basin water balance
Chloride mass balance	1. Undisturbed soil profile 2. Meteoric chloride concentration 3. Chloride concentration in soil water or groundwater 4. Mean annual precipitation	Arid, semi-arid and temperature climate where R > 10% MAP; sediment of any texture and pedogenic carbonates	High	Low	Conceptual model assumes (1) average rate of chloride deposition rate in P is constant, and (2) Pistol flow.
Stable isotope profile	1. Undisturbed soil profile 2. Water content profile 3. D and ^{18}O concentrations in soil moisture or groundwater	Arid and semi-arid climates where soil water movement is in quasi-steady state; sediments of any texture	Unknown	Low to moderate	Conceptual model assumes one-dimensional, vertical quasi-steady state soil water movement; non-routine soil water extraction process; requires further research to evaluate uncertainty
Groundwater age dating	1. Hydraulic gradient 2. Effective porosity 3. Distance to tracer peak 4. Apparent groundwater tracer age	Shallow unconfined aquifer; vertical hydraulic gradient near the water table; applicable to any climate, soil texture and vegetation	High	High	Groundwater age best determined by ^{14}C, $^{3}H/^{3}He$, Cl and/or CFCs; requires thorough understanding of aquifer flow system and careful application; very consistent results; high relative accuracy if source of ^{14}C and ^{3}H is known

	5.. Knowledge if other sources of C in aquifer				
Soil water balance models	1. Precipitation 2. Runoff 3. Evapotranspiration 4.Soil water storage 5. Hydraulic properties	Applicable to any conditions and any scale where vertical flow occurs	Low to moderate	Moderate to high	Relies on estimation of AET and unsaturated hydraulic conductivity; uncertainty varies by an order of magnitude or more
Soil water models based on Richards equation	1. Climatic data 2. Soil hydraulic properties 3. Depth to water table 4. In situ pressure head or water contents	Homogeneous soil profiles above a shallow water table, moist soils	Low to moderate	Moderate to high	Uncertainty is due to climatic data and hydraulic properties; extensive computational effort for deep water tables, dry heterogeneous soil.
Groundwater models	1. Aquifer geometry 2. Transmissivity 3. Aquifer boundary conditions 4. Initial head field	Applicable to any conditions and any scale	Moderate	Moderate to high	Cost can be considered if data are not compiled. Requires thorough calibration

Appendix C: Two-dimensional geo-electric resistivity models of the subsurface from the ERT geophysical survey in the Two Streams catchment.

Transect T1 (Clulow *et al*., 2011).

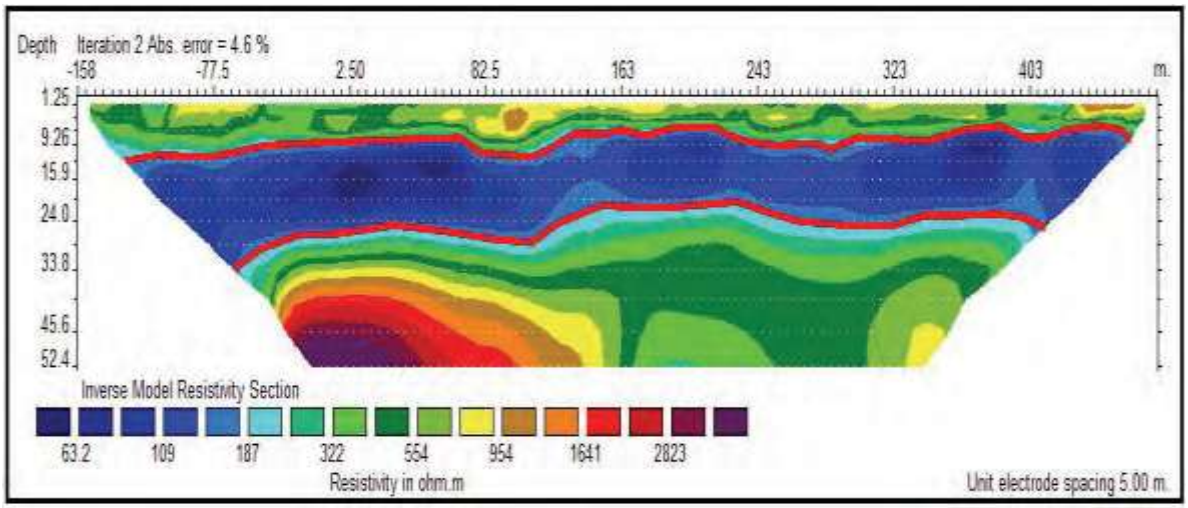

Transect T2 (Clulow *et al*., 2011)

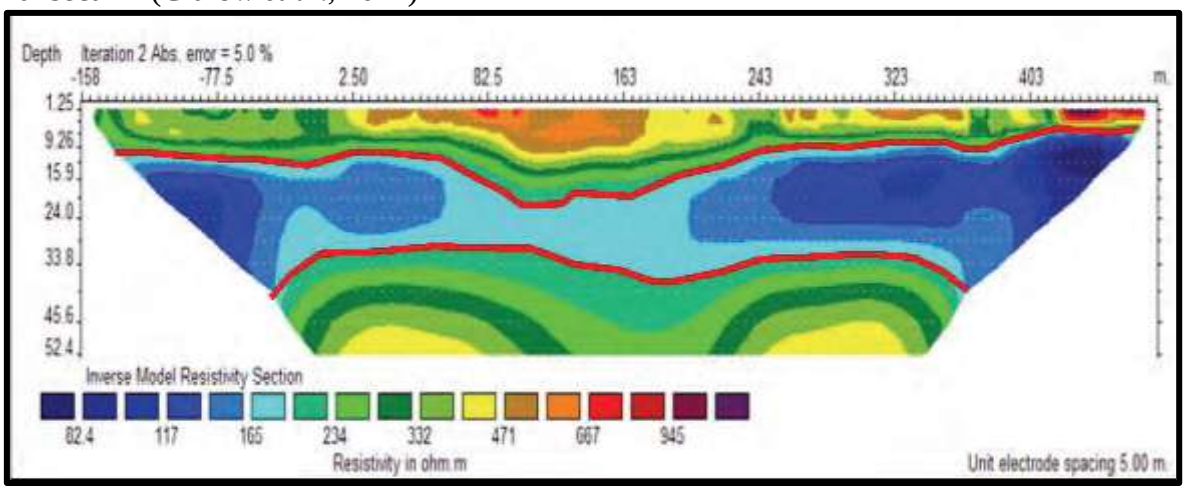

Transect T3 (Clulow *et al*., 2011)

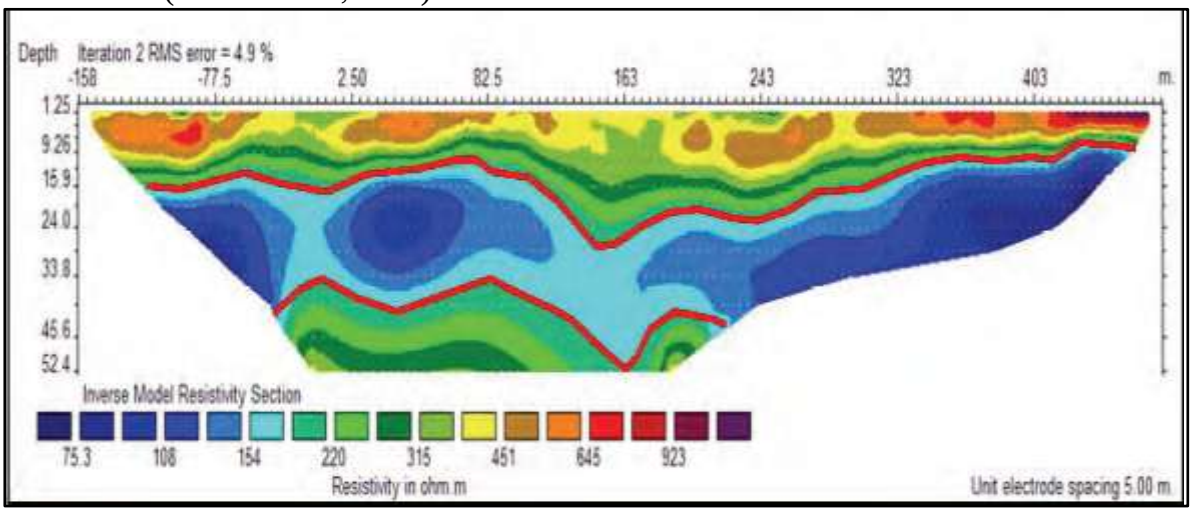

Transect tstert 2 (CWRR, 2009)

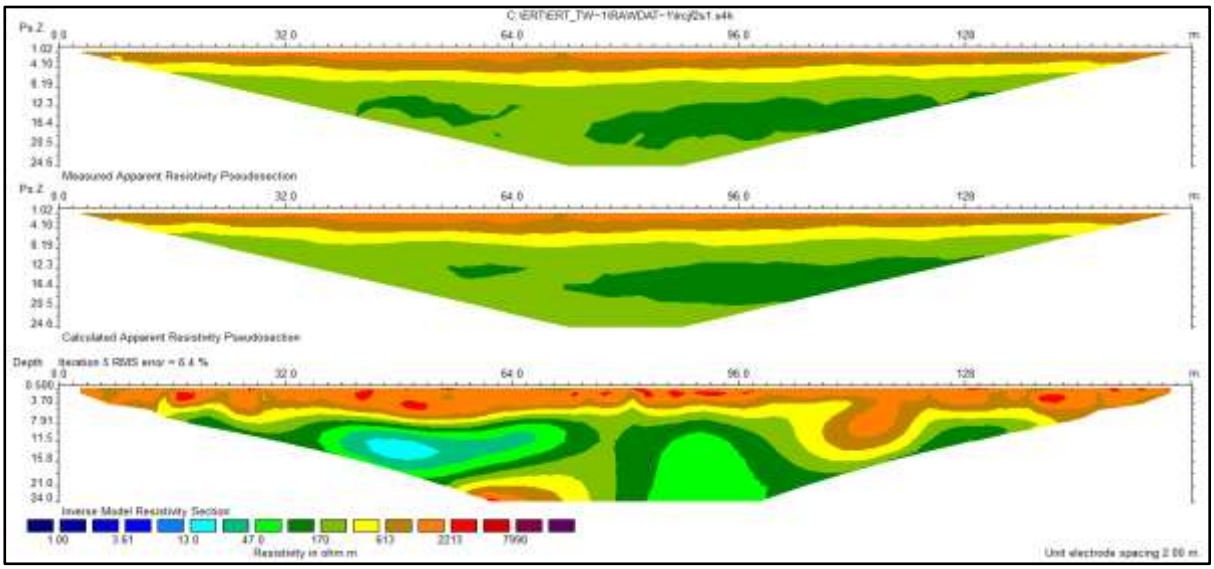

Transect tstert 3 (CWRR, 2009)

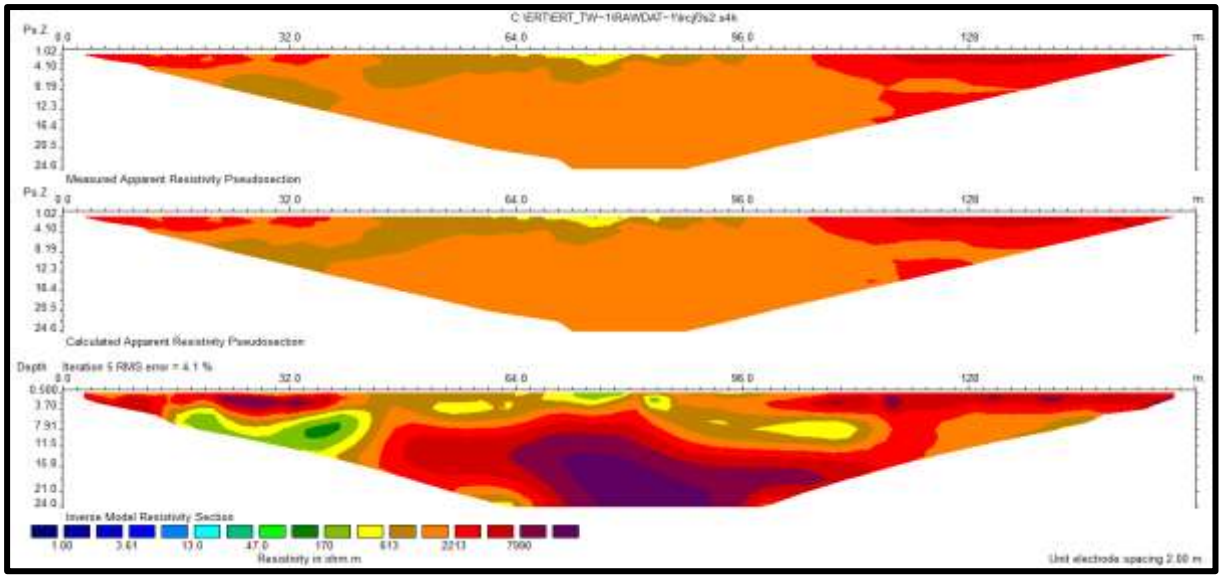

Transect 2ST001

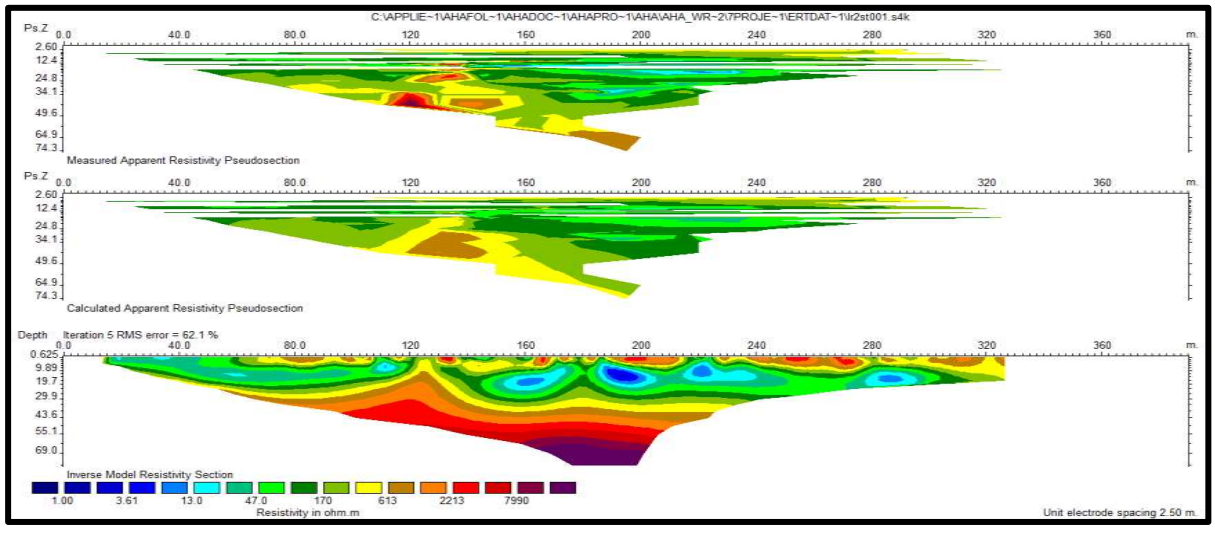

Transect 2ST002

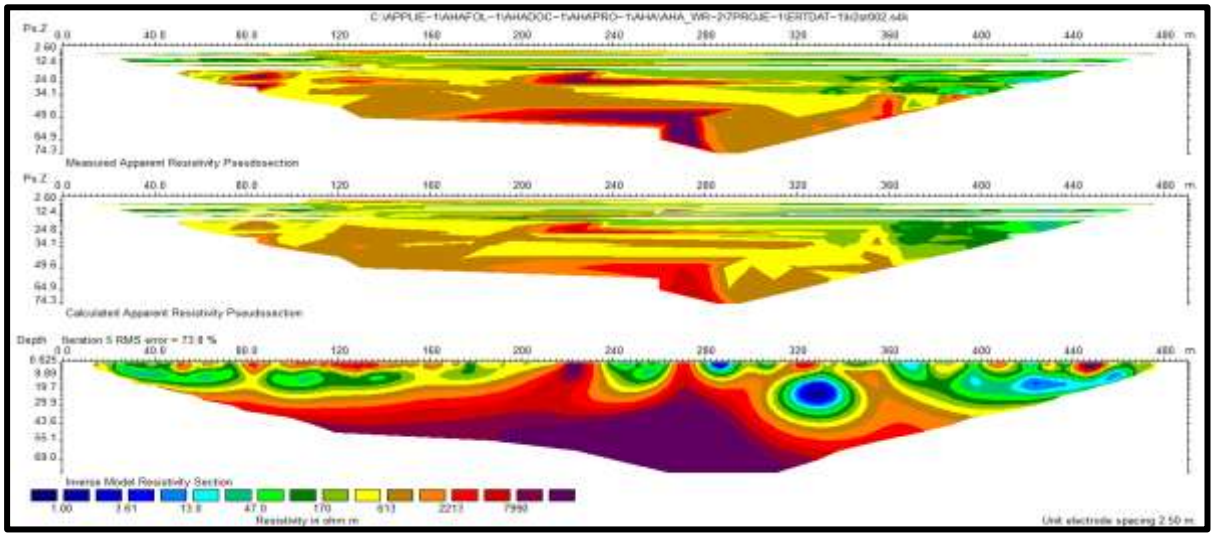

Transect 2ST004

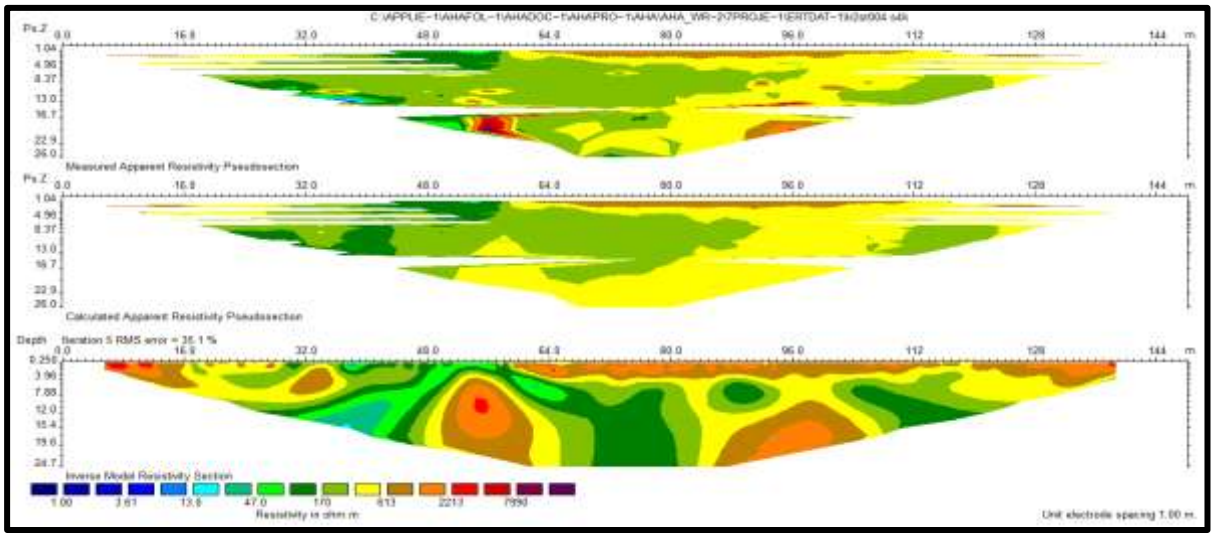

Appendix D: Borehole logs

2STBH1 (CENTRE)

Borehole no:	KZN07168			Map ref:		Date Started:	
Region:	KwaZulu Natal			Latitude:	30° 39' 03" E	Date Finished:	
District:	Umzinyathi			Longitude:	29° 12' 25.6" S	VBA Groundwater	
Farm:	Mistley 2034			Water level (m,b,g,l):		EC:	
Village:	SevenOaks			Collar height (m):		Ph:	
Altitude (m):				Air lift yield (l/s) :			
Water Strikes:	1	2	3	4	5		
Depth (m)							
Yield (l/s)							
Casing Detail:							
From/To (m):	16						
Type (S/P)	S	P					
Diameter (mm):	165						
Sanitary Seal:				DRILL CUTTINGS:			
B/H Diam	215mm 165mm						

Depth	Lithology, Colour, Grain Size, Weathering, etc.			
	b/h diam	casing diam		Description
				0-6m Red Brown Clay
				7-8m Light Red Brown Clay
10				9-14m Light Brown Clay
	215mm	165mm		15m Grey Fine Grained Shale
				16-40m Grey Granite
20				
30				
40	165mm			E.O.H

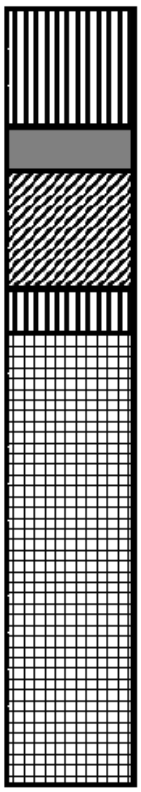

2STBH3 (NORTH)

Borehole no:	KZN07169			Map ref:			
Region:	KwaZulu Natal			Latitude:	30° 38' 49.7" E		
District:	Umzinyathi			Longitude:	29° 12' 20" S		
Farm:	Mistley 2034			Water level (m,b,g,l):			
Village:	SevenOaks			Collar height (m):			
Altitude (m):				Air lift yield (l/s) :		0.5	
Water Strikes:	1	2	3	4	5		
Depth (m)	31	41					
Yield (l/s)	Wetspot	0.5					
Casing Detail:							
From/To (m):	25						
Type (S/P)	S	P					
Diameter (mm):	165						
Sanitary Seal:				DRILL CUTTINGS:			

B/H Diam	215mm 165mm		

Depth	Lithology, Colour, Grain Size, Weathering, etc.		
	b/h diam	casing diam	Description
			0-14m Red Brown Clay
10			
			15-24m Light Brown Clay
20			
	215mm	165mm	25-43m Grey Fine Grained Shale
30			
40			
			43-60m Grey Granite
50			
60			E.O.H

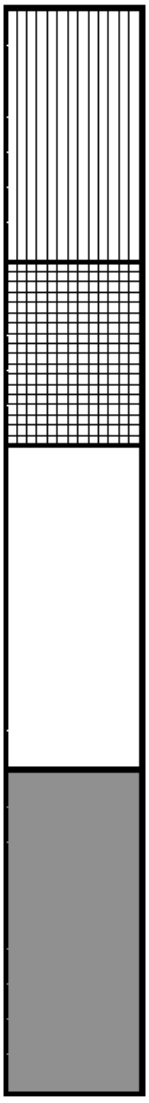

2STBH4 (WEST)

Borehole no:	KZN07170			Map ref:			
Region:	KwaZulu Natal			Latitude:	30° 39' 5.1" E		
District:	Umzinyathi			Longitude:	29° 12' 12" S		
Farm:	Mistley 2034			Water level (m,b,g,l):			
Village:	SevenOaks			Collar height (m):			
Altitude (m):				Air lift yield (l/s) :			
Water Strikes:	1	2	3	4	5		
Depth (m)							
Yield (l/s)							
Casing Detail:							
From/To (m):	22						
Type (S/P)	S	P					
Diameter (mm):	165						
Sanitary Seal:				DRILL CUTTINGS:			
B/H Diam	215mm 165mm						

Depth	Lithology, Colour, Grain Size, Weathering, etc.

b/h diam: 215mm (0–22m), 165mm (22–60m)

casing diam: 165mm (0–22m)

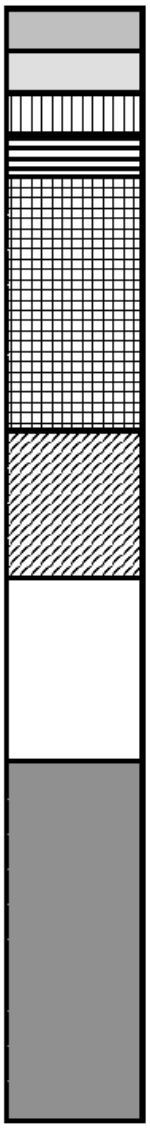

Description

0-1m Brown Clay

2-3m Red Brown Clay

4 Brown Clay

5-7 Light Brown Clay

8-22 Red Brown Clay

32-40m Grey Shale

41-60 Granite

E.O.H

Appendix E: Resistivities of some common rocks, minerals and chemicals (Loke, 2000).

Material	Resistivity (Ω•m)	Conductivity (Siemen/m)
Igneous and Metamorphic Rocks		
Granite	$5x10^{3}$ - 10^{6}	10^{-6} - $2x10^{-4}$
Basalt	10^{3} - 10^{6}	10^{-6} - 10^{-3}
Slate	$6x10^{2}$ - $4x10^{7}$	$2.5x10^{-8}$ - $1.7x10^{-3}$
Marble	10^{2} - $2.5x10^{8}$	$4x10^{-9}$ - 10^{-2}
Quartzite	10^{2} - $2x10^{8}$	$5x10^{-9}$ - 10^{-2}
Sedimentary Rocks		
Sandstone	8 - $4x10^{3}$	$2.5x10^{-4}$ - 0.125
Shale	20 - $2x10^{3}$	$5x10^{-4}$ - 0.05
Limestone	50 - $4x10^{2}$	$2.5x10^{-3}$ - 0.02
Soils and waters		
Clay	1 - 100	0.01 - 1
Alluvium	10 - 800	$1.25 x10^{-3}$ - 0.1
Groundwater (fresh)	10 - 100	0.01 - 0.1
Sea water	0.2	5
Chemicals		
Iron	$9.074x10^{-8}$	$1.102x10^{7}$
0.01 M Potassium chloride	0.708	1.413
0.01 M Sodium chloride	0.843	1.185
0.01 M acetic acid	6.13	0.163
Xylene	$6.998x10^{16}$	$1.429x10^{-17}$

Appendix F: Mean monthly groundwater levels for Two Streams monitoring boreholes

	2STBH1			2STBH3			2STBH4			2STBH5		
Month	Min	Max	**Mean WL**	Min	Max	**Mean WL**	Min	Max	**Mean WL**	Min	Max	**Mean WL**
18-Aug-06									32.33			
7-Sep-06									32.00			
19-Oct-06									33.30			
27-Nov-06									30.00			
23-Jan-07									29.40			
15-May-07									32.20			
21-Jun-07									32.28			
19-Jul-07									32.32			
29-Aug-07									32.22			
11-Oct-07			32.72			41.03			31.10			34.620
11-Dec-07			32.80			41.70			29.30			33.420
9-Feb-08			32.20			44.02			30.50			30.450
30-Apr-08			33.00			45.10			30.15			33.300
12-Jun-08			21.80			46.60			33.30			33.300
29-Aug-08			24.80			44.60			33.90			32.800
25-Sep-08			25.30			45.50			34.80			34.100
30-Oct-08			26.10			47.60			35.80			35.800
22-Dec-08	31.80	33.5	31.80	44.6	45.3	44.95	30.2	32.5	31.35	35.8	37.2	36.500
15-Jan-09			28.20			40.20			29.10			35.800
13-Feb-09			27.10			38.70			27.60			31.600
17-Mar-09			33.00			44.30			32.10			29.300
17-Apr-09			30.20			42.10			29.20			36.500
7-Jul-09			33.20			46.20			32.20			31.300
6-Aug-09			35.10			48.10			33.10			35.400
16-Sep-09			32.70			45.20			30.60			36.200
20-Nov-09			30.60			43.40			28.90			33.800
20-Jan-10			30.10			42.30			27.80			32.200
12-Feb-10			28.30			40.60			26.50			31.700
18-Mar-10			29.70			41.80			28.10			30.200
5-May-10			30.80			42.20			29.30			32.100
11-Jun-10			28.70			41.50			27.80			33.000
15-Jul-10			29.90			40.90			28.80			31.800
19-Aug-10			31.10			41.80			29.00			32.000
2-Dec-10			25.75			36.00			33.45			32.100

13-Jan-11			25.90			36.30			33.70			35.00
31-Mar-11			25.30			36.00			33.40			35.00
30-Jun-11			25.63			36.00			33.40			35.00
Sep-11	25.60	25.64	25.620	37.61	38.41	38.010	26.50	33.70	30.100	34.91	35.09	35.003
Oct-11	25.54	25.63	25.585	37.21	37.83	37.520	32.97	33.06	33.015	34.78	35.04	34.912
Nov-11	25.55	25.82	25.685	36.94	37.42	37.180	33.00	33.07	33.035	34.57	34.79	34.681
Dec-11	25.61	25.80	25.705	34.65	36.94	35.795	32.92	33.03	32.975	34.22	34.71	34.463
Jan-12	25.44	25.61	25.525	33.67	34.67	34.170	32.82	32.96	32.890	34.01	34.30	34.159
Feb-12	24.51	25.44	24.975	33.12	33.71	33.415	32.71	32.85	32.780	33.72	34.13	33.923
Mar-12	20.02	24.54	22.280	32.68	33.43	33.055	32.60	32.73	32.665	33.68	33.85	33.764
Apr-12	20.00	21.16	20.580	32.64	36.14	34.390	32.55	32.65	32.600	33.62	33.79	33.709
May-12	19.85	21.10	20.473	32.64	36.14	34.390	32.55	32.65	32.600	33.62	33.79	33.709
Jun-12	19.69	21.04	20.365	35.83	37.80	36.815	32.53	32.65	32.590	33.32	33.46	33.389
Jul-12	20.80	23.70	22.250	37.63	37.90	37.765	32.61	32.71	32.660	33.34	33.74	33.539
Aug-12	22.27	25.82	24.045	37.69	37.90	37.795	32.53	33.07	32.800	33.49	34.97	34.226
Sep-12	24.44	24.94	24.690	37.73	37.96	37.845				34.06	34.39	34.225
Oct-12	25.51	25.56	25.535	37.87	37.95	37.910				34.57	34.64	34.601
Nov-12	25.32	25.51	25.415	37.85	37.99	37.920				34.26	34.90	34.579
Dec-12	25.32	25.51	25.415	37.85	37.99	37.920				34.26	34.90	34.579
Jan-13	25.30	25.51	25.405	37.86	38.01	37.935				34.83	35.94	35.385
Feb-13	24.99	25.38	25.185	37.31	37.90	37.605				34.53	35.95	35.242
Mar-13	19.52	24.99	22.255	36.87	37.62	37.245				34.08	35.70	34.889
Apr-13	19.02	19.53	19.275	36.83	37.35	37.090	32.22	32.79	32.506	33.90	35.17	34.532
May-13	18.84	19.06	18.950	36.95	37.40	37.175	32.28	32.58	32.434	34.68	35.10	34.890
Jun-13	18.87	19.17	19.020	37.22	37.59	37.405	32.18	32.35	32.267	34.87	35.09	34.982
Jul-13	19.13	25.60	22.363	37.35	37.65	37.500	31.03	32.24	31.636	34.64	34.97	34.802
Aug-13	22.519	25.932	24.226	37.610	37.740	37.675	30.883	31.171	31.027	34.487	34.775	34.631
Sep-13	25.129	25.481	25.305	37.660	37.910	37.785	30.478	31.039	30.759	34.082	34.643	34.363
Oct-13	24.577	25.249	24.913	37.840	42.630	40.235	30.115	30.664	30.390	33.719	34.268	33.994
Nov-13	22.040	24.745	23.393	42.070	42.630	42.350	30.112	30.262	30.187	33.716	33.866	33.791
Dec-13	20.682	22.155	21.419	42.17	42.63	42.400	30.079	30.232	30.156	33.68	33.84	33.760
Jan-14	20.5	24.542	22.521	42.61	42.63	42.620	30.019	30.190	30.105	33.62	33.79	33.709
Feb-14	24.153	25.25	24.702	42.6	42.64	42.620	29.944	30.196	30.070	33.31	33.75	33.530
Mar-14	24.579	25.603	25.091	42.6	42.64	42.620	29.842	30.088	29.965	33.32	33.74	33.530
Apr-14	25.462	25.739	25.601	42.63	42.65	42.640	29.779	30.007	29.893	33.485	34.162	33.824
May-14	25.598	25.966	25.782	42.62	42.66	42.640	29.755	29.929	29.842	34.057	34.389	34.223
Jun-14	25.799	26.192	25.996	42.62	42.65	42.635	29.683	29.878	29.781	34.138	34.709	34.424
Jul-14	26.032	26.595	26.314	42.11	42.63	42.370	29.602	29.857	29.730	34.263	34.895	34.579
Aug-14	26.429	27.015	26.722	42.07	42.63	42.350	29.281	29.773	29.527	34.194	35.078	34.636
Sep-14	26.795	27.129	26.962	42.62	42.63	42.625	28.957	29.617	29.287	34.832	35.677	35.255
Oct-14	27.034	27.392	27.213	42.61	42.63	42.620	29.158	29.548	29.353	34.534	35.95	35.242
Nov-14	27.233	27.9	27.567	47.085	47.085	47.085	29.212	29.398	29.305	35.239	35.7	35.470
Dec-14	27.755	27.919	27.837	47.58	47.58	47.580	28.063	29.338	28.701	33.897	35.293	34.595
Jan-15	27.803	28.007	27.905	42.600	42.630	42.615	28.498	29.305	28.902	34.332	35.139	34.736
Feb-15	27.770	27.937	27.854	42.590	42.600	42.595	28.930	29.200	29.065	34.683	34.953	34.818

Mar-15	27.813	27.954	27.884				29.029	29.170	29.100	34.668	34.923	34.796
Apr-15	27.775	27.961	27.868				28.954	29.104	29.029	34.593	34.743	34.668
May-15	27.830	29.774	28.802				28.978	29.086	29.032	34.611	34.779	34.695
Jun-15	29.529	29.750	29.640							34.533	34.737	34.635
Jul-15	29.492	29.852	29.672							34.473	34.704	34.589
Aug-15	29.529	29.852	29.691							34.470	34.662	34.566
Sep-15	29.553	29.792	29.673							34.452	34.659	34.556
Oct-15	29.560	29.754	29.657							34.428	34.587	34.508
Nov-15	29.483	29.728	29.606							34.347	34.584	34.466
Dec-15	29.508	29.678	29.593							34.359	34.503	34.431
Jan-16	29.516	29.668	29.592							34.341	34.482	34.412
Feb-16	29.136	29.660	29.398							34.299	34.458	34.379
Mar-16	29.343	29.651	29.497							33.702	34.404	34.053
Apr-16	29.378	29.618	29.498							33.666	33.915	33.791
May-16	29.338	29.569	29.454							33.753	33.927	33.840
Jun-16	29.157	29.395	29.276							33.750	33.933	33.842
Jul-16	28.963	29.282	29.123							33.717	33.921	33.819
Aug-16	28.914	29.206	29.060							33.690	33.906	33.798
Sep-16	28.779	29.060	28.920							33.675	33.906	33.791
Oct-16	28.725	29.006	28.866	46.594	47.625	47.109	35.937	36.168	36.053	33.648	33.879	33.764
Nov-16	28.790	29.025	28.908	46.697	47.338	47.017	36.048	36.386	36.217	33.729	33.909	33.819
Dec-16	28.892	29.074	28.983	47.213	47.824	47.519	35.714	36.425	36.070	33.696	33.891	33.794
Jan-17	28.955	29.102	29.029	47.740	47.919	47.829	35.630	35.912	35.771	33.702	33.870	33.786
Feb-17	28.949	29.091	29.020	47.774	47.922	47.848	35.600	36.166	35.883	33.693	33.855	33.774
Mar-17	28.576	29.003	28.790	47.758	48.015	47.886	36.022	36.229	36.126	33.753	34.724	34.239
Apr-17	28.453	28.737	28.595	47.649	48.283	47.966	35.884	36.178	36.031	34.613	36.110	35.362

*WL is Water Level

Appendix G: Baseflow separation using the Web-based hydrograph analysis tool (WHAT) system.

		Local minimum method		**One parameter digital filter**		**Recursive digital filter**	
Date	Total discharge	Direct Runoff	Baseflow	Direct Runoff	Baseflow	Direct Runoff	Baseflow
	(m^3/d)	(m^3/d)	(m^3/d)	(m^3/d)	(m^3/d)	(m^3/d)	(m^3/d)
29-Feb-12	34.02	0	34.02	17.01	17.01	17.01	17.01
7-Mar-12	35.03	2.5	32.54	16.71	18.32	18.25	16.79
16-Mar-12	43.53	12.47	31.06	23.64	19.89	26.9	16.63
23-Mar-12	34.08	4.5	29.58	12.77	21.31	17.66	16.42
29-Mar-12	32.44	4.33	28.11	10.23	22.21	16.24	16.2
25-Apr-12	26.63	0	26.63	3.87	22.76	10.68	15.94
20-Jul-12	27.33	0	27.33	4.26	23.07	11.63	15.7
8-Aug-12	65.49	36.75	28.74	40.67	24.82	49.77	15.72
19-Aug-12	35	5.19	29.8	8.27	26.73	19.46	15.54
30-Aug-12	30.86	0	30.86	3.67	27.2	15.53	15.33
11-Apr-13	57.41	22.03	35.38	28.94	28.47	42.11	15.3
30-Apr-13	69.15	29.25	39.9	38.07	31.08	53.79	15.36
15-May-13	71.83	27.42	44.41	37.8	34.03	56.41	15.42
29-May-13	58.65	9.72	48.93	22.28	36.37	43.25	15.4
26-Jun-13	53.45	0	53.45	15.6	37.85	38.1	15.35
4-Jul-13	72.92	27.08	45.84	33.17	39.75	57.49	15.43
17-Jul-13	63.71	25.49	38.22	21.82	41.89	48.27	15.44
15-Feb-14	36.05	5.44	30.61	0	36.05	20.78	15.27
26-Mar-14	22.99	0	22.99	0	22.99	7.97	15.02
19-Apr-14	25.77	6.87	18.9	2.68	23.09	10.98	14.79
29-May-14	21.02	6.2	14.82	0	21.02	6.48	14.54
30-Jun-14	10.73	0	10.73	0	10.73	0	10.73
30-Jul-14	48.16	34.85	13.31	36.02	12.14	37.39	10.77
28-Aug-14	15.88	0	15.88	2.26	13.63	5.3	10.59
30-Sep-14	45.54	15.84	29.7	30.63	14.91	34.93	10.61
30-Oct-14	57.62	14.11	43.51	39.96	17.66	46.91	10.71
28-Nov-14	50.32	0	50.32	29.93	20.38	39.56	10.76
31-Dec-14	71.13	0	71.13	47.72	23.41	60.18	10.94
Total	**1216.74**	**290.04**	**926.70**	**527.98**	**688.77**	**813.03**	**403.71**

Appendix G: Baseflow separation using isotope techniques in the Two Streams catchment, baseflow is given by $Q_g = Q_t * (\delta_t - \delta_r)/(\delta_g - \delta_r)$.

Date	Daily Streamflow	Groundwater		Stream		Rainfall		Baseflow	Rainfall
	(m^3/d)	d^2H	$d^{18}O$	d^2H	$d^{18}O$	d^2H	$d^{18}O$	(m^3/d)	(mm)
29-Feb-12	34.015	-5.74	-1.90	-4.45	-1.92	7.69	-0.49	34.608	0.0
7-Mar-12	35.034	-4.70	-1.44	-6.35	-2.13	-40.87	-5.93	29.641	0.1
16-Mar-12	43.534	-8.94	-2.09	-5.95	-1.98	-17.89	-3.39	47.339	3.0
23-Mar-12	34.079	-7.79	-2.34	-4.96	-2.23	9.34	0.19	32.677	0.1
29-Mar-12	32.437	-7.49	-2.38	-6.49	-2.44	15.19	0.06	33.318	0.3
25-Apr-12	26.628	-8.77	-2.63	-5.17	-3.18	6.29	-1.98	49.150	0.0
20-Jul-12	27.329	-11.95	-4.43	-8.17	-3.62	10.37	-1.69	19.210	0.0
8-Aug-12	65.494	-11.97	-4.43	-25.79	-5.38	-85.65	-12.97	58.221	33.9
19-Aug-12	34.996	-12.46	-3.72	-9.66	-3.56	0.80	-2.44	30.639	0.0
30-Aug-12	30.861	-10.97	-3.65	-9.26	-3.46			29.258	0.0
11-Apr-13	57.410	-9.04	-2.63	-7.13	-2.33	0.47	-2.00	29.437	0.0
30-Apr-13	69.150	-9.60	-2.66	-6.40	-2.41			62.690	0.1
15-May-13	71.830	-10.17	-3.26	-6.55	-3.18	-12.49	-4.53	76.190	0.0
29-May-13	58.650	-8.38	-2.87	-7.04	-2.86	8.09	-1.39	58.048	0.1
26-Jun-13	53.450	-10.36	-2.97	-6.56	-2.85	-0.33	-2.69	29.585	0.1
4-Jul-13	72.920	-8.44	-2.95	-7.80	-2.98	-4.66	-2.88	105.324	2.6
17-Jul-13	63.710	-11.41	-3.78	-7.97	-2.85	10.54	-1.04	41.928	0.1
15-Feb-14	36.049	-11.69	-2.82	-8.71	-2.69	-4.94	-2.14	29.188	2.0
26-Mar-14	22.990	-11.41	-3.28	-8.40	-2.96	-12.85	-3.42	75.539	0.0
19-Apr-14	25.774	-8.73	-3.28	-8.65	-3.03			23.810	0.0
29-May-14	21.019	-10.41	-3.00	-7.34	-2.34			16.395	0.0
30-Jun-14	10.733	-9.35	-2.99	-7.79	-3.10			11.128	0.0
30-Jul-14	48.161	-8.89	-3.03	-7.84	-2.82	-1.59	-2.85	0.000	0.0
28-Aug-14	15.884	-9.51	-2.97	-7.92	-2.83	-1.42	-3.79	18.596	0.2
30-Sep-14	45.540	-6.90	-2.56	-5.09	-2.92	-1.74	-1.93	71.563	0.0
30-Oct-14	57.619	-10.38	-3.67	-6.86	-2.50	-2.62	-2.71	0.000	5.4

28-Nov-14	50.317	-9.47	-3.22	-8.10	-3.04	-2.62	-2.46	38.400	2.8
31-Dec-14	71.129	-11.16	-3.43	-10.36	-2.96	-4.94	-2.14	45.274	6.9
Total	**1216.742**							**1097.15**	**57.70**

Appendix I: Pumping test and FC program analysis

PUMPING TEST - CONSTANT DISCHARGE RATE & RECOVERY

Borehole No	2STBH1
Borehole Name	Centre
Borehole Depth	40 mbgl
Actual depth	36 mbgl
Static water level	28.085 mbgl
Pump intake	34 mbgl
Available drawdown	5.15 m

Constant Discharge Test				Recovery Test					
Elapsed Time	Pumping WL	Dradown	Pumping Rate	Recovery Time (T_1)	Total Time (T_2)	Ratio (T2/T1)	WL	Water level	Residual drawdown
(min)	(m)	(m)	(l/s)	(min)	(min)			(m)	(m)
0	28.085	0.000	0.03	0	40.0	0	34.000	33.70	5.62
0.5	28.150	0.065	0.03	0.5	40.5	81.0	33.15	32.85	4.77
1	28.250	0.165	0.03	1	41.0	41.0	33.12	32.82	4.74
1.5	28.350	0.265	0.03	1.5	41.5	27.7	33.10	32.80	4.72
2	28.645	0.560	0.03	2	42.0	21.0	33.08	32.78	4.70
3	29.020	0.935	0.03	3	43.0	14.3	33.06	32.76	4.68
4	29.300	1.215	0.03	4	44.0	11.0	33.06	32.76	4.67
5	29.460	1.375	0.03	5	45.0	9.0	33.06	32.76	4.67
6	29.680	1.595	0.03	6	46.0	7.7	33.05	32.75	4.67
7	29.850	1.765	0.03	7	47.0	6.7	33.05	32.75	4.67
8	30.020	1.935	0.03	8	48.0	6.0	33.05	32.75	4.67
9	30.210	2.125	0.03	9	49.0	5.4	33.05	32.75	4.67
10	30.520	2.435	0.03	10	50.0	5.0	33.05	32.75	4.67
11	30.700	2.615	0.03	11	51.0	4.6	33.05	32.75	4.67
12	30.850	2.765	0.03	12	52.0	4.3	33.05	32.75	4.67
15	31.280	3.195	0.03	15	55.0	3.7	33.05	32.75	4.67
20	31.940	3.855	0.03	20	60.0	3.0	33.05	32.75	4.67
25	32.400	4.315	0.03	25	65.0	2.6	33.05	32.75	4.67
30	32.960	4.875	0.03	30	70.0	2.3	33.05	32.75	4.67
35	33.200	5.115	0.03	35	75.0	2.1	33.05	32.75	4.67
40	33.700	5.615	0.03	40	80.0	2.0	33.05	32.75	4.67

DATA sheet: Enter general info and data of constant rate pumping test and recovery (optional)

Country:	SA	Main	**Geology:**	Granite
Region:	KwaZulu-Nata;		**Depth of BH:**	40
Owner:	UKZN	Diagnostic Plots / Derivative	**Water strikes:**	24 and 33 m below water level
X-coord:		Sust_Q	**Date of Test:**	2016
Y-coord:			**Contractor:**	C. Ngubo

CONSTANT RATE TEST DATA:

Borehole: 2STBH1

Distance from Rest WL to main water strike (m) = 5 | s_{max}= 5.62 | Recom. AD = 5.0

Q (l/s)= 0.03

Recovery data

AD= available drawdown for managing the borehole

AD = 5.15 **Time (y) =** 40

T (m^2/d) : Logan eq. 0.6

time = extrapolation time

t (min)	s (m)	avg s'	avg s"	avg T	avg S	Time t'	Res_s	t/t'	Wl rise	s'	Rec_T
0.50	0.065					0.5	5.62	81	-0		
1.00	0.165					1	4.77	41	0.845	1.95	
1.50	0.265	1.10	1.35			1.5	4.74	27.67	0.875	0.17	
2.00	0.56	1.69	0.96	0.24	1.05E-04	2	4.72	21	0.895	0.18	2.5
3.00	0.935	2.18	0.42	0.20	1.13E-04	2.5	4.7	17	0.915	0.23	2.7
4.00	1.215	2.28	0.14	0.21	1.13E-04	3	4.68	14.33	0.935	0.14	4.2
5.00	1.375	2.35	0.31	0.21	1.15E-04	4	4.67	11	0.945	0.05	#NUM!
6.00	1.595	2.55	0.74	0.19	1.20E-04	5	4.67	9	0.945	0.00	#NUM!
7.00	1.765	2.98	1.27	0.16	1.30E-04	6	4.67	7.667	0.945	0.00	#NUM!
8.00	1.935	3.65	1.54	0.13	1.39E-04	7	4.67	6.714	0.945	0.00	#NUM!
9.00	2.125	4.39	1.17	0.10	1.46E-04	8	4.67	6	0.945	0.00	#DIV/0!
10.00	2.435	4.80	0.29	0.09	1.49E-04	9	4.67	5.444	0.945	0.00	#DIV/0!
11.00	2.615	4.72	-0.20	0.10	1.49E-04	10	4.67	5	0.945	0.00	#DIV/0!
12.00	2.765	4.61	-0.13	0.11	1.49E-04	11	4.67	4.636	0.945	0.00	#DIV/0!
15.00	3.195	4.77	0.24	0.10	1.49E-04	12	4.67	4.333	0.945	0.00	#DIV/0!
20.00	3.855	5.15	0.30	0.09	1.49E-04	15	4.67	3.667	0.945	0.00	#DIV/0!
25.00	4.315	5.51	#NUM!	0.09	1.59E-04	20	4.67	3	0.945	0.00	#DIV/0!
30.00	4.875	#NUM!	#NUM!	0.08	1.66E-04	25	4.67	2.6	0.945	0.00	#DIV/0!
35.00	5.115	#NUM!	#NUM!	0.08	1.66E-04	30	4.67	2.333	0.945	0.00	#DIV/0!
40.00	5.615	#NUM!	#NUM!	0.08	1.66E-04	35	4.67	2.143	0.945	-7.37	#NUM!
						40	4.67	2			

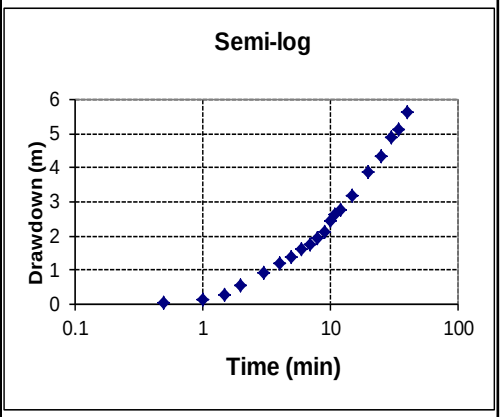

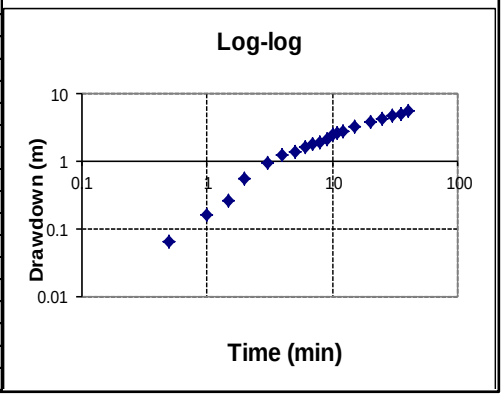

DIAGNOSTIC PLOTS

Main

Data

2STBH1

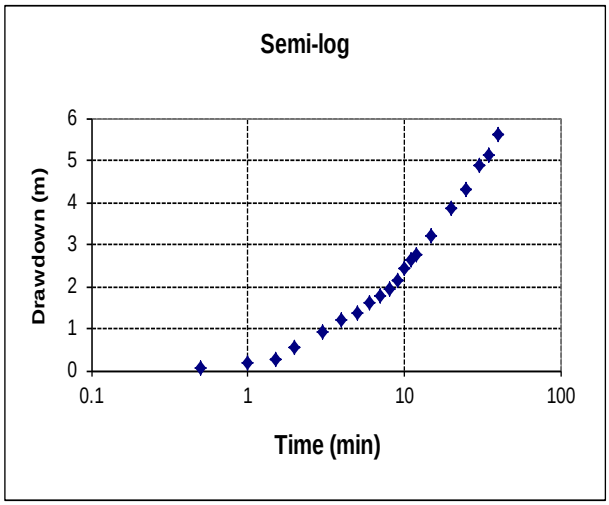

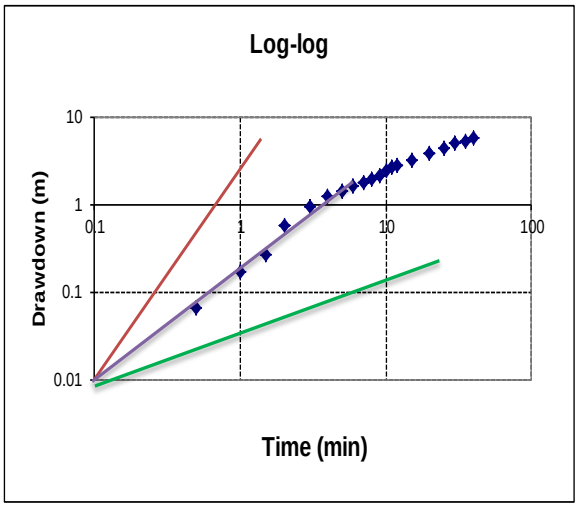

Recovery T : T = 0.05 m^2/d

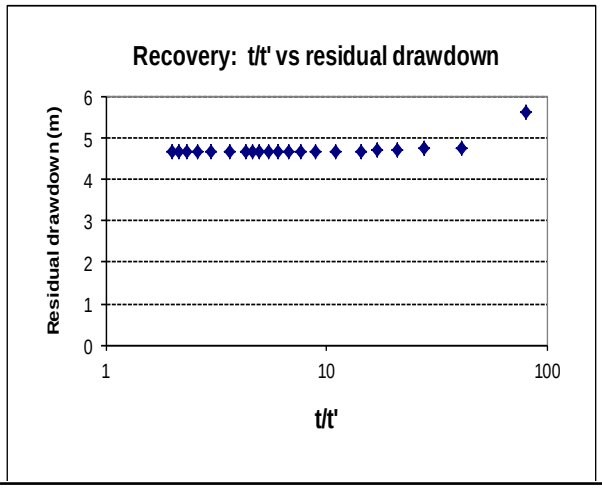

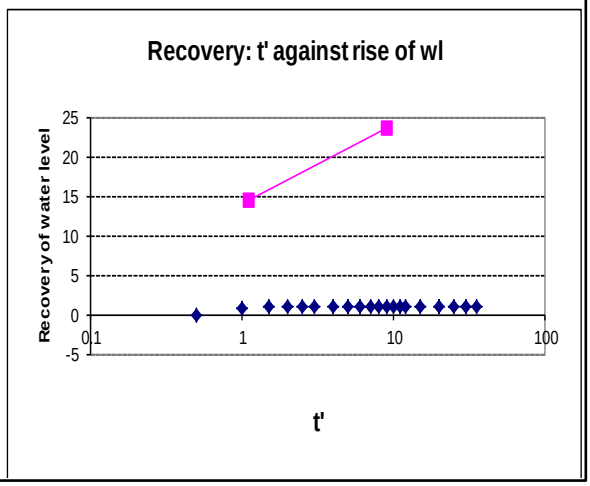

Appendix J: Hydrochemical constituents and stable isotope of water samples

Sample date	Site Name	pH	T	EC	EC	TDS	Na	K	Mg	Ca	CL	SO_4	NO_3	HCO3	Isotope	
		(Units)	(0C)	(uS/cm)	(mS/m)	(mg/l)	meq/l	meq/l	meq/l	meq/l	meq/l	meq/l	meq/l	meq/l	δ^2H	$\delta^{18}O$
14-Feb-14	2STBH1	6.6	18.5	440	44	245	0.71	0.01	0.77	1.85	0.13	2.49	0.00	0.71	-11.69	-2.82
26-Mar-14	2STBH1	6.4	18.8	470	47	230	0.54	0.00	0.70	2.01	0.12	1.97	0.01	1.15	-11.41	-3.28
19-Apr-14	2STBH1	6.7	18.6	510	51	250	0.63	0.00	0.84	2.38	0.12	2.04	0.01	1.69	-8.73	-3.28
29-May-14	2STBH1	6.6	19.9	510	51	250	0.81	0.05	1.03	2.77	0.12	1.99	0.00	2.53	-10.41	-3.00
30-Jun-14	2STBH1	6.8	17.9	480	48	240	0.87	0.05	1.07	2.87	0.13	2.18	0.01	2.55	-9.35	-2.99
30-Jul-14	2STBH1	6.7	17.8	480	48	240	0.84	0.05	1.05	2.83	0.14	2.06	0.01	2.56	-8.89	-3.03
28-Aug-14	2STBH1	6.7	18.4	510	51	270	0.73	0.04	0.94	2.54	0.13	2.08	0.01	2.03	-9.51	-2.97
30-Sep-14	2STBH1	6.8	19.2	550	55	270	0.74	0.05	0.94	2.62	0.14	1.72	0.00	2.49	-6.90	-2.56
30-Oct-14	2STBH1	6.9	19.6	580	58	290	0.74	0.05	0.95	2.66	0.14	1.79	0.00	2.46	-10.38	-3.67
28-Nov-14	2STBH1	6.9	19.0	590	59	300	0.72	0.05	0.95	2.64	0.12	2.07	0.00	2.16	-9.47	-3.22
31-Dec-14	2STBH1	6.9	17.6	610	61	310	0.74	0.05	1.02	2.64	0.12	2.01	0.00	2.32	-11.16	-3.43
30-Jan-15	2STBH1	6.7	19.9	640	64	320	0.69	0.05	1.00	2.66	0.12	2.07	0.00	2.20	-10.06	-2.99
14-Feb-14	2STBH2	8.0	29.0	263	26.3	112	0.97	0.01	0.57	0.97	0.22	0.49	0.01	1.79	-10.75	-3.06
26-Mar-14	2STBH2	7.8	30.8	340	34	170	0.89	0.02	0.55	0.93	0.22	0.51	0.01	1.65	-9.31	-3.22
19-Apr-14	2STBH2	7.7	30.9	300	30	110	0.91	0.02	0.55	0.92	0.17	0.35	0.01	1.88	-8.53	-3.18
29-May-14	2STBH2	7.3	23.9	290	29	140	1.22	0.02	0.71	1.21	0.25	0.85	0.00	2.06	-10.04	-2.93
30-Jun-14	2STBH2	7.6	23.9	240	24	120	1.20	0.02	0.71	1.19	0.23	0.56	0.01	2.32	-9.16	-3.11
30-Jul-14	2STBH2	7.9	23.2	250	25	120	1.21	0.02	0.70	1.19	0.24	0.53	0.01	2.35	-10.84	-2.83
28-Aug-14	2STBH2	7.6	24.3	280	28	140	1.21	0.02	0.71	1.20	0.24	0.70	0.00	2.19	-8.51	-3.10
30-Sep-14	2STBH2	7.4	25.2	310	31	150	1.10	0.02	0.56	1.24	0.23	0.40	0.00	2.28	-9.39	-3.05
30-Oct-14	2STBH2	7.1	25.4	270	27	130	1.10	0.02	0.57	1.25	0.23	0.39	0.01	2.31	-9.36	-3.1
28-Nov-14	2STBH2	7.3	19.9	270	27	130	0.65	0.04	0.54	1.20	0.23	0.39	0.00	1.81	-10.27	-3.34
31-Dec-14	2STBH2	7.5	19.3	270	27	130	0.91	0.02	0.54	1.22	0.23	0.40	0.00	2.06	-9.06	-3.05
30-Jan-15	2STBH2	7.0	27.0	280	28	130	0.92	0.03	0.54	1.19	0.23	0.40	0.00	2.05	-8.35	-3.04
14-Feb-14	2STBH3	6.7	17.9	320	32	160	0.59	0.00	1.07	0.56	0.20	1.56	0.01	0.46	-8.10	-2.69
26-Mar-14	2STBH3	6.4	20.1	280	28	130	0.58	0.00	1.03	0.54	0.17	1.58	0.01	0.39	-10.91	-3.42
19-Apr-14	2STBH3	6.5	19.5	270	27	140	0.59	0.00	1.08	0.55	0.18	1.61	0.01	0.42	-7.99	-3.12
29-May-14	2STBH3	6.5	18.5	300	30	150	0.78	0.07	1.37	0.88	0.19	1.70	0.00	1.21	-9.13	-3.29
30-Jun-14	2STBH3	6.7	18.8	250	25	130	0.76	0.06	1.27	0.94	0.18	1.70	0.01	1.15	-8.46	-3.01
30-Jul-14	2STBH3	6.9	18.3	700	26	130	0.74	0.05	1.29	0.84	0.21	1.76	0.01	0.93	-9.82	-2.72
28-Aug-14	2STBH3	6.9	18.0	270	27	130	0.70	0.06	1.16	1.12	0.17	1.82	0.01	1.03	-8.75	-3.17
30-Sep-14	2STBH3	6.9	19.3	290	29	140	0.66	0.05	1.14	1.11	0.15	1.61	0.00	1.20	-8.67	-2.64
30-Oct-14	2STBH3	7.4	19.3	300	30	150	0.65	0.04	1.15	1.18	0.15	1.60	0.00	1.26	-10.93	-3.41
28-Nov-14	2STBH3	7.7	20.2	320	32	160	0.64	0.04	1.15	1.30	0.14	1.60	0.00	1.40	-9.91	-3.09
31-Dec-14	2STBH3	6.8	18.1	320	32	160	0.64	0.05	1.15	1.29	0.13	1.61	0.00	1.39	-9.85	-2.94
30-Jan-15	2STBH3	7.1	19.3	330	33	160	0.64	0.04	1.16	1.32	0.13	1.65	0.00	1.37	-9.23	-3.00
14-Feb-14	2STBH4	6.9	19.8	190	19	100	0.40	0.00	0.40	0.38	0.15	0.54	0.01	0.47	-10.22	-3.23
26-Mar-14	2STBH4	6.5	19.1	200	20	100	0.22	0.00	0.18	0.29	0.15	0.48	0.01	0.05	-7.47	-3.02
19-Apr-14	2STBH4	7.1	18.3	230	23	110	0.06	0.00	0.54	0.54	0.15	0.52	0.01	0.47	-9.71	-3.49
29-May-14	2STBH4	7.8	18.1	220	22	110	0.67	0.05	0.76	0.71	0.12	1.07	0.01	0.98	-10.84	-2.81
30-Jun-14	2STBH4	7.4	18.3	170	17	80	0.66	0.05	0.75	0.69	0.16	1.18	0.01	0.81	-9.17	-3.32
30-Jul-14	2STBH4	6.9	18.6	180	18	90	0.68	0.05	0.74	0.72	0.14	1.11	0.02	0.92	-9.15	-2.70
28-Aug-14	2STBH4	6.7	19.1	240	24	100	0.59	0.05	0.60	0.73	0.12	0.58	0.01	1.26	-11.36	-3.16
30-Sep-14	2STBH4	6.7	19.2	180	18	90	0.57	0.05	0.59	0.73	0.15	0.40	0.00	1.40	-6.28	-2.4
30-Oct-14	2STBH4	6.9	20.5	180	18	90	0.55	0.05	0.59	0.74	0.15	0.39	0.00	1.37	-7.03	-2.55
28-Nov-14	2STBH4	7.2	19.9	180	18	90	0.48	0.04	0.56	0.70	0.15	0.38	0.00	1.26	-10.37	-3.52
31-Dec-14	2STBH4	6.7	18.0	210	21	100	0.49	0.04	0.57	0.70	0.14	0.39	0.00	1.27	-7.37	-3.17
30-Jan-15	2STBH4	6.8	19.5	190	19	90	0.48	0.04	0.56	0.69	0.14	0.39	0.00	1.24	-9.26	-3.22

14-Feb-14	2STBH5	6.9	19.2	330	33	160	0.62	0.01	1.05	1.05	0.13	1.13	0.01	1.46	-6.92	-2.91
26-Mar-14	2STBH5	6.3	19.6	330	33	160	0.57	0.01	0.99	0.93	0.12	1.03	0.01	1.35	-9.71	-2.92
19-Apr-14	2STBH5	6.6	18.4	330	33	170	0.61	0.01	1.03	1.08	0.12	0.83	0.00	1.78	-8.63	-3.36
29-May-14	2STBH5	6.8	18.0	310	31	150	0.80	0.11	1.19	1.44	0.14	1.06	0.01	2.34	-8.05	-3.1
30-Jun-14	2STBH5	6.7	17.9	280	28	140	0.77	0.10	1.16	1.52	0.12	1.08	0.01	2.34	-7.52	-2.97
30-Jul-14	2STBH5	6.6	17.7	300	30	150	0.85	0.09	1.16	1.88	0.12	1.17	0.01	2.68	-8.48	-2.89
28-Aug-14	2STBH5	6.8	18.7	290	29	150	0.80	0.10	0.98	1.87	0.13	1.02	0.02	2.58	-8.60	-3.14
30-Sep-14	2STBH5	7.1	19.6	380	38	180	0.79	0.09	1.00	1.81	0.12	1.15	0.00	2.42	-8.05	-3.1
30-Oct-14	2STBH5	7.1	19.8	370	37	160	0.81	0.08	0.98	1.91	0.12	1.20	0.00	2.46	-9.16	-3.02
28-Nov-14	2STBH5	7.2	20.2	380	38	190	0.71	0.08	0.97	1.74	0.13	1.06	0.00	2.31	-8.49	-2.83
31-Dec-14	2STBH5	6.4	18.0	370	37	180	0.65	0.07	0.96	1.72	0.13	1.01	0.00	2.27	-8.24	-2.35
30-Jan-15	2STBH5	6.7	19.3	410	41	200	0.67	0.08	0.97	1.73	0.13	0.86	0.01	2.46	-9.35	-3.2
14-Feb-14	2STRIV1	6.7	19.7	177	17.7	98	0.31	0.00	0.39	0.42	0.31	1.21	0.01	0.41	-8.42	-2.84
26-Mar-14	2STRIV1	6.4	18.1	210	21	100	0.49	0.00	0.62	0.62	0.30	1.61	0.02	0.17	-7.86	-3.32
19-Apr-14	2STRIV1	6.7	16.1	230	23	110	0.46	0.00	0.62	0.62	0.30	1.64	0.04	0.27	-11.99	-3.47
29-May-14	2STRIV1	7.0	13.8	240	24	120	0.66	0.04	0.86	0.90	0.33	1.77	0.01	0.34	-6.49	-2.35
30-Jun-14	2STRIV1	6.6	12.8	200	20	100	0.66	0.05	0.87	0.90	0.34	1.79	0.02	0.34	-7.76	-2.85
30-Jul-14	2STRIV1	7.3	15.2	200	20	100	0.67	0.07	0.81	0.86	0.34	1.67	0.02	0.39	-8.21	-2.86
28-Aug-14	2STRIV1	6.2	15.8	210	21	100	0.66	0.06	0.61	0.89	0.35	1.62	0.02	0.23	-6.36	-2.8
30-Sep-14	2STRIV1	6.4	17.8	220	22	100	0.63	0.06	0.61	0.78	0.37	1.33	0.01	0.36	-5.91	-3.01
30-Oct-14	2STRIV1	6.2	20.3	220	22	110	0.56	0.05	0.61	0.76	0.32	1.41	0.00	0.25	-6.85	-2.96
28-Nov-14	2STRIV1	6.3	19.3	230	23	110	0.56	0.05	0.61	0.79	0.30	1.47	0.00	0.23	-5.10	-2.53
31-Dec-14	2STRIV1	6.9	18.8	220	22	110	0.48	0.05	0.61	0.78	0.29	1.51	0.00	0.11	-6.07	-2.69
30-Jan-15	2STRIV1	6.5	20.5	220	22	110	0.45	0.04	0.63	0.84	0.31	1.55	0.00	0.11	-3.9	-3.08
14-Feb-14	2STRIV2	6.9	18.9	210	21	110	0.43	0.00	0.56	0.46	0.24	1.27	0.01	0.07	-8.63	-2.94
26-Mar-14	2STRIV2	6.7	18.4	210	21	100	0.44	0.00	0.57	0.48	0.23	1.31	0.03	0.07	-8.67	-3.15
19-Apr-14	2STRIV2	6.5	16.4	230	23	110	0.47	0.01	0.61	0.49	0.25	1.34	0.01	0.02	-8.58	-3.37
29-May-14	2STRIV2	7.0	13.4	210	21	100	0.64	0.07	0.79	0.67	0.24	1.41	0.01	0.52	-7.86	-3.13
30-Jun-14	2STRIV2	6.8	11.9	180	18	90	0.63	0.08	0.79	0.65	0.24	1.51	0.01	0.39	-8.79	-3.23
30-Jul-14	2STRIV2	6.9	12.2	190	19	100	0.66	0.09	0.83	0.75	0.24	1.55	0.01	0.54	-8.33	-3.07
28-Aug-14	2STRIV2	6.9	18.7	210	21	100	0.64	0.03	0.63	0.73	0.23	1.54	0.00	0.25	-6.46	-2.40
30-Sep-14	2STRIV2	6.7	22.7	210	21	100	0.54	0.04	0.68	0.78	0.21	1.43	0.00	0.40	-7.28	-2.65
30-Oct-14	2STRIV2	6.7	28.5	220	22	110	0.51	0.01	0.65	0.76	0.24	1.46	0.00	0.23	-6.49	-2.47
28-Nov-14	2STRIV2	7.2	22.5	220	22	100	0.47	0.02	0.63	0.71	0.23	1.35	0.00	0.25	-7.80	-2.96
31-Dec-14	2STRIV2	7.0	18.0	200	20	100	0.44	0.03	0.65	0.70	0.22	1.29	0.00	0.33	-8.77	-2.7
30-Jan-15	2STRIV2	6.9	24.4	200	20	100	0.43	0.04	0.53	0.68	0.23	1.25	0.00	0.19	-8.82	-2.92
14-Feb-14	2STWEIR	6.3	19.6	175	17.5	98	0.28	0.00	0.28	0.29	0.23	1.65	0.01	1.03	-8.71	-2.69
26-Mar-14	2STWEIR	6.6	19.6	200	20	100	0.48	0.00	0.57	0.53	0.25	1.67	0.01	0.35	-8.40	-2.96
19-Apr-14	2STWEIR	5.8	17.1	210	21	100	0.48	0.00	0.56	0.53	0.23	1.51	0.03	0.19	-8.65	-3.03
29-May-14	2STWEIR	6.4	16.4	220	22	110	0.66	0.05	0.76	0.72	0.28	1.73	0.01	0.19	-7.34	-2.34
30-Jun-14	2STWEIR	6.8	14.6	200	20	100	0.67	0.05	0.79	0.74	0.27	1.77	0.01	0.20	-7.79	-3.10
30-Jul-14	2STWEIR	7.0	15.0	220	22	110	0.68	0.07	0.81	0.78	0.25	1.78	0.01	0.29	-7.84	-2.82
28-Aug-14	2STWEIR	6.1	17.8	230	23	111	0.67	0.06	0.61	0.77	0.27	1.79	0.00	0.04	-7.92	-2.83
30-Sep-14	2STWEIR	6.5	23.8	220	22	111	0.57	0.06	0.62	0.78	0.24	1.63	0.00	0.16	-5.09	-2.92
30-Oct-14	2STWEIR	6.2	26.3	230	23	110	0.55	0.04	0.62	0.77	0.28	1.65	0.00	0.04	-6.86	-2.5
28-Nov-14	2STWEIR	6.5	21.8	230	23	110	0.55	0.03	0.60	0.75	0.20	1.67	0.00	0.06	-8.1	-3.04
31-Dec-14	2STWEIR	6.7	18.5	230	23	110	0.49	0.04	0.61	0.76	0.22	1.66	0.00	0.02	-10.36	-2.96
30-Jan-15	2STWEIR	5.9	23.2	240	24	120	0.45	0.04	0.58	0.75	0.22	1.67	0.00	0.06	-3.85	-3.37

Appendix K: Statistical analysis of hydrochemical constituents of water samples

ALL SAMPLES						
Parameter	**Unit**	**Min**	**Max**	**Mean**	**Median**	**Std. Dev.**
Temp	^{0}C	11.9	30.9	19.6	19.1	3.47
pH	units	5.82	8.00	6.84	6.82	0.43
EC	mS/m	17.00	64.00	28.51	24.00	10.86
TDS	mg/l	80.0	320.0	140.2	116.0	55.4
Na	mg/l	0.06	1.22	0.66	0.65	0.20
K	mg/l	0.0008	0.1085	0.0394	0.0439	0.0267
Mg	mg/l	0.1823	1.3743	0.7813	0.7073	0.2432
Ca	mg/l	0.2876	2.8707	1.1175	0.8505	0.6492
Cl	mg/l	0.1159	0.3731	0.1985	0.2003	0.0674
SO_4	mg/l	0.3473	2.4934	1.3100	1.4674	0.5312
NO_3	mg/l	0.00003	0.03531	0.00601	0.00568	0.00631
HCO_3	mg/l	0.0154	2.6823	1.1342	1.0908	0.8822
GROUNDWATER						
pH	units	6.32	8.0	7.0	6.9	0.41
Temp	^{0}C	17.60	30.9	20.2	19.3	3.07
EC	mS/m	17.00	64.0	32.8	30.0	11.73
TDS	mg/l	80.00	320.00	161.28	150.00	60.75
Na	mg/l	0.06	1.22	0.73	0.71	0.21
K	mg/l	0.001	0.108	0.041	0.044	0.028
Mg	mg/l	0.182	1.374	0.864	0.949	0.261
Ca	mg/l	0.288	2.871	1.368	1.194	0.704
Cl	mg/l	0.116	0.246	0.158	0.142	0.041
SO_4	mg/l	0.347	2.49	1.172	1.096	0.619
NO_3	mg/l	0.000	0.02	0.00	0.01	0.00
HCO_3	mg/l	0.051	2.68	1.66	1.74	0.69
SURFACE WATER						
pH	units	5.82	7.30	6.61	6.61	0.35
Temp	^{0}C	11.90	28.50	18.55	18.55	3.84
EC	mS/m	17.5	24.0	21.311	21.311	1.613
TDS	mg/l	90.0	120.0	104.944	104.944	6.604
Na	mg/l	0.282	0.675	0.540	0.540	0.105
K	mg/l	0.002	0.093	0.037	0.037	0.025
Mg	mg/l	0.280	0.871	0.644	0.644	0.120
Ca	mg/l	0.291	0.904	0.700	0.700	0.139
Cl	mg/l	0.202	0.373	0.266	0.266	0.045
SO_4	mg/l	1.210	1.786	1.540	1.540	0.168
NO_3	mg/l	0.00003	0.035	0.008	0.008	0.009
HCO_3	mg/l	0.015	1.029	0.253	0.253	0.190